26812

National Library of Canada | Bibliothèque nationale du Canada

CANADIAN THESES ON MICROFICHE | THÈSES CANADIENNES SUR MICROFICHE

NAME OF AUTHOR/*NOM DE L'AUTEUR* YIU-FAI LAM

TITLE OF THESIS/*TITRE DE LA THÈSE* Nuclear Magnetic Resonance Studies in Biological Systems

UNIVERSITY/*UNIVERSITÉ* U. of Alberter

DEGREE FOR WHICH THESIS WAS PRESENTED/ *GRADE POUR LEQUEL CETTE THÈSE FUT PRÉSENTÉE* Ph. D.

YEAR THIS DEGREE CONFERRED/*ANNÉE D'OBTENTION DE CE GRADE* FALL, 1975.

NAME OF SUPERVISOR/*NOM DU DIRECTEUR DE THÈSE* Dr. G. Kotowycz

Permission is hereby granted to the NATIONAL LIBRARY OF CANADA to microfilm this thesis and to lend or sell copies of the film.

The author reserves other publication rights, and neither the thesis nor extensive extracts from it may be printed or otherwise reproduced without the author's written permission.

L'autorisation est, par la présente, accordée à la BIBLIOTHÈQUE NATIONALE DU CANADA de microfilmer cette thèse et de prêter ou de vendre des exemplaires du film.

L'auteur se réserve les autres droits de publication; ni la thèse ni de longs extraits de celle-ci ne doivent être imprimés ou autrement reproduits sans l'autorisation écrite de l'auteur.

DATED/*DATÉ* 30th Sept. 1975 SIGNED/*SIGNÉ* Yiu-Fai Lam

PERMANENT ADDRESS/*RÉSIDENCE FIXE* 7/F, A-3, Elegance House
630, Kings Rd North Point
Hong Kong

NL-91 (3-74)

THE UNIVERSITY OF ALBERTA

NUCLEAR MAGNETIC RESONANCE STUDIES IN BIOLOGICAL SYSTEMS

by

Yiu-Fai Lam (C)

A THESIS

SUBMITTED TO THE FACULTY OF GRADUATE STUDIES

IN PARTIAL FULFILMENT OF THE REQUIREMENTS FOR THE DEGREE

OF DOCTOR OF PHILOSOPHY

DEPARTMENT OF CHEMISTRY

EDMONTON, ALBERTA

FALL, 1975

THE UNIVERSITY OF ALBERTA

FACULTY OF GRADUATE STUDIES

The undersigned certify that they have read, and recommend to the Faculty of Graduate Studies for acceptance, a thesis entitled

NUCLEAR MAGNETIC RESONANCE

STUDIES IN

BIOLOGICAL SYSTEMS

submitted by Yiu-Fai Lam in partial fulfilment of the requirements for the degree of Doctor of Philosophy.

George Kotowycz
Supervisor

R.B. Jordan

H.B. Dunford

W.M. Bowers

Dallas W. Hobbs

Jan C. Smith
External Examiner

Date 5th Sept, 1975.

To My Parents

and

Mr. Chu On-Hong

ABSTRACT

Three studies using nuclear magnetic resonance (NMR) techniques on systems of biological interest are reported in this thesis.

The first study is concerned with the binding of Mn(II) ions with the enzyme succinyl-CoA-synthetase. Four equivalent metal ion binding sites are found in the enzyme with an average dissociation constant of 4.1×10^{-4}M at 25°C. Once the Mn(II) ions bind to the enzyme, their tumbling motion is hindered and the corresponding rotational rate decreases significantly. The resultant tumbling motion, the NMR exchange and the electronic relaxation all affect the nuclear relaxation of the water protons at the metal ion binding sites of the enzyme.

The second study is concerned with the binding between Mn(II) ions and adenosine-5'-triphosphate (ATP). The metal ions bind to the three phosphate groups of ATP and, in addition, some of them also bind to the adenine N-7 nitrogen of the same ATP molecule. The two Mn(II)-ATP complexes, together with the unbound ATP, constitute a three-site exchange system. In this system, the NMR exchange process between the two complexes is a very fast

step, with a rate constant of 2.7×10^7 sec^{-1} at 27°C. The distances between the Mn(II) ion and the adenine carbons are also determined. Thus, a model for the Mn(II)-ATP complex, in which the metal co-ordinates to the adenine base, is proposed.

Finally, the conformation and the mode of association of folic acid in aqueous solutions is studied. It is found that folic acid exists in an extended conformation. Furthermore, these molecules form intermolecular stacks. In these stacks, the molecules orientate themselves in an alternative manner such that their hydrophilic ends uniformly extend out into the solvent.

ACKNOWLEGMENTS

I would like to express my sincere thanks for Dr.G.Kotowycz as my research advisor during the course of these studies.

Special thanks to my wife, Siu-Kim, for her understanding and encouragement throughout these years.

To Dr.W.A.Bridger for providing the enzyme and his advice on the enzyme study.

I am also indebted to my wife for programming the manuscript, to Mr.G.Bigam and Mr.E.Brownie for their technical assistance. Finally, financial support from the University of Alberta and the National Research Council of Canada is greatly appreciated.

TABLE OF CONTENTS

PAGE

LIST OF TABLES xii

LIST OF FIGURES xiv

CHAPTER

I GENERAL INTRODUCTION 1

A. The Object of these Studies 1

B. Methodology 2

C. Outline of the Thesis 5

II MAGNETIC RESONANCE STUDIES OF MANGANESE(II) ION BINDING WITH SUCCINYL CoA-SYNTHETASE . . . 7

A. Introduction 7

1. The Catalytic Functions and Molecular Properties of the Enzyme 7

2. Catalytic Mechanism of SCS 9

3. The Object and Approach of the Present Study 13

B. Theory Section 16

1. Stoichiometry of the EM complex 17

2. Water PRR of the Enzyme-free and the Enzyme-bound complexes 19

3. Temperature and Frequency Dependence of Water PRR 27

3A. The NMR Exchange Rate 27

PAGE

3B. The Nuclear Relaxation Rate at the Mn(II) Ion Complexes 29

3C. The Correlation Times 32

C. Experimental Section 37

1. Materials 37

2. Enzyme Assays and Buffer 39

3. Sample Preparation and ESR Measurements. . 40

4. Sample Preparation and NMR Measurements. . 42

D. Results and Discussion 48

1. Binding of Mn(II) Ions with Phospho-SCS. . 48

2. Frequency and Temperature Dependence of Water PRR 59

2A. Water PRR of Mn(II) Solutions in the Absence of the Enzyme 59

2B. Water PRR of the Mn(II) Enzyme Solutions 63

3. Quantitative Analysis of the Water PRR for the Enzyme-bound Complex 68

E. Conclusions 76

III ^{13}C NMR RELAXATION STUDIES ON THE Mn(II) ADENOSINE-5'-TRIPHOSPHATE COMPLEX IN SOLUTION. . 77

A. Introduction 77

1. Biochemistry of the Metal Ion ATP Complexes 77

2. Stoichiometry of the Metal Ion ATP Complexes 79

PAGE

3. Structures of the Metal Ion ATP Complexes 83

4. Object of the Present Study. 86

B. Theory Section 88

1. A Two-Site System 88

2. A Three-Site Exchange System 92

2A. The Spin-Spin Paramagnetic Relaxation Rate 94

2B. The Spin-Lattice Paramagnetic Relaxation Rate 98

3. Nuclear Relaxation Mechanisms Between the Mn(II) Ion and the ATP Nuclei . . . 100

C. Experimental Section 104

1. Materials and Sample Preparation . . . 104

2. ^{13}C NMR Measurements 107

3. ^{1}H NMR Measurements 111

D. Results 112

E. Discussion 122

1. The Dominant Relaxation Mechanism of ^{13}C T_2p^{-1} in the Present Study 122

2. The Temperature Dependence of T_2p^{-1} . . . 125

3. The Three-Site Scheme 132

3A. The T_2p^{-1} Temperature Dependence . . 132

3B. The T_1p^{-1} Temperature Dependence . . 135

4. Geometry of the Backbound Mn(II) ATP Complex 137

PAGE

F. Conclusions 143

IV SELF-ASSOCIATION OF FOLIC ACID IN AQUEOUS SOLUTION BY PROTON MAGNETIC RESONANCE 145

A. Introduction 145

B. Experimental Section 151

1. Materials and Sample Preparation . . . 151

2. Instrumental Techniques 153

C. Results 155

1. Proton NMR Spectra 155

2. The Concentration Dependence of the Chemical Shifts. 159

3. The Temperature Dependence of Chemical Shifts of the Folate Protons 165

D. Discussion 168

1. The Folate Conformation in Aqueous Solution 168

2. The Intermolecular Association of Folate 170

E. Conclusions 176

* * *

BIBLIOGRAPHY 177

APPENDIX A 193

APPENDIX B 207

LIST OF TABLES

Table		Page
II-1	Data of the water proton relaxation enhancements at 100.0 MHz	50
II-2	The ESR M-titration data	54
II-3	A least-squared analysis on the M-titration data	56
II-4	Parameters for Mn(II) ions in the enzyme-bound and the enzyme-free complexes	69
III-1	Summary of ^{13}C T_1p^{-1} and T_2p^{-1} values for the Mn(II) ATP solutions	116
III-2	The T_1p^{-1} temperature dependence of the ^{13}C nuclei in ATP	119
III-3	The T_1p^{-1} temperature dependence of the ^{1}H and ^{31}P nuclei in ATP	120
III-4	Parameters obtained in the water proton T_2p analysis	128
III-5	Scalar coupling constants between the base carbon nuclei of ATP and Mn(II) ion	134
III-6	The activation parameters and the NMR exchange rate for the $3 \rightleftharpoons 2$ process in the Mn(II)-ATP system	135
III-7	Metal-nuclei distances (A) for the Mn(II) ATP backbound complex	139

Table		Page
IV-1	The concentration dependence of proton chemical shifts of disodium folate in D_2O at 30.5°C and a pD of 7.1	161
IV-2	The concentration dependence of proton chemical shifts of folate solution and compound I solution at 12.9 pD and 30.5°C	162
IV-3	The comparison of chemical shifts between the protons in folate and those in model compound II	164
IV-4	The temperature dependence of the proton chemical shifts of disodium folate in D_2O at 7.1 pD in two different concentrations	167

LIST OF FIGURES

Figure		Page
II-1	Proposed molecular mechanism of a concerted reaction for SCS enzyme	12
II-2	Determination of T_1 using the 180°, τ, 90° pulse sequence	44
II-3	Water proton signals plotted as a function of τ, in a 180°, τ, 90° pulse experiment to determine the spin-lattice relaxation time	47
II-4	Water proton relaxation enhancement as a function of the enzyme concentration	51
II-5	X-band EPR spectra of aqueous Mn(II) ions at 25°C in tris-buffer	52
II-6	The Scatchard plot for the enzyme solution titrated with Mn(II) ions	55
II-7	Frequency and temperature dependence of the normalized water proton T_1 induced by the enzyme-free $Mn(II).(H_2O)_6^{+2}$ complex in tris-buffer	61
II-8	Frequency and temperature dependence of the normalized water proton T_1 induced by the enzyme-bound $Mn(II).(H_2O)_4^{+2}$ complex in tris-buffer	64
II-9	Frequency dependence of the normalized water proton T_1 induced by the enzyme-bound complex in tris-buffer at 23°C	66
II-10	Frequency and temperature dependence of the correlation times in Mn(II) SCS solutions	73
II-11	Frequency and temperature dependence of water proton dipolar correlation time τ_c and its function $F(\tau_c)$ in the enzyme-bound Mn(II) complex	74

Figure		Page
III-1	Formula structure of ATP in aqueous solutions at neutral pH	78
III-2	A sample set of ^{13}C NMR spectra of the Adenine carbons of ATP, obtained in a 180°, τ, 90° pulse experiment	110
III-3	Proton-decoupled natural abundance ^{13}C FT NMR spectrum of ATP	113
III-4	The effect of Mn(II) ions on the ^{13}C longitudinal relaxation rates of the adenine base nuclei of ATP	114
III-5	The effect of Mn(II) ions on the ^{13}C transverse relaxation rates of the adenine base nuclei of ATP	115
III-6	The temperature dependence of T_2p^{-1} of the ATP ^{13}C nuclei	118
III-7	The temperature dependence of the water proton transverse relaxation times in a Mn(II-ATP solution	121
III-8	The analysis of the temperature dependence of T_2p^{-1} for the carbon nuclei C-5 and C-8	130
III-9	Proposed structure for the Mn(II-ATP backbound complex in solution	141
IV-1	Formula structures of folic acid and the two model compounds	146
IV-2	The 100.0 MHz NMR spectrum of 0.049m disodium folate in D_2O	156
IV-3	The 100.0 MHz ^1H NMR spectra of the model compounds in D_2O at 30.5°C	158

Figure		Page
IV-4	The concentration dependence of the proton chemical shifts of disodium folate in D_2O	160
IV-5	The temperature dependence of the proton chemical shifts of disodium folate in D_2O	166
IV-6	The proposed, alternating, head to tail intermolecular stacking model for folate ions in aqueous solution	175

CHAPTER I

GENERAL INTRODUCTION

A. THE OBJECT OF THESE STUDIES

The work described in the thesis involves three different compounds of biological interest and they were studied by means of nuclear magnetic resonance (NMR). The appropriate principles, theory, and techniques that were employed in each study are discussed together with the analysis and interpretation of the data. Throughout these studies, an attempt was made to achieve a clear understanding on the specific problem and, at the same time, to learn the NMR principles that may be applied to other similar biological systems.

B. METHODOLOGY

Three characteristic NMR parameters were measured in the reported studies. They are the spin-lattice relaxation time T_1, the spin-spin relaxation time T_2 and the chemical shift. The first study (Chapter II) deals mainly with T_1 measurements. The second study (Chapter III) involves both T_1 and T_2 measurements, whereas the last topic under study (Chapter IV) deals only with chemical shift measurements . These three NMR parameters have been treated and discussed in detail in a number of monographs (Slichter, 1963; Poole and Farach, 1971 and 1972). In the following paragraphs, a brief outline of these parameters is presented using proton nucleus, with spin quantum number of 1/2, as an example.

Nuclear magnetism is a macroscopic phenomenon (Bloch, 1946). The observed behavior of an NMR resonance reflects the overall effect arising from all the nuclear spins in identical chemical and magnetic environments. In the presence of a static magnetic field H_0, the nuclear spins experience a magnetic field given by H_{0i}, depending on their location in a molecule. On the microscopic scale, the nuclear spins distribute themselves between two energy levels. The population of these levels is governed by the Boltzmann law. The energy difference between the two

levels is given by μH_{0_i} , where μ is the magnetic moment of the nucleus. In addition, the nuclear spins interact with each other (spin-spin interaction) due to the very small time-dependent fluctuating magnetic field arising from the environment. Thus, they precess with no phase coherence at the Larmor precession frequency ω_i given by $\mu H_{0_i} / \gamma$ where γ is the magnetogyric ratio.

In order to induce a resonance of the nuclei in question, a suitable electromagnetic radiation at the frequency ω_i is used. The difference between the frequency and that of a certain reference signal is known as the chemical shift of the nuclei. When such radiation is applied to the spin system, the original thermal distribution is perturbed , due to the absorption of a certain amount of energy from the radiation, and at the same time, the nuclei precess momentarily in phase with the radiation. As soon as this perturbation is removed, the nuclei relax via two relaxation processes. In the first, the spins return to the original thermal distribution by transferring the absorbed energy to the surroundings (the lattice). This process is known as spin-lattice relaxation which has a characteristic time constant T_1, generally known as the spin-lattice (or longitudinal) relaxation time. In addition, the spins tend to resume their random-phased

precession. This latter process is known as spin-spin relaxation which has a characteristic time constant T_2, known as the spin-spin (or transverse) relaxation time.

Recent improvements in instrumentation allow the measurement of these nuclear phenomena very accurately and in a reasonable period of time for many different types of nuclei, such as ^{1}H, ^{31}P and ^{13}C. The advances are very important for NMR studies on those delicate compounds which may either be unstable or available only in very small quantities. Consequently, the application of NMR techniques in the area of biological research has become increasingly useful (Dwek, 1973; Bovey, 1972).

C. OUTLINE OF THE THESIS

Since several different biological compounds were investigated and the NMR techniques employed were different for each study, the thesis is divided into three chapters. In each chapter, the object of the research and the biological aspects of the compound are introduced together with the relevant theory, experimental procedure, results, discussion and conclusions.

Chapter II deals with the binding between a divalent metal ion and an enzyme [Mn(II) ion and phosphosuccinate-CoA-synthetase]. Using pulsed NMR techniques, the relaxation times T_1 of the solvent water protons in the enzyme-metal solutions were measured as a function of the magnetic field strength and temperature. From these data, the relevant mechanism for nuclear relaxation at the metal ion binding sites on the enzyme was worked out. In addition to the NMR measurements, the stoichiometry of the Mn(II) ion enzyme complex was determined by electron paramagnetic resonance.

Chapter III describes the studies on the structures of the Mn(II) ion complex with a nucleotide: adenosine-5'-triphosphate(ATP). By means of Fourier transform pulsed NMR techniques, both the T_1 and T_2 values

of the natural abundance ^{13}C nuclei of ATP in the presence of Mn(II) ions were measured. The temperature dependence of the T_2 processes were followed. The data are best interpreted in terms of a three-site exchange system. The ^{13}C T_1 data allow the metal ion to adenine carbon distances to be calculated. A model for the Mn(II)-nucleotide complex is proposed.

Finally, in Chapter IV, the mode of self-association of a commonly occuring coenzyme, folic acid, as well as its conformation were studied by ^1H NMR. The chemical shifts of folic acid and that of two model compounds were measured as a function of temperature and concentration. Results indicate that folic acid exists in an extended conformation in solution. In addition, these molecules stack in solution and a possible model for this intermolecular association is proposed.

CHAPTER II

MAGNETIC RESONANCE STUDIES OF MANGANESE(II) ION BINDING WITH SUCCINYL CoA-SYNTHETASE

A. INTRODUCTION

1. The Catalytic Functions and Molecular Properties of the Enzyme

Succinyl-CoA-Synthetase, abbreviated as SCS, is one of the most important and complex enzymes in the phosphorus metabolism (Kaufman et al, 1953). Among various sources, the enzyme isolated from Escherichia coli is the one that has been most thoroughly investigated (Nishimura, 1972; Bridger, 1974). It is composed of two subunits (α and β) (Ramaley et al, 1967; Bridger, 1971). In the phosphorylated form of the enzyme, the smaller α subunit contains a phosphorylated histidine group (Bridger, 1971). At high enzyme concentrations (above 1 mg/ml), the enzyme exists as an $\alpha_2\beta_2$ tetramer and has an oligomeric molecular weight around 140,000 (Ramaley et al, 1967; Krebs and Bridger, 1974). At lower concentrations, it begins to dissociate into an $\alpha\beta$ dimer. The enzyme exists mainly in the random coil conformation with small fractions of α-

helix and β-pleated sheet structure in the ratio 0.78, 0.14 and 0.08, respectively (Krebs and Bridger, 1974). The amino acid compositions of the enzyme have been determined (Leitzmann et al, 1970). However, the complete sequence has not been worked out.

SCS catalyzes the following reversible reaction in the presence of divalent cations:

$$\text{succinyl-CoA} + \text{NDP} + \text{Pi} \overset{M^{+2}}{\rightleftharpoons} \text{succinate} + \text{CoA} + \text{NTP} \qquad \text{(II-1)}$$

where CoA stands for Coenzyme A; Pi stands for inorganic orthophosphate; NDP and NTP are, respectively, nucleoside di- and tri-phosphates. M^{+2} is the divalent metal ion(Mg^{+2} is most commonly used). The forward reaction represents phosphorylation in the tricarboxylic acid cycle (Kaufman et al, 1953; Hift et al, 1953), which is important in the metabolism of higher organisms. The reverse reaction is a nucleoside triphosphate-dependent synthesis of succinyl-CoA, an important anabolic precursor for several essential biological molecules such as heme and cystathionine. The catalytic mechanism and structural features of the enzyme have been the subject of intensive research and have been critically reviewed (Nishimura, 1972; Bridger, 1974).

2. Catalytic Mechanism of SCS

Various techniques such as isotope labelling, rapid mixing and quenching have been used to study the kinetic and catalytic mechanism of the enzyme (Bridger, 1974). It has been shown that the phosphorylated form of the enzyme is an important obligatory intermediate in the catalysis (Bridger et al, 1968; Grinnell and Nishimura, 1969).

Recent steady state kinetic studies (Moffet and Bridger, 1970, 1973) indicate that the main reaction pathways can be represented by the following scheme:

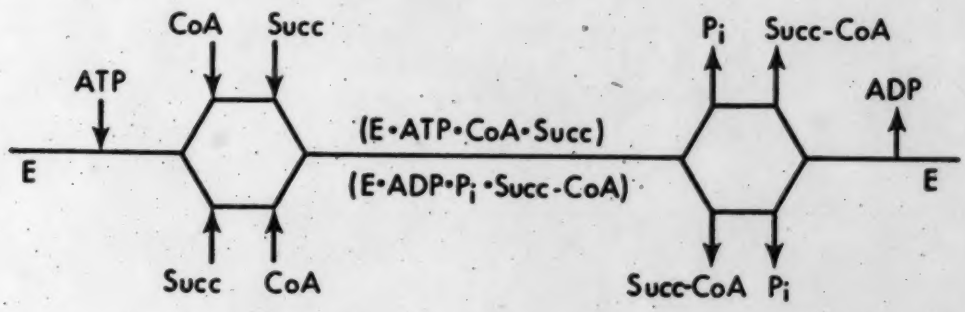

(II-2)

The reaction is initiated by ATP addition to the enzyme, followed by random association of succinate or CoA. A central complex represented by (E.ATP.CoA-Succ) or (E.ADP.Pi-Succ.CoA) was proposed to account for the "substrate synergism" character of the enzyme. This

property was first noted by Bridger et al (1968). In their studies of ^{32}P isotope exchange rate between ADP and ATP in the presence of phospho-SCS enzyme, it was found that the rate of exchange of ^{32}P per unit of enzyme was much slower than the net catalytic rate when all substrates are present. Addition of individual substrates (CoA or Succinate) alone has no effect on the exchange rate, whereas the introduction of Succinyl-CoA (which possesses the essential functional groups) increases the exchange rate to the full net catalytic rate level. In their studies, these researchers also showed that the enzyme may be phosphorylated very rapidly by NTP. The reaction between SCS and NTP, leading to the formation of a phosphorylated enzyme (E-P), can therefore be regarded as an initial rapid equilibrium (pre-steady state) in the overall catalytic mechanism (Kaufman, 1955; Bridger et al, 1968).

Consequently, the overall catalytic reaction may be written as the following scheme:

$$E + NTP \overset{M^{+2}}{\rightleftharpoons} E\text{-}P + NDP \qquad \text{(II-3)}$$

$$E\text{-}P + \text{succinate} + CoA \overset{M^{+2}}{\rightleftharpoons} E + \text{succinyl-CoA} + Pi \qquad \text{(II-4)}$$

The various intermediates in the second reaction Eq.(II-4) are still not completely known. Two possible schemes have been presented for this process.

(i) The first scheme (Hager, 1962; Grinell and Nishimura, 1969; Walsh et al, 1970) requires the presence of an enzyme-bound phosphorylated succinate (E-succinyl-P) as a discrete intermediate. The scheme may be written as:

$$\text{E-P} + \text{succinate} \underset{}{\overset{M^{+2}}{\rightleftharpoons}} \text{E-succinyl-P} \qquad \text{(II-5)}$$

$$\text{E-succinyl-P} + \text{CoA} \overset{M^{+2}}{\rightleftharpoons} \text{E} + \text{succinyl-CoA} + \text{Pi} \qquad \text{(II-6)}$$

(ii) The second scheme (Hager, 1962; Robinson et al, 1969) involves a concerted mechanism which may be written as:

$$\text{E-P} + \text{succinate} + \text{CoA} \overset{M^{+2}}{\rightleftharpoons} \text{E-P.succinyl-CoA} \qquad \text{(II-7)}$$

$$\text{E-P.succinyl-CoA} \overset{M^{+2}}{\rightleftharpoons} \text{E} + \text{succinyl-CoA} + \text{Pi} \qquad \text{(II-8)}$$

Fig. II-1 illustrates this concerted scheme in more detail.

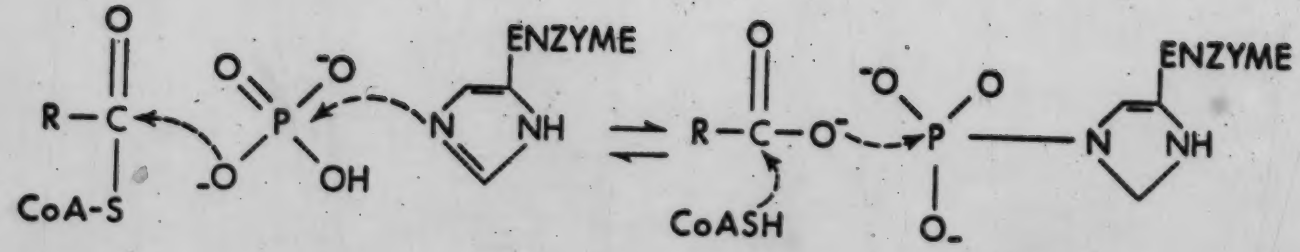

FIGURE II-1. Proposed molecular mechanism of a concerted reaction for SCS enzyme (Robinson et al , 1969)

3. The Object and Approach of the Present Study

In all the reactions of the enzyme described previously, the divalent cation Mg(II) is always required (Kaufman, 1955; Bridger, 1974 and references therein). The present work is to study the possible binding between the metal ions and the phosphorylated enzyme (phospho-enzyme), as the phospho-enzyme is the most stable and important form of the enzyme in the catalytic reaction (Moffet *et al*, 1972; Moffet and Bridger, 1973). In this study, Mn(II) ions are used because they resemble closely Mg(II) ions in most biological systems (Vallee, 1960; Cleland, 1967; Daune, 1974) and also because the paramagnetic property of the Mn(II) ions facilitates the NMR measurements. The approach is briefly outlined in the following paragraphs.

When Mn(II) ions bind to an enzyme, the environment around the bound metal ions is quite different from that of the unbound metal ions in the same solvent. Since a paramagnetic Mn(II) ion has five unpaired electrons in its d orbitals, these electrons interact significantly with any neighboring nuclei. Hence, these environmental changes will be experienced by the solvent water protons when the water molecules reside in the coordination spheres of the metal ions. Since the water molecules are exchanging between these ions and the bulk solvent, the observed

between these ions and the bulk solvent, the observed magnetic properties of the proton nuclei of the bulk solvent will then contain all contributions from the enzyme-bound metal ions, the free metal ions as well as from the pure solvent.

By means of ^1H NMR, these magnetic properties can be measured quantitatively in terms of the proton relaxation rates (PRR) of the water solvent (Einsinger et al, 1962; Cohn and Leigh, 1962). Furthermore, the proton relaxation rate arising from the bound metal ions on the enzyme may be isolated from the total observed relaxation rate when the concentrations of the bound and unbound (free) metal ions are known. This rate will be useful in the study of structural feature of the portion in the enzyme where the metal ion is bound (Reuben and Cohn, 1970). In many cases, the results thus obtained from NMR compare favourably with those from other techniques (Dwek, 1973). For example, in the case of Concanavalin-A, the same number of water molecules at the metal binding site in the enzyme were observed both from NMR (Koenig et al, 1973) and from X-ray study (Becker et al, 1975).

In the following sections, the relevant theory and equations will be discussed in order to show the design of the experiments for the study. The stoichiometry and

the dissociation constant of the enzyme-Mn(II) complex were measured using electron spin resonance (ESR) techniques. With this information, NMR experiments on water PRR were carried out as a function of temperature (4--38°C) and frequency (6.--60.0MHz). Combining these results, the relaxation rates are analyzed in detail to study the structural features of the enzyme around the bound metal ions.

B. THEORY SECTION

When an enzyme with n equivalent metal ion binding sites is introduced into an aqueous solution of Mn(II) ions, some of the metal ions will bind to the binding sites in the enzyme. Consequently, two types of metal ion complexes exist in solution:

a) The original hexa-aquo Mn(II) ion complex, $[Mn(H_2O)_6]^{+2}$, which is enzyme-free and abbreviated as M_f from now on.

b) The enzyme-bound Mn(II) ion complex, $[Mn(E')(H_2O)]^{+2}$, abbreviated as M_b. The coordination sites in this complex are now occupied by the water molecules and some ligands, E', of the enzyme. The complex is therefore also known as a binary EM complex (Dwek, 1973).

The formation of the enzyme-bound complex may be represented by the following equilibrium:

$$M_f + E' \underset{}{\overset{K_D}{\rightleftharpoons}} M_b \qquad \text{(II-9)}$$

where [E'] is the concentration of the metal binding sites in the enzyme. For an enzyme with n equivalent

metal binding sites, [E'] is equal to $nx[E]$, where [E] is the enzyme concentration. K_D is the dissociation constant (to be discussed in the following section), and the concentrations of the complexes, $[M_f]$ and $[M_b]$ are related to the total metal ion concentration $[M_t]$ as:

$$[M_t] = [M_f] + [M_b] \qquad \text{(II-10)}$$

1. Stoichiometry of the EM Complex

The dissociation constant of the complex for the equilibrium [Eq.(II-9)] is defined as (Mildvan and Cohn, 1963):

$$K_D = \frac{[M_f]\,[E']}{[M_b]} = \frac{[M_f]\,\left\{n\,x[E_t] - [M_b]\right\}}{[M_b]} \qquad \text{(II-11)}$$

where $[E_t]$ is the total enzyme concentration and the other symbols were defined previously.

This equation can be further rearranged into the following linear form, from which the values of K_D and n may be obtained easily:

$$\frac{\bar{\nu}}{[M_f]} = \frac{n}{K_D} - \frac{\bar{\nu}}{K_D} \qquad \text{(II-12)}$$

where $\bar{\nu} = \frac{[M_b]}{[E_t]}$

A linear plot of $\bar{\nu}$ vs $\bar{\nu}/[M_f]$ is known as a Scatchard plot (Scatchard, 1949). From this plot, the slope of the line gives $-1/K_D$ and the intercept gives n/K_D .

Experimentally, $\bar{\nu}$ and $\bar{\nu}/[M_f]$ for the Scatchard plot are obtained by titrating a fixed amount of enzyme, $[E_t]$, with Mn(II) ion solution. For each metal ion concentration, the concentration of the M_f complex can be measured from the electron spin resonance (ESR) spectrum of the Mn(II) ions (Cohn and Townsend, 1954; Cohn and Leigh, 1962). Then, using Eq.(II-10), $[M_b]$ can be calculated from $[M_t]$ and $[M_f]$. The above procedure for obtaining the values of K_D and n is often referred to as an M-titration (Mildvan and Cohn, 1963; Reuben and Cohn, 1970).

2. Water PRR of the Enzyme-free and the Enzyme-bound Complexes

The NMR measurements in the present study are on the spin-lattice relaxation rate (T_1^{-1}) of the water protons. Hence, the principles of the study are discussed along with the relevant equations for the spin-lattice relaxation time (T_1). The corresponding equations for the spin-spin relaxation time (T_2) will be described and used in the next study [Chapter III]. For simplicity of notation in this chapter, the term "water proton relaxation rate or water PRR" is used to stand for the relevant spin-lattice relaxation rate.

First of all, let us consider the effect on the water PRR due to the enzyme-free Mn(II) complex [i.e. when no binding to the enzyme occurs]. The presence of the complex gives rise to two types of environment [two-site] for the water protons:

(i) the original bulk solvent, and

(ii) the co-ordination sphere of the metal complex.

In NMR terminology, the exchange of a water ligand between these two sites can be generalized in the following form (Gutowsky et al, 1953; Gutowsky and Saika, 1953):

$$ML_{n-1}L^* + L \underset{}{\overset{\tau_m^{-1}}{\rightleftharpoons}} ML_n + L^*$$

or abbreviated as:

$$M \underset{}{\overset{\tau_m^{-1}}{\rightleftharpoons}} L$$

(II-13)

where L and L* are the same chemical species (water), but in different magnetic environments. n is the number of solvent molecules (water molecules) in the first coordination sphere of the metal ion, and M stands for the enzyme-free complex in the present case (or for the enzyme-bound complex in the next case to be considered).

Furthermore, it is noted that the concentration of the Mn(II) complex is very small (10^{-2} - 10^{-3}M is used in most studies). Hence, the experimentally observable quantity is the bulk solvent signal since it is of much higher concentration. Nevertheless, the water molecules are exchanging between the two sites, both of these magnetic properties therefore contribute to the observed water PRR (O'Reilley and Poole, 1963; Luz and Meiboom, 1964). The contribution to the water PRR from the paramagnetic Mn(II) complex can

be isolated from that of the bulk solvent in the following way:

$$T_{1p_f}^{-1} = T_1^{-1} - T_{1,o}^{-1} \qquad \text{(II-14)}$$

where T_1^{-1} is the water PRR measured on the Mn(II) solution and $T_{1,o}^{-1}$ is that measured on a blank solution (pure water).

The contribution is referred to as "water PRR of the M_f complex" or "$T_{1p_f}^{-1}$" from now on. It is related to the nuclear relaxation and the exchange rates and is given by (O'Reilley and Poole, 1963; Luz and Meiboom, 1964):

$$T_{1p_f}^{-1} = \frac{P_m \cdot q}{T_{1m_f} + \tau_{m_f}} \qquad \text{(II-15)}$$

or written as

$$(P_m \cdot T_{1p_f})^{-1} = \frac{q}{T_{1m_f} + \tau_{m_f}}$$

where

$$P_m = \frac{[M_t]}{[H_2O]} = \frac{[M_t]}{55.5}$$

The terms in the above equations are defined as follows:

(i) The quotient, $(P_m \cdot T_{1p_f})^{-1}$, is commonly known as the normalized water PkR. It is the water PkR of the complex per unit metal ion concentration.

(ii) $[M_t]$ is the total Mn(II) ion concentration, as we are discussing the effect when all the Mn(II) ions are in the enzyme-free complex. This point will be further clarified in the subsequent discussion on Eq.(II-17).

(iii) q is the number of water molecules in the first coordination sphere of the metal ion. It is equal to six for the enzyme-free Mn(II) complex.

(iv) T_{1m_f} is the water proton spin-lattice relaxation time, when the water molecule is in the coordination sphere of the metal ion.

(v) Finally, τ_{m_f} is the NMR exchange lifetime with which the water molecule exchanges from the complex to the bulk solvent.

These last two terms, (iv) and (v), are further discussed in the next section.

In analogy to the preceding discussions, if all the Mn(II) ions exist as the enzyme-bound M_b complex, the corresponding water PRR of the complex is:

$$(P_m \cdot T_{1p_b})^{-1} = \frac{q^*}{T_{1m_b} + \tau_{m_b}} \qquad \text{(II-16)}$$

where the terms are similarly defined as those in Eq.(II-15), and the subscript b is used to indicate that the term is for the enzyme-bound complex. q* is the number of water molecules in the first coordination sphere of the complex and is ≤ 6 in the case of the enzyme-bound Mn(II) ion.

In practice, not all the metal ions are bound to the enzyme. Hence, the analysis of the observed water PRR has to take into account the presence of both complexes. The overall PRR is therefore the <u>weighted</u> sum of the individual PRR as given in the two preceding equations (II-16) and (II-17) (Eisinger <u>et al</u>, 1962; Mildvan and Cohn, 1963):

$$T_{1p_{obs}}^{*\,-1} = \frac{[M_f]}{[M_t]} \cdot T_{1p_f}^{-1} + \frac{[M_b]}{[M_t]} \cdot T_{1p_b}^{-1}$$

(II-17)

where $[M_b]$ and $[M_f]$ are, respectively, the concentration of the enzyme-bound and enzyme-free complexes and are related in the equilibrium as given by Eqs.(II-9) to (II-11).

Conventionally, the above equation is expressed in the following forms:

$$\frac{T_{1p_{obs}}^{*\,-1}}{T_{1p_f}^{-1}} = \frac{[M_f]}{[M_t]} + \frac{[M_b]}{[M_t]} \cdot \frac{T_{1p_b}^{-1}}{T_{1p_f}^{-1}}$$

or

$$\varepsilon_{obs}^{*} = \frac{[M_f]}{[M_t]} + \frac{[M_b]}{[M_t]} \cdot \varepsilon_b$$

(II-18)

where the relaxation rate ratio at the left hand side of the equation is known as the observed water enhancement, ε_{obs}^{*}, since such ratio has always been found to be larger than unity in all the enzyme-metal complexes studied (Eisinger et al, 1962; Dwek, 1973).

The relaxation rate ratio at the right hand side of the equation is known as the binary enhancement of the complex, ε_b .

Experimentally, the water PRR of the enzyme-bound complex is therefore calculated using Eq.(II-17) by measuring the related terms in the equation:

(i) The concentrations of the two complexes, which are obtained using the EPR techniques as previously described.

(ii) The overall water PRR, which is measured by the NMR experiments that yield T_1^* and $T_{1,o}^*$:

$$T_{1p_{obs}}^{*\,-1} = T_1^{*\,-1} - T_{1,o}^{*\,-1} \qquad \text{(II-19)}$$

where $T_{1,o}^*$ is the water proton spin-lattice relaxation time of a solution that only contains the enzyme, and T_1^* is the T_1 of a solution that contains the enzyme and Mn(II) ions at a concentration of $[M_t]$.

(iii) Finally, the water PRR of the enzyme-free complex

which is obtained in a similar manner as described with Eq.(II-14) in which the Mn(II) ion concentration is the <u>same</u> as the one used in the preceding measurements - (ii).

3. Temperature and Frequency Dependence of Water PRR

The NMR exchange rates and the nuclear relaxation rates related to the water PRR of the complexes are discussed in this section. Emphasis is on the temperature and frequency (magnetic field strength) effects on these rates, as these dependences form the basis of the present NMR study.

3A. The NMR Exchange Rate

The NMR exchange lifetime in the exchange-system [Eq.(II-13)] can be generalized in the following definition (Gutowsky and Saika, 1953):

$$\tau_m^{-1} = k_m = \frac{\text{Rate of disappearance of a species } m}{\text{Concentration of the same species } m}$$

In the present exchange system, τ_{m_j} (j=f, b) is the exchange lifetime of the water molecule which exchanges from the M_j complex to the bulk solvent. Due to the appearance of the definition, NMR exchange rate, τ_m^{-1} or k_m, is also known as a "pseudo-" first order rate constant [with respect to the species under observation].

The overall temperature variation of the exchange rate can be expressed in terms of the activation parameters from the transition-state theory (Eyring, 1935; Glasstone et al, 1941):

$$\tau_{m_i}^{-1} = \frac{R \cdot T}{N \cdot h} \cdot \exp\left[-\frac{\Delta H_i^{\ddagger}}{R \cdot T} + \frac{\Delta S_i^{\ddagger}}{R}\right] \qquad \text{(II-20)}$$

where subscript m_i (i=f, b) denotes that the exchange rate is of the enzyme-free and the enzyme-bound complexes respectively. R is the gas constant, N is Avogadro's number, h is Planck's constant, and T is the absolute temperature. $\Delta H_i^{\ddagger}$ and $\Delta S_i^{\ddagger}$ are, respectively, the activation enthalpy and entropy for the corresponding exchange from the M_i complex to the bulk solvent.

As seen from the definition, the exchange rate is not a function of frequency [magnetic field strength]. However, in some cases, the exchange rate may depend on other factors such as the concentration, the pH, and the ionic strength of an exchange system, and hence it is very useful to the studies of complex solution kinetics (e.g. Dodgen et al, 1973; Fuhr and Rabenstein, 1973). These variables are not used in the present study and are

not discussed in detail in the thesis.

3B. The Nuclear Relaxation Rate at the Mn(II) Ion Complexes

The T_{1m_f} and T_{1m_b} relaxation times of the water protons in the enzyme-free and the enzyme-bound complexes are now considered. As mentioned previously, only the equations for the spin-lattice relaxation times are used in the present discussion.

When a water molecule is in the coordination sphere of the Mn(II) ion, the nuclear relaxation of the water protons is induced by the dipolar and the scalar interactions between the nuclear spin and the unpaired electrons of the Mn(II) ion (Solomon, 1955; Solomon and Bloembergen, 1956; Bloembergen, 1957). In the high frequency range used in most studies (100.0MHz to 4MHz for ^1H), the contribution of the scalar interaction to the spin-lattice relaxation is very small and is negligible with respect to the dipolar interaction (King and Davidson,

1958; Bernheim *et al*, 1959; Pfeifer, 1962; Peacocke *et al*, 1969; Reuben and Cohn, 1970). At very low frequencies ($\leq$ 1MHz), however, the scalar contribution will also become significant to the T_1 relaxation (Codrington and Bloembergen, 1958). Furthermore, discrepancies for the scalar interaction from the Solomon-Bloembergen equation have been found at high temperatures (95°C) and at low frequencies ($\leq$ 1MHz) (Pfeifer *et al*, 1966; Collingwood and White, 1969). Nevertheless, in the present study, the frequency used is between 6MHz and 100.0MHz and the temperature was between 4°C and 38°C. Therefore, the spin-lattice relaxation is controlled mainly by the dipolar interaction. The Solomon-Bloembergen equation for the spin-lattice relaxation time is (Reuben *et al*, 1970; Rubinstein *et al*, 1971):

$$T_{1M_i}^{-1} = \frac{C_D}{R_i^6}\left[\frac{3\,\tau_{c1}}{1+\omega_I^2\tau_{c1}^2} + \frac{7\,\tau_{c2}}{1+\omega_s^2\tau_{c2}^2}\right]_i$$

$$= \frac{C_D}{R_i^6} \cdot F_i \qquad (i=f,b) \qquad \text{(II-21)}$$

The symbols in the above equation are described as follows.

(i) For both complexes,

$$C_D = \frac{2}{15} S(S+1) \gamma_I^2 g^2 \beta^2$$

where S is the resultant electron spin angular moment and is 5/2 for the Mn(II) ions, γ_I is the nuclear magnetogyric ratio of the proton, g is the "isotropic" g factor, and β is the Bohr magneton.

(ii) R_i (i=f,b) is the distance between the nucleus and the paramagnetic ion in the enzyme-free and in the enzyme-bound complexes respectively.

(iii) ω_I and ω_S are the nuclear and electronic Larmor precession frequencies.

(iv) τ_{c1} τ_{c2} are the dipolar correlation times which are characteristic lifetimes for the dipolar coupling between the nuclear and electron spins. These times affect the resultant form of F_i for different complexes, the details are described in the next section.

3C. The Correlation Times

The dipolar interactions are commonly induced by three types of processes: the NMR exchange, the rotational motion of the metal complex, and the electronic relaxation of the unpaired electrons in the complex. Hence, the dipolar correlation times consist of all the individual correlation times of the relevant processes. The equations are

$$\tau_{c1}^{-1} = \tau_m^{-1} + \tau_R^{-1} + \tau_{1S}^{-1}$$

$$\tau_{c2}^{-1} = \tau_m^{-1} + \tau_R^{-1} + \tau_{2S}^{-1}$$

(II-22)

In the above equations, τ_m is the exchange lifetime as previously described [Section 3A]. τ_R is the rotational time of the complex and is due to the reorientational motion between the nuclear spin and the unpaired electrons. The rotational correlation time is affected by temperature but not by frequency. The temperature dependence is

$$\tau_{Ri} = \tau_{Ri}^{\circ} \exp \left(E_{Ri} / RT \right)$$

$$(i=f,b)$$

(II-23)

where subscript i is used to denote that different com-

plexes may have different rotational correlation times and temperature dependence. τ_R^o is the standard (or reference) state of the rotation time and E_R is the corresponding activation energy of the rotation motion.

Finally, the τ_{1S} and τ_{2S} in Eq.(II-22) are the spin-lattice and the spin-spin relaxation times of the unpaired electrons. In contrast to the two previous correlation times, the electronic relaxation times are functions of temperature and frequency, the details are further described in the last paragraph.

In different Mn(II) ion complexes, the interactions between the nuclear spin and the electron spin may vary. Consequently, the magnitudes of those correlation times are not always the same and hence the resultant effect on the nuclear relaxation rates are different. Two common cases are described as follows.

(a) In the case of small Mn(II) ion complexes, such as the hexa-aquo complex which can rotate freely and rapidly in water, Bloembergen and Morgan (1961) have shown that the rotational time of the complex is so short that it dominates the dipolar correlation time and also makes the

product $(\omega_I \tau_{c1})^2 << 1$. Therefore, the F_f term in the T_{1M_f} equation [Eq.(II-21)] becomes

$$F_f = \tau_{R_f} \cdot \left(3 + \frac{7}{1 + \omega_S^2 \tau_{R_f}^2} \right) \qquad \text{(II-24)}$$

where the subscript f is to denote that the expression is for the enzyme-free or the hexa-aquo Mn(II) ion complexes.

(b) In the case of macromolecule-Mn(II) ion complexes, as the metal ions are bound, the rotational rate may decrease. Hence, the rotational time is no longer dominant and in some cases, the electronic relaxation time may also contribute to the nuclear relaxation (Peacocke et al, 1969; Reuben and Cohn, 1970). Nevertheless, in the nuclear relaxation for such complexes, the term that contains the spin-lattice relaxation time often dominates and hence the distinction between the spin-lattice and the spin-spin relaxation times for the electrons is not necessary as far as the nuclear relaxation is concerned (Koenig et al, 1971; Koenig et al, 1972). In fact, when the modulation process of the electronic relaxation is fast, i.e. $(\omega_S \tau_V)^2 < 1$ [where τ_V is the relevant correlation time of the modulation] the two electronic relaxation times have been shown to be equal (Rubinstein et al, 1971). In addition, even when $(\omega_S \tau_V)^2 \geq 1$, Rubinstein et al (1971) have shown that the electronic relaxation times may be approximated by the

single electronic relaxation time τ_{1S} as derived by Bloembergen and Morgan (1961). Hence, those two dipolar correlation times [Eq.(II-22)] may be approximated with the τ_{1S} and this has been applied satisfactorily in many Mn(II)-enzyme studies (Dwek et al, 1974). The approximation is

$$\tau_c^{-1} = \tau_{c1}^{-1} = \tau_{c2}^{-1} = \tau_{m_b}^{-1} + \tau_{R_b}^{-1} + \tau_{1S}^{-1} \qquad \text{(II-25)}$$

where subscript b is to denote that the correlation times are of the enzyme-bound Mn(II) ion complexes. Consequently, the F_b term in the T_{1M_b} equation [Eq.(II-21)] becomes

$$F_b = \left[\frac{3\,\tau_c}{1 + \omega_I^2\,\tau_c^2} + \frac{7\,\tau_c}{1 + \omega_S^2\,\tau_c^2} \right] \qquad \text{(II-26)}$$

In order to sort out the possible contribution of the electronic relaxation time, the frequency and temperature dependence of τ_{1S} is now considered. Various theoretical studies have shown that it is a function of temperature, frequency and the zero-field splitting of the metal ion complex (Bloembergen and Morgan, 1961; Atkins and

Kivelson, 1966; Mclachlan, 1964; Burlamacchi, 1970).

In the case of Mn(II)-ion complexes, the main relaxation mechanism arises from the modulation of the zero field splitting (Reed et al, 1971; Rubenstein et al, 1971). The equation is given as (Bloembergen and Morgan, 1961):

$$\tau_{1S}^{-1} = B \left[\frac{\tau_v}{1 + \omega_S^2 \tau_v^2} + \frac{4\,\tau_v}{1 + 4\,\omega_S^2 \tau_v^2} \right] \qquad \text{(II-27)}$$

where

$$B = \frac{2}{50} \Delta^2 \left\{ 4 \quad S (S + 1) - 3 \right\}$$

Δ is the zero-field splitting, and τ_v is the correlation time of the relevant physical relaxation process.

This correlation time is also dependent upon the temperature as:

$$\tau_v = \tau_v^{\,o} \exp \left[E_v / RT \right] \qquad \text{(II-28)}$$

where $\tau_v^{\,o}$ is the standard state for the correlation time and E_v is the activation energy of the modulation process.

C. EXPERIMENTAL SECTION

1. Materials

Phosphorylated SCS from E.Coli. (Crooke's strain) was supplied by Dr. W.A. Bridger, Department of Biochemistry, University of Alberta. After the standard purification procedure (Leitzman et al, 1970; Moffet and Bridger, 1973), the enzyme extract was stored as a precipitate in a 75% saturated ammonium sulfate solution at 4°C.

Further steps were taken to prepare the enzyme samples for the present studies. First of all, the precipitate was dissolved in a tris-buffer at a pH of 7.2. The buffer was made up with 0.1M potassium chloride and 10^{-4}M EDTA, the latter is used to eliminate heavy metal ion impurities that may de-activate the enzyme (Ramaley et al, 1967; Grinnell et al, 1969). The buffered enzyme solution was then introduced into a column packed with (1.0x3.0 cm) Sephadex G-25 (fine) resin at the bottom, and the (1.0x4.0 cm) AG-1 anion exchange resin at the top to eliminate the EDTA and any EDTA-metal ion complexes. Before use, the column had been equilibrated with EDTA-free tris-buffer. The pH of all solutions was 7.2. The effluent enzyme solution was concentrated with a DIA-flow cell.

All of the above processes were carried out at 4°C and the purified enzyme solutions were also kept at 4°C between measurements to prevent denaturation. Preliminary studies showed that a 20 to 30% drop in activity may occur over a period of twenty days, when the enzyme is in the EDTA-free tris-buffer solution.

All glassware was cleaned with concentrated nitric acid, then washed and rinsed thoroughly with triply distilled water.

The tris-HCl-buffer was obtained from Schwarz-Mann Co., potassium chloride from J.T.Baker Chem.Co., and manganese (II) chloride from Fisher Scientific Co. The Sephadex was purchased from Pharmacia Fine Chemicals, Sweden and AG-1 resin from Bio-Rad Lab., California, U.S.A.. The purity of these reagents was found to be satisfactory from previous kinetic experiments carried out in Dr. Bridger's Laboratory.

The molar concentration and specific activity of each sample were measured spectroscopically (methods to be described in the following section). NMR and EPR experiments were immediately carried out and completed within one week after the samples were prepared. The specific activity was then rechecked and some of the NMR and EPR

measurements were repeated. The results were reproducible. Samples which experienced a large change in activity (> 25%) were discarded.

2. Enzyme Assays and Buffer

Molar concentration of the enzyme was determined by U.V. absorption at 280nm. The extinction coefficient, $E_{1cm}^{1\%}$, is 4.9±0.2 (Krebs and Bridger, 1974). The enzyme activity was measured spectroscopically at 25°C on an assay mixture, which was prepared with 0.1 to 1.5 micromoles of enzyme, 10 micromoles of disodium succinate, 0.1 micromoles of CoA, 0.4 micromoles of ATP (in tris-buffer pH 7.2), 10 micromoles of magnesium chloride and 50 moles of Tris-buffer (pH 7.2). The total volume was one ml.

The specific activity is expressed in units per mg of enzyme where one unit is the quantity of succinyl-CoA (in micromoles) generated per minute at 25°C, calculated using the molar extinction coefficient of 4.5×10^3 (Stadtman et al, 1957; Ramaley et al, 1967) for the succinyl-CoA at

230nm. All samples used in the following ESR and NMR measurements were prepared in tris-buffer. The buffer was made up with 0.1MKCl, 0.05M tris (hydroxyl methyl) amino methane and at a pH of 7.2.

3. Sample Preparation and ESR Measurements

For the ESR experiments, the samples were prepared in such a way that they all had the same enzyme concentration of 0.074mM, but different Mn(II) ion concentrations ranging from 0.08mM to 1.0mM. Similarly, a series of reference samples with the same range of Mn(II) ion concentrations but no enzyme were prepared. All samples were carefully sealed into small capillary tubes (1mm I.D.) and had the same volume of 30micro-litre.

The ESR spectrum of the reference and the enzyme samples with the same total Mn(II) ion concentrations were obtained under controlled instrumental settings and for the same number of scans (ranging from three to six, depending on the metal ion concentration). The experimental uncertainty in these measurements was ±5%. The intensities

of the spectrum were then measured by adding the six peak to peak heights of the ESR signals. The free Mn(II) ion concentrations in the enzyme samples were calculated from the relative signal intensities with respect to the blank reference signals (Cohn and Townsend, 1954). Prior to all of these measurements, the spectrometer was calibrated using reference samples (0.01mM to 2mM). The intensities are linear to the concentrations.

The measurements were carried out on a Varian X-4502 EPR spectrometer (9.2 GHz). For very dilute Mn(II) ion (<0.25mM), the EPR signals were accumulated using a Varian C-1024 signal averager to improve the accuracy of the measurements. The temperature was controlled using the Varian V-4557 temperature control unit and was measured with a copper-constantan thermocouple.

4. Sample Preparation and NMR Measurements

There are two types of NMR experiments in the study:

(i) The first type of measurements was carried out at fixed frequency (100.0MHz) and temperature (25°C). Samples were prepared in such a way that they all had the same Mn(II) ion concentration (0.050mM) but different amounts of enzyme (0.09mM to 0.017mM). A reference sample with the same amount of Mn(II) ions in tris-buffer was prepared. These samples were used for the enhancement experiments.

(ii) The second type of measurements was carried out at variable frequency and temperature. With the knowledge of the dissociation constant from the previous ESR results (section 3) the samples were prepared in such a way that the ratio of the enzyme-bound Mn(II) ions to the enzyme-free Mn(II) ions was maximized. The concentration of the Mn(II) ions and the enzyme used were, respectively, 0.14mM and 0.078mM. A reference sample containing only 0.14mM Mn(II) ion in tris-buffer was also prepared. All samples for this type of experiment were prepared in the same conditions, and small aliquots were taken for

each temperature measurement. All samples were carefully sealed in (5mmx4cm) NMR tubes, and each had a volume of 75micro-litre.

Water proton spin-lattice relaxation times (T_1) were measured as a function of temperature over the range for which the enzyme is stable (4° to 38°C). Spin-lattice relaxation times over the frequency range of 6.0 MHz to 60.0 MHz were measured with a Bruker SXP NMR Spectrometer. The 100.0 MHz experiments were carried out using a Varian HA-100-15 NMR Spectrometer interfaced with the Digilab pulse unit (FTS/NMR-400-1).

The relaxation times (T_1) were measured using the Carr-Purcell 180°- τ -90° pulse sequence (Carr and Purcell, 1954). A schematic diagram is shown in Fig. II-2 and the principle is briefly described as follows. In the rotating-frame co-ordinates (x',y',z') (Fig. II-2), the net magnetization moment of the nuclei may be represented by a vector M which is aligned with the field H_0 at thermal equilibrium (Bloch, 1946). At time "0", a selective radio-frequency pulse (with intensity H_1 and at the resonance frequency of the nucleus) is applied so that the magnetization vector rotates an angle 180° along the z' axis (Fig.II-2A). Then, after a time " τ ", a 90° pulse is applied (Fig.II-2B).

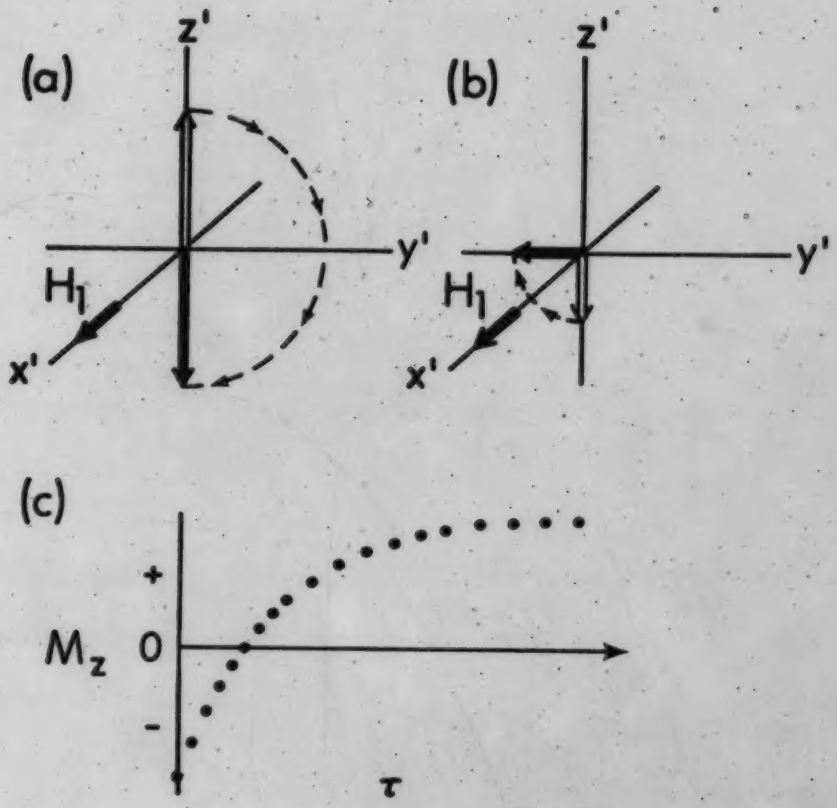

FIGURE II-2. Determination of T_1 using the 180°, τ, 90° pulse sequence. (a) M is inverted by a 180° pulse at time 0 (b) after a time τ, a 90° pulse rotates M to the y' axis for observation. (c) The observed signal intensity M_z is plotted as a function of τ.

The magnetization, M_z , is then measured experimentally as the signal intensity. A typical plot of M_z vs τ is shown in Fig.II-2C. Some representative spectra obtained from the pulse experiments on water protons are shown in Fig.II-3. The intensities correlate with the time interval τ according to the following equation:

$$M_z = M_\infty \left[1 - 2\exp(-\tau/T_1) \right] \qquad \text{(II-29)}$$

where M_∞ is the thermal equilibrium magnetization of the nuclei, measured from the signal intensity at large τ values ($> 5T_1$).

From the above Eq.(II-29), the value of T_1 was calculated using the linear least-squares technique [Appendix A] on at least twenty data pairs ($M_{z(\tau)}$, τ). Four series of data pairs were measured for each sample, giving T_1 values with a standard deviation of 4 to 2%. A computer program was written to handle the large volume of data and the listing is given in Appendix A. The program also includes another useful technique for the analysis of the data (Guggenheim, 1926). This technique is useful when values of M_∞ are not available or not easily accessible, e.g. when the nucleus has very long relaxation time T_1.

Nevertheless, the present data can all be calculated using the common technique with Eq.(II-29).

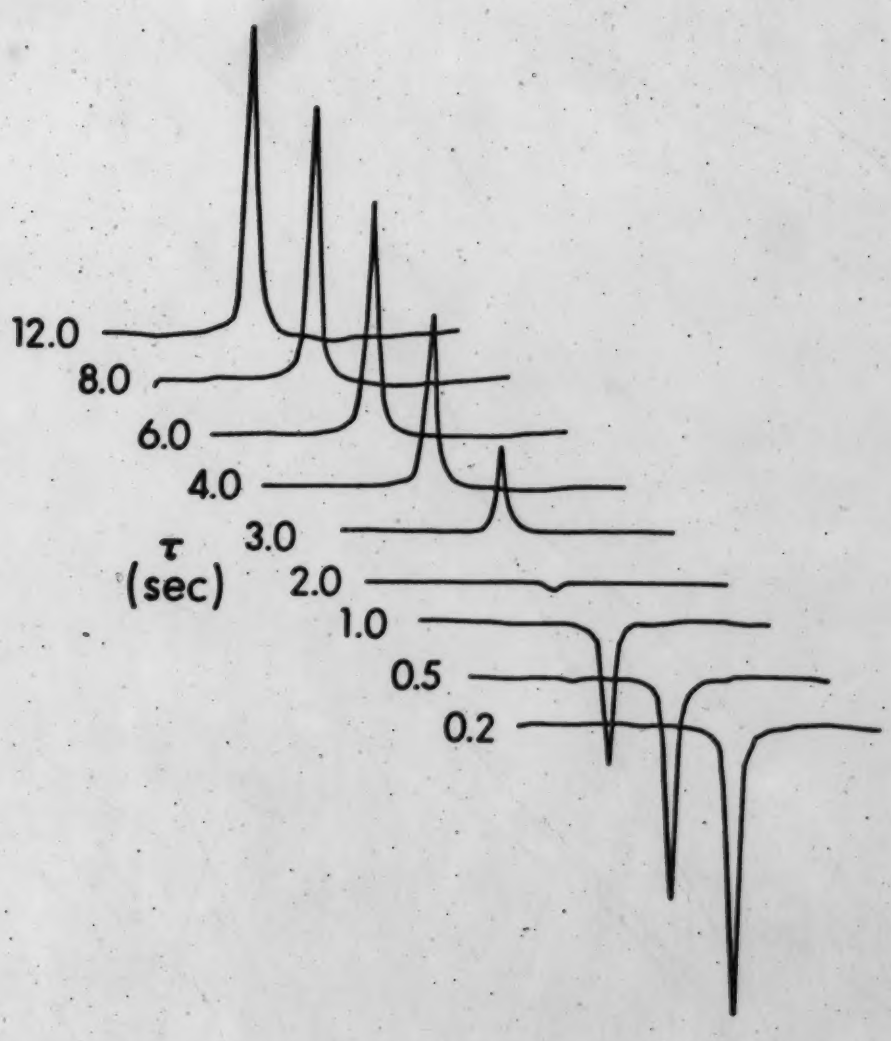

FIGURE II-3. Water proton signals plotted as a function of τ, in a 180°, τ, 90° pulse experiment to determine the spin-lattice relaxation time. The experiment was carried out at 100.0MHz and 27°C on a non-degassed tris-buffer solution (0.1M KCl, 0.05M tris-buffer). The T_1 was found to be 2.73sec.

D. RESULTS AND DISCUSSION

1. Binding of Mn(II) Ions with phospho-SCS

In order to show the presence of a binary EM complex between the Mn(II) ions and phospho-SCS, two types of experiments with NMR and ESR techniques were carried out. First of all, NMR measurements at a fixed frequency and temperature were performed using the samples and the procedures as described in the experimental section (C-4). The experimental data are listed in Table II-1. The results are reported in terms of the observed water enhancement as defined in Eq.(II-18). They are plotted in Fig. II-4 as a function of the total enzyme concentration. From the figure, it is seen that the enhancements are all different from unity.

Secondly, ESR measurements were used to detect any changes in the free-Mn(II) ion concentration in the presence of the enzyme. A typical ESR spectrum of a Mn(II)-phospho-SCS solution, together with that of a blank Mn(II) ion solution (reference), are shown in Fig. II-5. Only a significant decrease in the ESR spectrum intensity was observed on the addition of the enzyme. Hence, both results from NMR and ESR indicate that some Mn(II) ions are likely bound to the enzyme. The decrease indicates that

some of the original Mn(II) ions were bound to the enzyme. In such state, the ESR signal from the unpaired electrons of the metal ions may experience significant homogeneous or/and inhomogeneous line broadening effects (Reed and Cohn, 1970; Reed et al, 1971). Subsequent results based on NMR measurements (Tabble II-4) indicate that the spin-lattice electronic relaxation time, τ_{1S}, for both the enzyme-bound and the enzyme-free Mn(II) ion complexes are of similar magnitude. For example, at 27 °C and 9.2GHz (X band), the values of τ_{1S}, calculated using Eq.(II-27), are 1.6×10^{-8}sec and 2.1×10^{-8}sec, respectively, for the enzyme-bound and enzyme-free complexes. Therefore, the absence of the ESR signal for the enzyme-bound Mn(II) ion is likely due to the extreme shortening of the electronic spin-spin relaxation time in the enzyme-bound complex.

TABLE II-1 Data of the Water Proton Relaxation Enhancements at 100.0 MHz.‡

Solutions*	Spin-Lattice Relaxation Times
A. Buffer	3.51±0.03 sec
Buffer + $MnCl_2$(0.05mM)	1.423±0.002 sec
B. Enzyme$^{\xi}$	3.49±0.02 sec
Enzyme + $MnCl_2$(0.05mM)	
$[E_t]$ (mM)	T_1^* (sec)
0.0152	1.19
0.0229	1.15
0.0305	1.10
0.0412	1.04
0.0457	0.960
0.0617	0.900
0.0686	0.840
0.0823	0.819
0.0914	0.766

‡ The experiments were carried out at 100.0 MHz at 25°C in Fourier Transformed mode.

* All solutions were in 0.05M tris-buffer, 0.1M KCl and at a pH of 7.2.

ξ The values of T_1 are independent of the enzyme concentration studied.

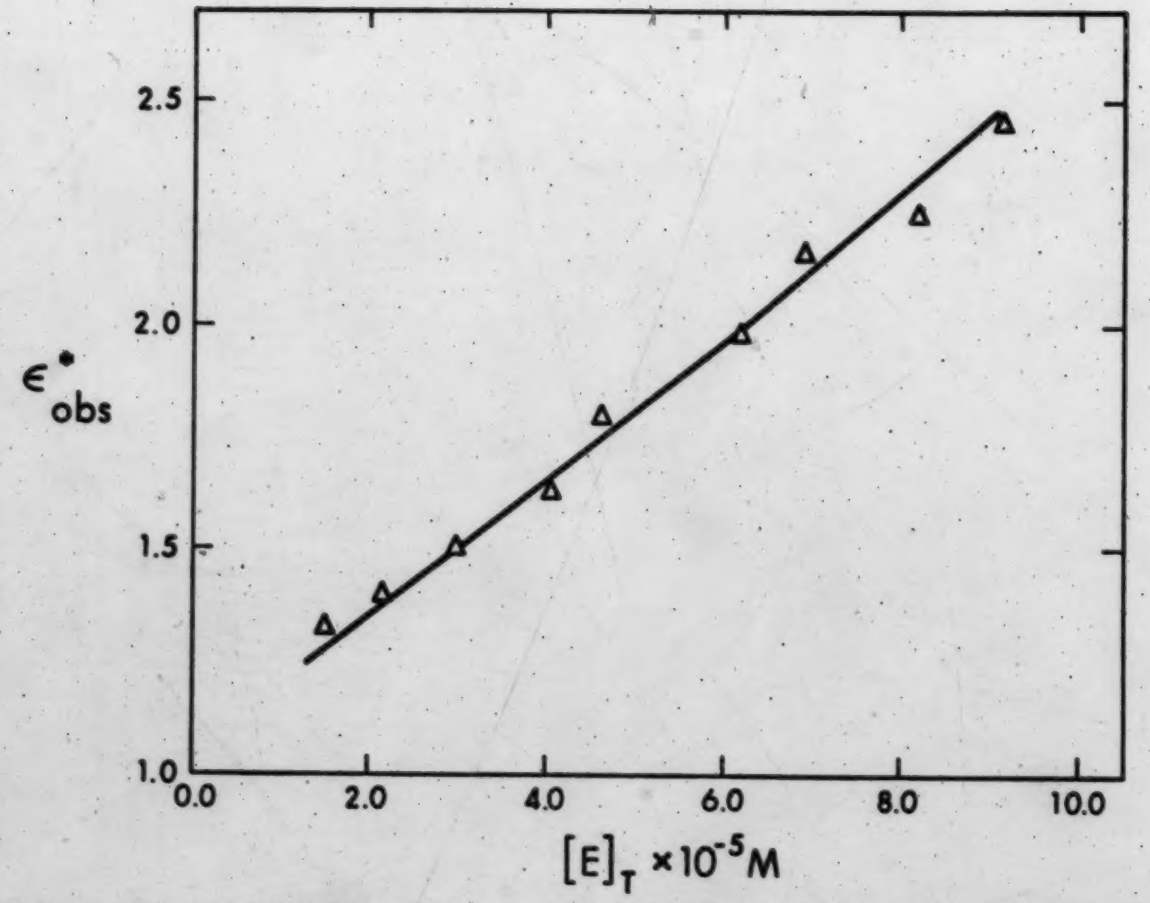

FIGURE II-4. Water proton relaxation enhancement as a function of the enzyme concentration . Experiments were carried out at 100 MHz at 25°C in tris-buffer (0.05M), 0.1MKCl and 0.050mM Mn(II) ions.

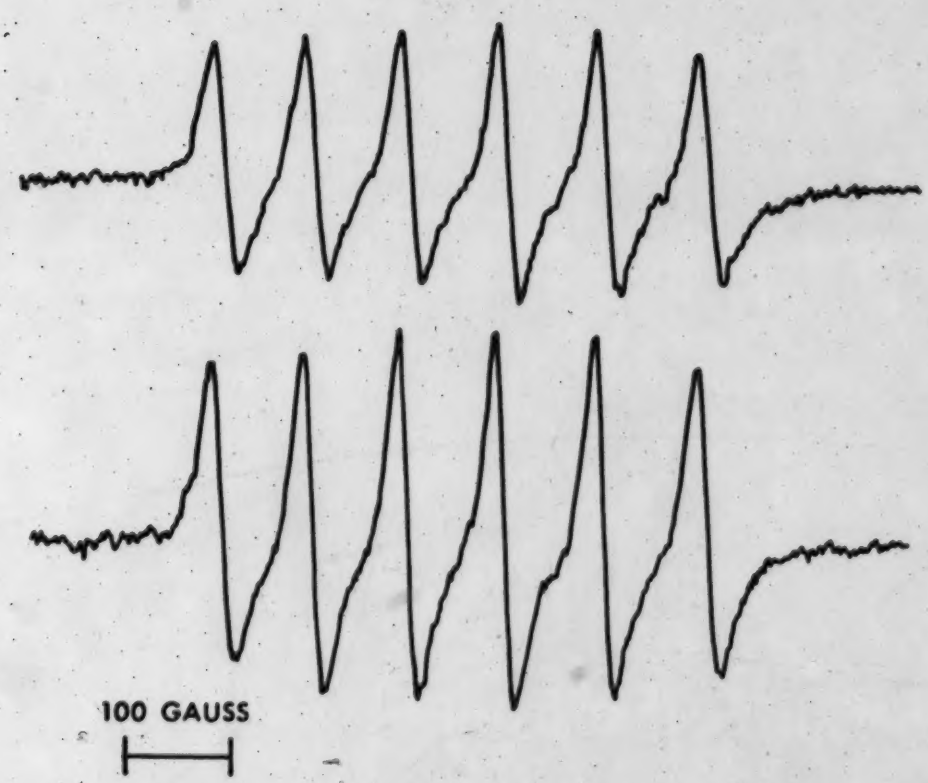

FIGURE II-5. X-band EPR spectra of aqueous Mn(II) ions at 25°C in tris-buffer (pH7.2; 0.1MKCl). The bottom spectrum contains only 0.34 mM Mn(II) ion. The top spectrum contains the same amount of Mn(II) ion and an additional 0.074 mM of the enzyme.

In order to describe the stoichiometry of the enzyme-Mn(II) complex quantitatively, the dissociation constant, K_D, and the number of metal ion binding sites, n, were further determined by the the M-titration procedure using the ESR techniques as described in the experimental section(C-2). The experimental results are tabulated in Table II-2. These data were analysed with the Scatchard plot as described in the theory section(B-1). Using Eq.(II-12), the data are plotted in Fig. II-6.

From a least-squares analysis to these data, the dissociation constant is $4.1\pm0.4\times10^{-4}$M at 25°C and a mole of phospho-SCS contains 3.7±0.5 moles of metal binding sites (Table II-3). Similar values (7.1×10^{-4}M and 3.4) were also obtained by Battlaire and Cohn (1971, private communication).

TABLE II-2 The ESR M-titration Data‡.

$[M_t]^{\xi}$	ESR Spectral Intensities**		$[M_f]^{\Xi}$
	Reference Sample	Enzyme Sample	
(mM)	(cm)	(cm)	(mM)
0.063	48.4	29.8	0.039
0.084	74.2	46.5	0.053
0.126	82.8	55.0	0.0837
0.251	96.6	64.8	0.168
0.336	95.4	67.2	0.237
0.503	99.3	73.0	0.370
0.670	106.3	82.0	0.517
1.010	127.8	105.9	0.837

‡ Experiments were carried out at 25°C and 9.1KGauss. All samples were prepared in 0.05M tris-HCl buffer (pH7.2) and 0.1M KCl. $[E_t]$ = 0.074mM.

ξ The recorder gain for samples with different $[M_t]$ was readjusted in order to maximize the output signal amplitude. However, for samples with a given value of $[M_t]$, all conditions were kept constant.

** The intensities were obtained by adding the six peak to peak heights of the ESR spectrum (Section C-3). The experimental errors are ±5%.

Ξ The free Mn(II) ion concentrations were calculated from the relative spectral intensities of the enzyme and the reference samples.

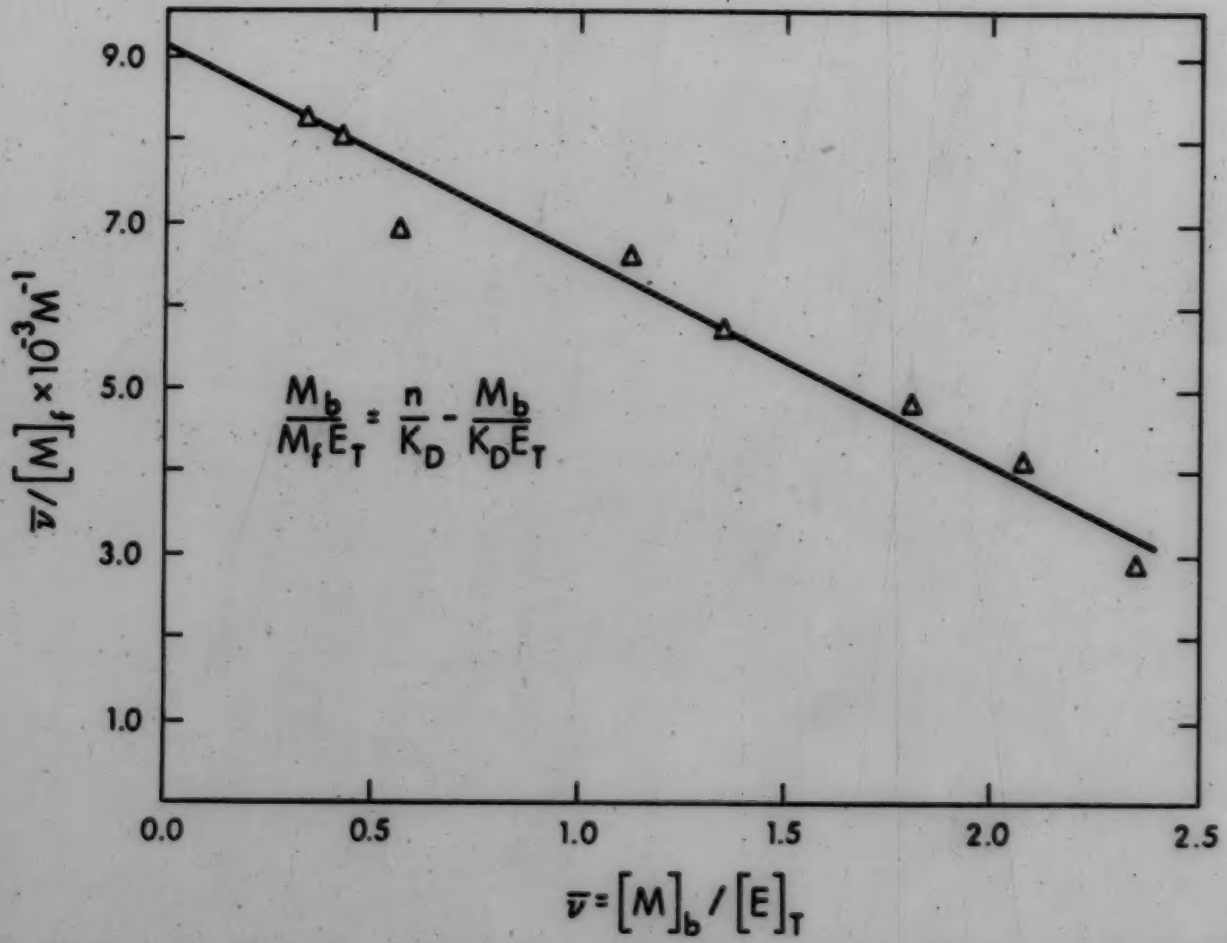

FIGURE II-6. The Scatchard plot for the enzyme solution titrated with Mn(II) ions in a 0.05M tris-HCl buffer (pH7.2) and 0.1MKCl at 25°C. The enzyme concentration (M.W. 140,000) is 0.074 mM.

TABLE II-3 A Least-squares Analysis on the M-Titration Data.‡

$\bar{\nu} = [M]_b / [E]_T$	$\bar{\nu}/[M]_f \times 10^{-3} M^{-1}$	
	(observed)	(calculated) *
0.33	8.5	8.26
0.43	8.1	8.02
0.576	6.88	7.65
1.13	6.73	6.29
1.35	5.70	5.75
1.81	4.89	4.62
2.08	4.20	3.95
2.35	2.81	3.29

Slope ($-1/K_D$) = $-2.46 \pm 0.22 \times 10^3$

Intercept (n/K_D) = $9.07 \pm 0.32 \times 10^3$

‡ The experimental data are listed in Table II-2. They were analysed using Eq.(II-12) with the least-squares technique (the computer program is given in Appendix A: subroutine LSQSM).

* The prediced values are calculated from the best fit slope and intercept of Eq.(II-12) to the data.

The M-titration results indicate that there are nearly two Mn(II) ions per $\alpha\beta$ subunits of the enzyme. However, the exact distribution of these metal binding sites cannot be assigned at the present study (such as one metal ion per subunit), since the native enzyme consists of two different subunit pairs ($\alpha_2\beta_2$). Since the standard deviation of the dissociation constant (the slope) is about ±10% (Table II-3), the linearity of the plot indicates that Mn(II) ion binding sites are very similar, otherwise, a change in the slope or non-linearity in the plot should be detected. Slight difference among these metal binding sites may still exist, nevertheless, the subsequent NMR treatment assumes that these sites have similar magnetic environment within experimental error (about 20%).

The binding between the Mn(II) ions and the enzyme is not very strong. The value of 4.1×10^{-4}M for K_D is not very small compared to most values of K_D in Mn(II)-enzyme complexes obtained under similar conditions (pH 7.0, 0.1M KCl). For example, the K_D for the Mn(II)-pyruvate kinase complex is 6.5×10^{-5}M (25°C) (Mildvan and Cohn, 1965), and the K_D for Mn(II)-glutamine synthetase is 4×10^{-6}M (24°C) (Villafranca and Wedler, 1974). This comparatively weak affinity between Mn(II) ions and phospho-SCS made the present experiments a little more

difficult, since the enzyme-bound complex does not exist in large quantities.

In addition, the solubility of the enzyme is not large and hence the most concentrated enzyme solution available was about 22mg per ml. As a comparison, in the Mn(II)-pyruvate kinase studies, the kinase concentration used in the EPR experiments was around 250mg/ml (M.W. of pyruvate kinase being 237,000) (Reed and Cohn, 1973). Nevertheless, both results from NMR and EPR indicate that the phospho-enzyme does bind with Mn(II) ions.

2. Frequency and Temperature Dependence of Water PRR

2A. Water PRR of Mn(II) Solutions in the Absence of the Enzyme

The water PRR of the hexa-aquo M_f complex in tris-buffer was studied as a function of temperature (4° to 38°C) and at various frequencies (6.0, 12.0, 25.0, 40.3 and 60.0 MHz), using the procedures and samples as described in Section C-4. The values of T_{1p_f} were calculated using Eq.(II-14). The normalized water PRR, $(P_M T_{1p_f})^{-1}$, of this enzyme-free complex are shown in Fig. II-7. Comparable magnitude such as the $(P_M T_{1p_f})^{-1}$ of $4.7 \times 10^5 sec^{-1}$ at 24.3MHz and 25°C was reported in a recent review (Mildvan and Engle, 1972).

Similar behavior on aqueous Mn(II) ion solutions has been studied (Bloembergen and Morgan, 1961; Reuben and Cohn, 1970). Nevertheless, the values obtained in the present controlled experiments were useful in the subsequent study, since samples both with and without the enzyme were added with the same amount of the stock Mn(II) ion solutions and the T_1 of these samples were measured successively under the same experimental conditions (Section C-4).

In Fig. II-7, the water PRR at a given temperature are seen to decrease monotonically as the frequency increases. At a constant frequency, the water PRR all decrease with an increase in temperature. Since the exchange rate, τ_{m_f} , is independent of frequency and increases with an increase in temperature [Eq.(II-20)], therefore, the T_{1M_f} term of the M_f complex must dominate the observed water PRR [Eq.(II-15)].

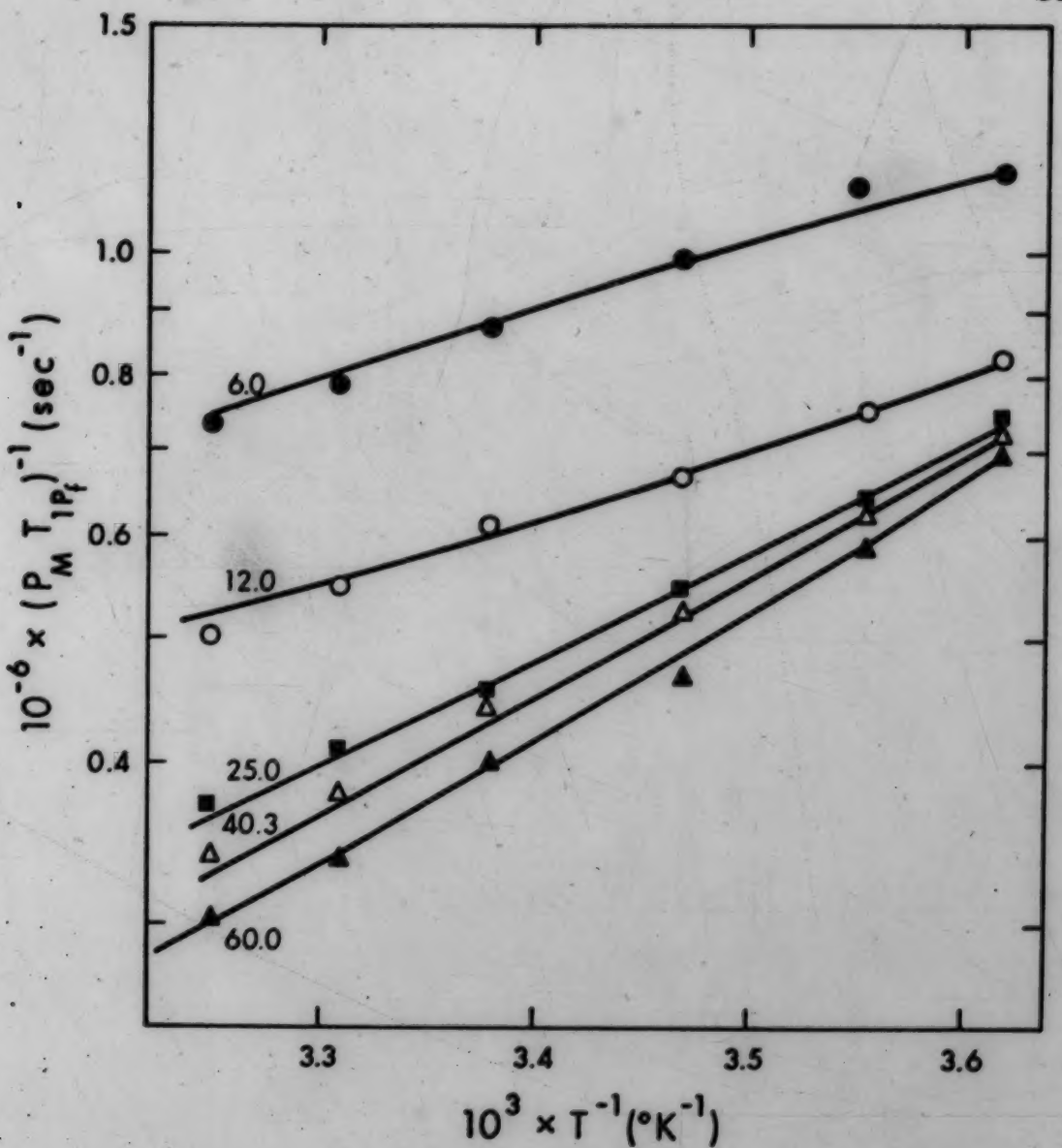

FIGURE II-7. Frequency and temperature dependence of the normalized water proton $T_{1P_f}^{-1}$ induced by the enzyme-free $Mn(II).(H_2O)_6^{+2}$ complex in tris-buffer. P_M = $[Mn^{+2}]/[H_2O] = [Mn^{+2}]/[55.5]$. The solution (pH7.2) consisted of 0.1M KCl; 0.05M tris-buffer; and 0.14mM Mn(II) ion. Solid curves are the computer fit to the data.

Using the relevant equations (II-15, 21 and 24) for the enzyme-free Mn(II) ions, the data were fitted as a function of temperature and frequency by varying $\tau_{R_f}^{o}$ and E_{R_f} in Eq.(II-23). From the least-squares analysis to the data, the best fit curves are shown in Fig. II-7 and the best fit parameters are:

(i) 4.8 Kcal/mole for E_{R_f} ,

(ii) 1.0×10^{-14} sec for $\tau_{R_f}^{o}$.

These values are similar to those observed by other researchers:

a) Bloembergen and Morgan (1961)

4.5Kcal/mole ; 1.6×10^{-14}sec.

b) Pfeifer (1962)

4.3Kcal/mole ; 2.1×10^{-14}sec.

In summary, in the absence of the enzyme, the water protons are relaxed through the dipolar mechanism which arises mainly from the tumbling motion of the complex.

2B. Water PRR of the Mn(II)-enzyme Solutions

In the presence of the enzyme, the normalized water PRR behaved quite differently (Fig. II-8). First of all, at a given temperature, these values do not vary monotonically with frequency. Secondly, at a given frequency, the sharp increase of the PRR with an increase in 1/T observed in Fig. II-7 does not exist. Instead, at the highest frequency (60.0MHz), a slight decrease of the PRR with an increase in 1/T is observed.

If only the 60.0MHz data were considered, a possible interpretation of the data would be that the rates were controlled by the NMR exchange process [Eq.(II-20)]. However, the water PRR are a function of the frequency (Fig. II-6), and some of the data shows a slight increase with (an increase in) 1/T . Therefore, the exchange term alone is not sufficient to interpret the data and the T_{1m_b} term is also important for the analysis [Eq.(II-16)].

FIGURE II-8. Frequency and temperature dependence of the normalized water proton $T_1p_b^{-1}$ induced by the enzyme-bound Mn(II).$(H_2O)_4^{+2}$ complex in tris-buffer. P_M = $[Mn^{+2}]/[55.5]$. The solution (pH7.2) consisted of 0.1M KCl, 0.05M tris-buffer, 0.14mM Mn(II) ion and 0.078mM phospho-SCS. Solid curves are computer fit to the data.

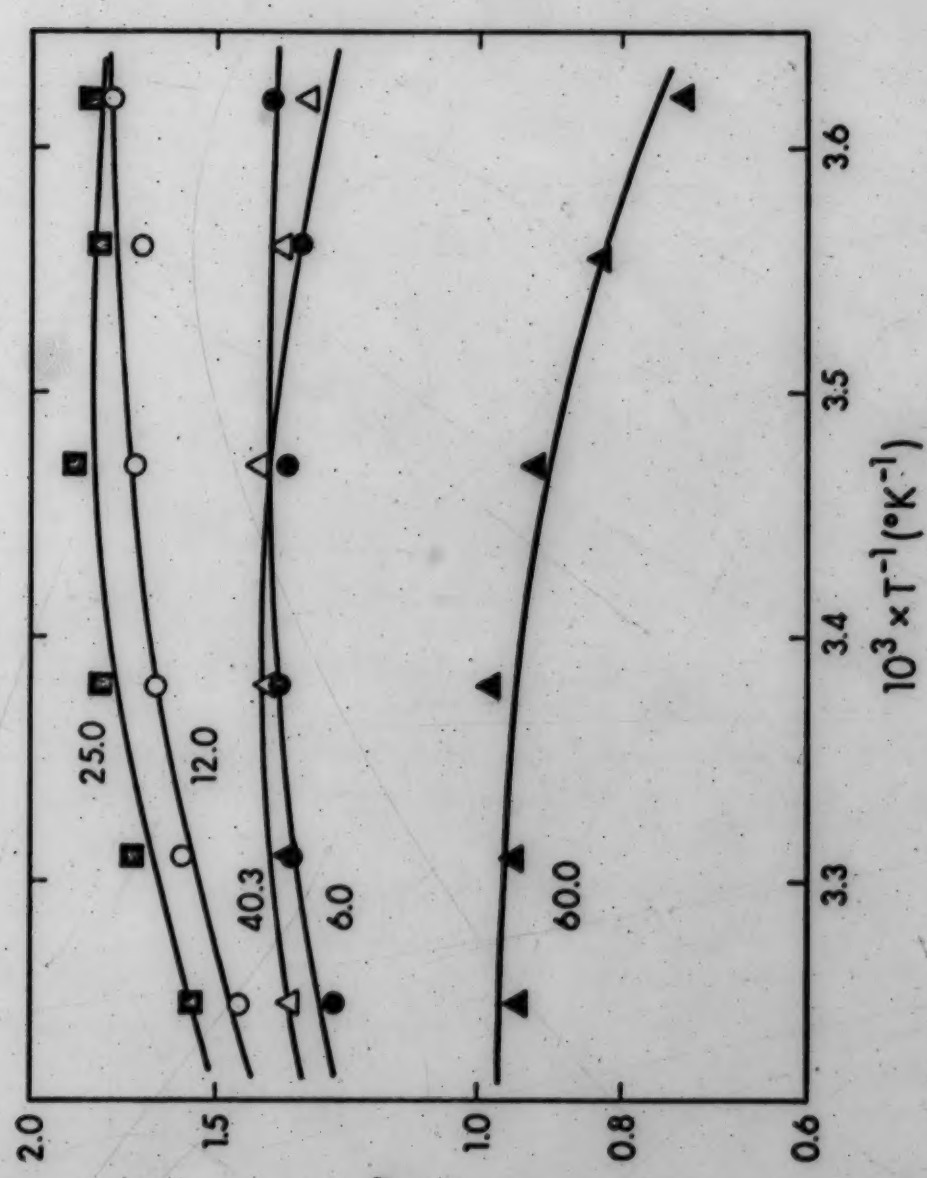
25.0
12.0
40.3
6.0
60.0
2.0
1.5
1.0
0.8
0.6
3.3
3.4
3.5
3.6
$10^3 \times T^{-1}(°K^{-1})$
$10^{-7} \times (P_M \ T_{1P_b})^{-1}(sec^{-1})$

The special variation of the water PRR with frequency is now considered. If only the rotational motion and the exchange process are dominant in the dipolar mechanism of the water protons, Eqs. II-22, II-20 and II-23 indicate that the resultant correlation time is again frequency independent as observed in the absence of the enzyme. Hence, a monotonic decrease in PRR with frequency would be predicted [Eq.(II-21)]. This does not explain the present data (Fig. II-8).

As shown with the EPR results, in the presence of the enzyme, some of the Mn(II) ions become bound and their mobility may decrease. Consequently, the reorientation time τ_{R_b} of the water protons with respect to unpaired electrons in the enzyme-bound Mn(II) ions will be longer than that in the enzyme-free Mn(II) ions. In other words, $\tau_{R_b}^{-1}$ may decrease to an extent where all the other possible correlation rates, τ_{1S}^{-1} and $\tau_{m_b}^{-1}$, significantly contribute to the resultant τ_c^{-1}.

When the frequency dependence of the electronic time is considered, a plausible explanation of the observed PRR can be given as follows. For ease of reference, the frequency dependence of the PRR at a fixed temperature (286°K) are plotted in Fig. II-9.

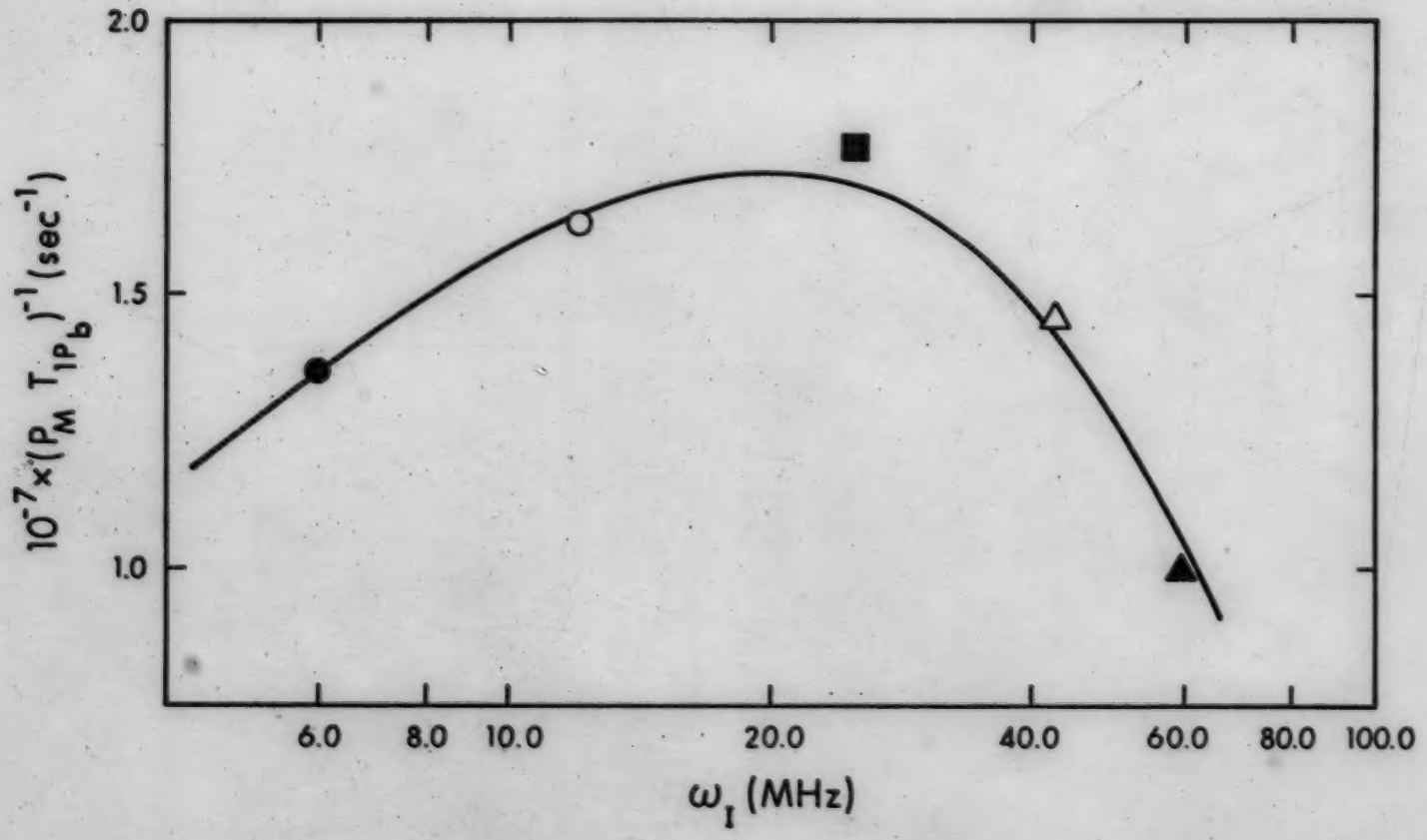

FIGURE II-9. Frequency dependence of the normalized water proton $T_1p_b^{-1}$ induced by the enzyme-bound Mn(II).$(H_2O)_4^{+2}$ complex in tris-buffer at 23°C.

(i) In the high frequency region of the curve (60.0 and 40.0MHz), the electron relaxation time is long [Eq.(II-26)] (τ_{1S}^{-1} is small). The dipolar correlation time, τ_c, is governed mainly by τ_{m_b} and τ_{R_b} and is therefore essentially frequency independent as explained previously. The frequency dependence of water PRR can only come about via the $(1+\omega_i^2\tau_c^2)^{-1}$ terms (i=I or S) in Eq.(II-26). [From now on, this term is referred to as $F(\tau_c)$]. Hence, a decrease in the frequency (Fig. II-9) causes an increase in the relaxation rate in the high frequency range.

(ii) When the frequency is further decreased, τ_{1S} decreases and eventually dominates τ_c, while the $F(\tau_c)$ terms approach unity. Hence, at the low frequencies (6.0 and 12.0MHz), the frequency dependence of the PRR is controlled mainly by τ_c, which in turn is controlled by τ_{1S}. A decrease in frequency shortens the τ_{1S} and hence the PRR as observed (Fig. II-9).

3. Quantitative Analysis of the Water PRR for the Enzyme-bound Complex

In order to include both the frequency and temperature dependence of the water PRR under study, a least-squares analysis to fit all the data was carried out using all the relevant equations for the enzyme-bound complex as described in the theory (section B-2 and 3). These equations are (II-16), (II-20 to 23) and (II-25 to 27). All parameters in these equations were varied until the root mean square deviation between the experimental and calculated values reached 6%. The best fit parameters for the enzyme-bound complex are tabulated in Table II-4, together with the corresponding literature values for the enzyme-free Mn(II) ion complex. Using the best fit parameters, the computed results are plotted in Fig. II-8 as solid curves.

A comparison of the values for these parameters (Table II-4) shows the differences between the enzyme-bound and the enzyme-free complexes.

TABLE II-4. Parameters for Mn(II) Ions in the Enzyme-bound and the Enzyme-free Complexes.

Parameter	Enzyme-bound Mn(II) ions	Enzyme-free Mn(II) ions
q (water molecules)	4.0 [α]	6.0 [β]
τ_R^o (sec).....	2.2×10^{-10}	1.0×10^{-14}; 1.6×10^{-14} [φ]
E_R (Kcal/mole)...	1.8	4.8 ; 4.5 [φ]
$\Delta H^{\neq}$ (Kcal/mole)...	7.1	7.5 [φ] ; 7.82 [δ]
$\Delta S^{\neq}$ (e.u.).....	0.97	1.3 [φ] ; 1.38 [δ]
τ_V^o (sec).....	1.4×10^{-13}	3.6×10^{-15} [φ]
E_V (Kcal/mole)...	2.7	3.9 [φ]
B (rad^2/sec^2)...	0.5×10^{19}	0.1×10^{20} [β]

[α] Value based on R= 2.78 A.

[β] Value from Reuben and Cohn (1970) and references therein.

[φ] Value from Bloembergen and Morgan (1961).

[δ] Value from ^{17}O NMR study (Zetter, et al, 1972).

(1) q* and R

From the least-squares analysis, these two parameters were found to be perfectly correlated. In other words, the value of q* depends on that of R and vice versa. Hence, a set of q* values was used to calculate the distance between the water proton and the Mn(II) ion in the enzyme:

q*	3	4	5
	2.65	2.78	2.88

Since the major paramagnetic relaxation is due to the binding in the first coordination sphere of the metal ion, the distance of 2.78A is the closest value to the average distance (2.81A) used in other Mn(II)-enzyme studies in aqueous solutions (Reuben and Cohn, 1970; Villafranca and Wedler, 1974; Jones et al, 1974b). However, the values of R may range from 2.82 to 2.92A for hexa-aquo Mn(II) complexes in solid state (Zalkin et al, 1964; Montgomery et al, 1966), the value of five for q may still be possible. Nevertheless, the coordination sites available for the water ligands decrease once the Mn(II) ions are bound to the enzyme.

(2) τ_R^o and E_R

The reorientation time of the water proton is much

longer for the M_b complex than for the M_f complex. This is due to the decreased mobility of the Mn(II) ion once it is bound to the SCS enzyme. Consequently, the other correlation rates $\tau_{m_b}^{-1}$ and τ_{1S}^{-1} can also contribute to τ_c^{-1}. The frequency and temperature dependence of all three correlation rates will be analyzed in more detail at the end of this section.

(3) $\Delta H^{\ddagger}$ and $\Delta S^{\ddagger}$

These constants are similar for both complexes. This indicates that the water molecules can readily exchange between the enzyme-bound Mn(II) complex to the bulk solvent.

(4) τ_v^{o}, E_v and B

These constants are different for the M_b and M_f complexes. Similar changes have been observed in other metal-enzyme systems, for example, in Gd(III)-bovin serum albumin (Reuben, 1971); in Mn(II)-ATP-phospho-fructokinase (Jones et al, 1974a) and in Mn(II)-ATP (Jones et al, 1974b). This was interpreted in terms of a conformational change of the enzyme around the Mn(II) ion. In principle, the effect induced by these parameters will change the electronic relaxation times, and hence the EPR

spectrum of the binary complex. This could be checked by a variable frequency EPR study (Reed and Cohn, 1970). In addition, information may be obtained about the rotational correlation time since it may be related to the EPR linewidth of the complex (Wilson and Kivelson, 1966; Angerman and Jordan, 1970). However, these experiments at present cannot be carried out since the EPR signal of the SCS-Mn(II) complex cannot be detected.

Finally, in order to show explicitly the frequency and temperature dependence of $T_{1_{p_b}}^{-1}$, values for the individual correlation rates at four representative frequencies are shown in Fig. II-10. These results were calculated from the best-fit parameters of the enzyme-bound Mn(II) ion in Table II-4. Furthermore, using Eq.(II-25), the resultant dipolar correlation rates were calculated and are shown in Fig. II-11 together with the $F(\tau_c)$ for ω_I [i.e. $(1+\omega_I^2\tau_c^2)^{-1}$].

FIGURE II-10.

Frequency and temperature dependence of the correlation times in Mn(II)-SCS solutions, calculated with the parameters listed in Table II-4 The dashed lines represent the reciprocals of electronic relaxation time at four different frequencies. The solid lines represent the reciprocals of reorientation time and exchange time respectively.

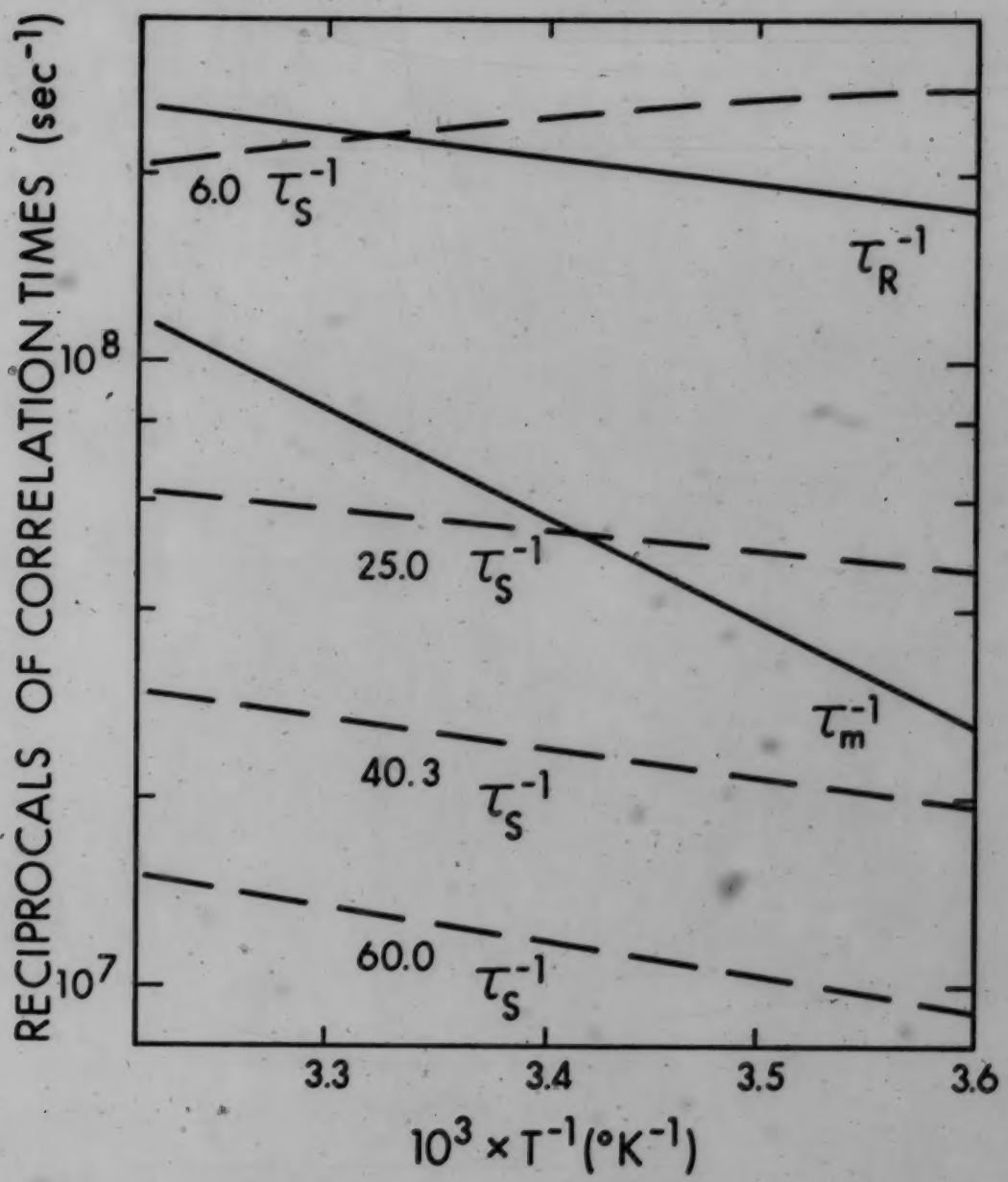
RECIPROCALS OF CORRELATION TIMES (sec^{-1})
10^8
10^7
6.0 τ_S^{-1}
τ_R^{-1}
25.0 τ_S^{-1}
τ_m^{-1}
40.3 τ_S^{-1}
60.0 τ_S^{-1}
3.3
3.4
3.5
3.6
$10^3 \times T^{-1}(°K^{-1})$

FIGURE II-11. Frequency and temperature dependence of water proton dipolar correlation time τ_c and its function $F(\tau_c)$ in the enzyme-bound Mn(II) complex, calculated using the parameters listed in Table II-4.
The curves with solid symbols (● ■ ✖ ▲) are for the functions at various frequencies (in MHz). The curves with open symbols (○ □ △) are for the corresponding correlation rates τ_c^{-1}.

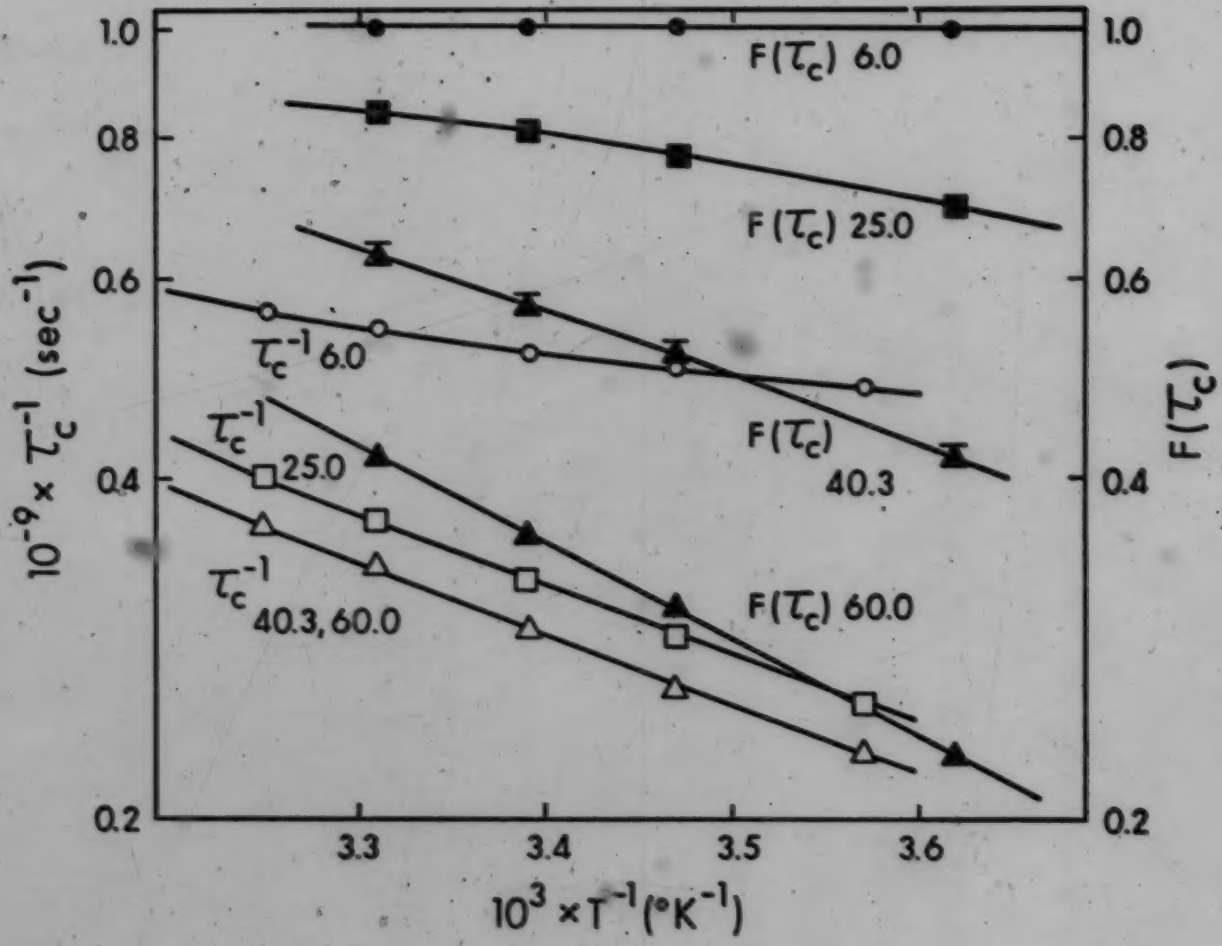
1.0
0.8
0.6
0.4
0.2
3.3
3.4
3.5
3.6
$10^{-9} \times \tau_c^{-1}$ (sec^{-1})
$10^3 \times T^{-1}$(°K^{-1})
F(τ_c)
F(τ_c) 6.0
F(τ_c) 25.0
F(τ_c) 40.3
F(τ_c) 60.0
τ_c^{-1} 6.0
τ_c^{-1} 25.0
τ_c^{-1} 40.3, 60.0

The previous qualitative explanation on the relative importance of τ_{1S}^{-1} compared to the other correlation times is now expressed in detail over the temperature range studied (Fig. II-10). The electronic relaxation rates vary with frequency and hence those at the low frequencies are comparable to the rotational and the exchange correlation rates. This induces opposite effects on the dipolar correlation times and their functions $F(\tau_c)$ (Fig. II-11). In the figure, at lower frequencies, τ_c^{-1} is frequency dependent whereas at high frequencies, $F(\tau_c)$ is frequency dependent. A similar function, $(1+\omega_S^2\tau_c^2)^{-1}$, which also appears in the T_{1M_b} expression (Eq. II-26) is very small (10^{-4} to 10^{-6}) with respect to unity. Therefore, it contributes a negligible amount to the observed rates and is not discussed.

E. CONCLUSIONS

From both water proton enhancement (NMR) and Mn titration (ESR) data, a binary Mn(II)-SCS complex was shown to be present. There are nearly four metal ion-binding sites on the phosphorylated enzyme with an average dissociation constant of 4.1×10^{-4}M at 25°C.

The analysis of the water PRR at variable frequencies and as a function of temperature yields valuable information concerning the changes around the Mn(II) ion binding sites compared with respect to the Mn(II) ion in the enzyme-free state (i.e. the hexaquo-Mn(II) ion). The Mn(II) ions rotate(tumble) much slower once they are bound to the enzyme. Consequently, the electron relaxation time does contribute to the observed water PRR of the enzyme-bound complex. The sensitivity of water PRR measurements in the present study shows the validity of the approach and technique. Similar approach may be applied to further studies in determining the possible ternary and quarternary SCS-Mn(II)-substrate complexes.

CHAPTER III

^{13}C NMR RELAXATION STUDIES ON THE Mn(II)-ADENOSINE-5'-TRIPHOSPHATE COMPLEX IN SOLUTION

A. INTRODUCTION

1. Biochemistry of the Metal Ion ATP Complexes

Adenosine-5'-triphosphate (ATP) is one of the most important coenzymes and a major supplier of energy in most biological reactions and organisms (Hutchinson, 1964; Kit, 1970). An ATP molecule consists of an adenine base, a ribose sugar and three phosphate groups as shown in Fig. III-1 (Todd, 1958). In aqueous solutions at neutral pH, most of the ATP molecules (about 80%) exist as tetravalent anions (ATP^{-4}), and the rest (about 20%) as $ATPH^{-3}$ with the terminal phosphate protonated (Smith and Alberty, 1956a). At physiological temperature, both anions are mainly in the anti-conformation in which the C-8 end of the adenine ring is facing the phosphate groups (Danyluk and Hruska, 1968; Schweizer *et al*, 1968).

In all the enzymatic reactions involving ATP, some divalent metal ions, especially Mg(II) ions, are always required (Bock, 1960; Kit, 1970). Examples are numerous, such as the reactions catalysed by thymidine

kinase (Brent *et al*, 1965), by purine nucleoside kinases (Gotto *et al*, 1964), and by nucleoside monophosphokinase (Nakamura and Sugino, 1966; Hiraga and Sugino, 1966). The affinity between ATP and divalent metal ions is very strong (Phillips, 1966) and the resultant metal ion-ATP complexes

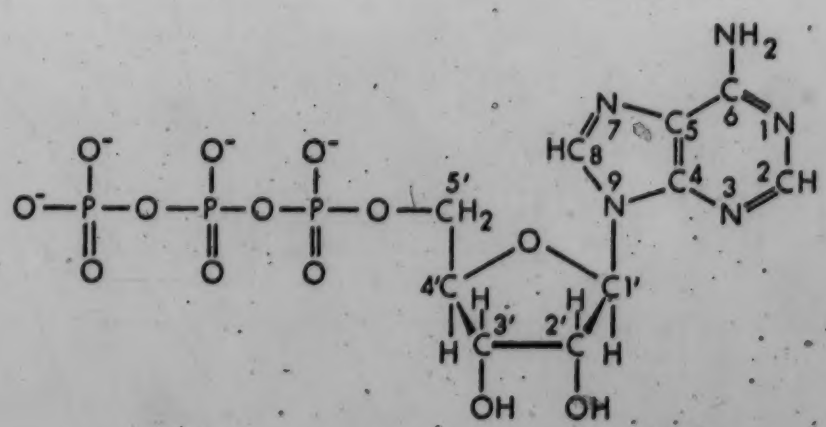

ATP

FIGURE III-1. Formula structure of ATP in aqueous solutions at neutral pH.

have been shown to be the actual substrates for a number of enzymes, such as creatine kinase (Morrison and James, 1965), pyruvate kinase (Reynard et al, 1961; Cleland, 1967) and arginine kinase (Uhr et al, 1966).

Among various metal ions, Mn(II) ions closely resemble Mg(II) ions both in their chemistry (Williams, 1970; Hughes, 1972) and in their biological effects on many enzymes (Vallee, 1960; Daune, 1974). In some cases, Mn(II) ions may even have larger activating or unique effects than those of Mg(II) ions, such as the reactions with polynucleotide phosphorylase (Hsieh and Buchanan, 1967) and with pancreatic deoxyribonuclease (Wiberg, 1958). The present study is concerned with the Mn(II) ion-ATP complexes.

2. Stoichiometry of the Metal Ion ATP Complexes

A large volume of thermodynamic and stoichiometric data on different metal ion ATP complexes has been summarized (Phillips, 1966; Izatt et al, 1971). In the case of Mn(II) ions, pH titration studies have been carried out on dilute ATP solutions (5mM) for two Mn(II):ATP ratios (10:1 and 1:1) (Taqui Khan and Martell, 1962). These researchers proved that the Mn(II) ion and ATP mainly

form a 1:1 Mn(II)-ATP complex, instead of either a 2:1 or 1:2 Mn(II)-ATP complex. Recent selective ion electrode measurements, also on dilute ATP slutions (~1.5mM) with several Mn(II) ion to ATP ratios (1:4 to 1:1), also yield the same conclusions (Mohan and Rechnitz, 1974). In the Mn(II)-ATP complex, the ATP anions exist mainly as ATP^{-4}, because this anion binds more strongly to the metal ion when it is compared to the $ATPH^{-3}$ anion; for example, the formation constant of $[Mn(II)\text{-}ATP]^{-2}$ is $3.1 \times 10^{6} M^{-1}$, whereas that of $[Mn(II)\text{-}ATPH]^{-1}$ is $3.7 \times 10^{4} M^{-1}$ (Mohan and Rechnitz, 1974).

AT higher ATP concentrations (~ 0.1M), self-association of ATP molecules becomes significant (Sternlicht et al, 1965b). Nevertheless, these researchers reported in the same paper a comparative ^{1}H NMR study on 0.35M and 0.02M ATP solutions in the presence of Mn(II) ions (~ 1 to 0.1mM). Results at both ATP concentrations were found to be the same and hence the effect of self-association does not affect the stoichiometry of the Mn(II)-ATP complex to any significant extent (Sternlicht et al, 1965b). Nevertheless, an additional 1:2 $[Mn(II)\text{-}ATP_2]^{-6}$ complex was proposed in a subsequent Mn(II) ion-competition study on equimolar AMP-ATP solutions (0.25M) in the presence of dilute Mn(II) ions (~ 0.1mM) (Sternlicht et al, 1968).

However, the original NMR data, which were used to support the presence of the 1:2 complex, were irreproducible (Wee et al, 1974). Furthermore, the conditions of the proposed kinetic scheme involving the 1:2 complex have also been questioned by Frey and Stuehr (1973). Therefore, in the present study, the stoichiometry of the Mn(II)-ATP complex is belived to be mainly in a 1:1 ratio.

The 1:1 complex may exist in several structures. For metal ions including Mg(II), Ca(II), Ni(II) and Co(II), kinetic studies based on temperature jump (T-jump) techniques showed the presence of two equilibrium states and hence two kinetically distinct metal ion-ATP complexes. The first process is represented by the following scheme and the related temperature jump relaxation times are dependent on the ATP concentrations (Diebler et al, 1960; Hammes and Levison, 1964; Hammes and Miller, 1967):

$$\begin{array}{ccc} M^{+2} + ATP^{-4} & \rightleftharpoons & M\text{-}ATP^{-2} \\ & \rightleftharpoons & \\ & ATPH^{-3} & \end{array} \qquad \text{(III-1)}$$

where M^{+2} stands for Mg(II), Ca(II), Ni(II) and Co(II). The $M\text{-}ATP^{-2}$ complex can undergo further structural rearrangement. In this second process, the relaxation times are faster than that of the first process, yet

independent of the ATP concentration. The process is represented by the following scheme (Hammes and Miller, 1967; Frey and Stuehr, 1972; Frey et al, 1972):

$$M\text{-}ATP^{-2} \rightleftharpoons [M\text{-}ATP^{-2}]^{\ddagger} \qquad \text{(III-2)}$$

Several possible structures for the second $[M\text{-}ATP^{-2}]^{\ddagger}$ complex were proposed, yet no definite conclusion was made based on the kinetic data alone.

For Mn(II)-ATP complexes, the initial process [Eq.(III-1)] leading to the formation of a binary complex is also present. The relaxation times from the T-jump experiments for this process were found to be too fast to be measured accurately even at a very dilute ATP concentration [$\leq 10^{-4}$M]. Hence, only the limits on the reaction rates of the process were estimated. The forward rate (leading to $M\text{-}ATP^{-2}$) was $> 10^9$ sec and the reverse rate was about 10^4 sec at 25°C and at an ATP concentration of 10^{-4}M (Hammes and Levison, 1964). At higher concentrations, no new relaxation times can be detected (Hammes and Miller, 1967). Two possibilities were suggested (Frey and Stuehr, 1973): (i) the relaxation rates may be too fast to be measured as the first process is already at the instrumental limit, or (ii) the second Mn(II)-ATP^{-2} complex [given in Eq.(III-2)] may not exist in significant amount and hence is not observed.

3. Structures of the Metal Ion ATP Complexes

In an ATP molecule (Fig. III-1), there are several potential ligands for metal ion binding, namely the oxygens of the phosphate groups and nitrogens of the adenine base. Therefore, a variety of structures have been proposed for different metal ion-ATP complexes (Izatt et al, 1971).

In the case of Mg(II) ions, the dominant metal binding ligands are the phosphate groups (Hammes et al, 1961; Cohn and Hughes, 1962). Several studies have shown that the N-7 nitrogen of the adenine ring may not be involved in the metal ion binding. These studies include optical rotatory dispersion (McCormick and Levedahl, 1959), ^{1}H NMR (Cohn and Hughes, 1962) and ^{15}N NMR (Happe and Morales, 1966).

For Mn(II) ions used in the present study, it is generally accepted that the three phosphates are bound to the metal ion (Cohn and Hughes, 1962; Sternlicht et al, 1965a, 1968; Brown et al, 1973). The involvement of the adenine ring is still under active discussion. Schneider et al (1964) carried out a comparative U.V. study on adenosine, Mn(II)-adenosine, ATP and Mn(II)-ATP solutions. No significant Mn(II)-adenine ring binding is observed in

adenosine. In the case of ATP, which has three additional phosphate groups in the ribose compared with that in adenosine, only a small fraction of the Mn(II) ions is involved in the binding with the adenine ring. These researchers then proposed that Mn(II)-ATP complexes exist mainly in a structure in which only the phosphates are bound to the Mn(II) ion as suggested from other titration studies (Taqui Kahn and Martell, 1962; Martell and Schwarzenbach, 1956; Smith and Alberty, 1956a,b). This complex will be refered to as $M_{(p)}ATP$ from now on.

From ^1H NMR studies, Sternlicht et al (1965b) confirmed that the adenine H-8 proton of ATP is preferentially affected by Mn(II), Co(II), Ni(II) and Cu(II) ions (Cohn and Hughes, 1962). In addition, the bindings are not affected by the concentration and self-association of ATP. These authors then proposed that the adenine ring is also bound to the metal ion [via the N-7 nitrogen]. This binding gives rise to a backbound complex which was proposed by Szent-Gyorgyi (1957). In this complex, both the three phosphates and the adenine base of the same ATP molecule are bound to the metal ion. This complex is designated as $M_{(p+r)}ATP$ from now on.

The exact structure of the backbound complex may vary even among the transition metal ion series as observed

in some subsequent studies. For Ni(II) and Co(II) ions, ^{17}O NMR studies on the number of exchangeable water molecules coordinated to the metal ion have been carried out (Glassman et al, 1971; Kuntz et al, 1972). On the assumption that there is only one type of metal ion-ATP complex, both metal ions are shown to be indirectly bound to nitrogen N-7 of the base via a water molecule "bridge". For Mn(II) ions, another ^{17}O NMR study (Zetter et al, 1973) showed that there are about three water molecules in the Mn(II)-ATP complex. Nevertheless, their data could not distinguish whether the water molecules are kinetically different and hence a similar "bridge" water complex cannot be confirmed (Zetter et al, 1973). In these three studies, as only the properties of the solvent water were followed, a complete metal ion-ATP structure was not worked out.

4. Object of the Present Study

In this study, an attempt is made to determine the number of Mn(II)-ATP complexes (or structures) present in solution as well as to determine the favorable geometry resulting from the Mn(II)-adenine ring interaction. The experiments were carried out using natural abundance ^{13}C NMR techniques which enable more nuclei to be observed when it is compared to the ^{1}H NMR and ^{31}P NMR studies.

^{13}C NMR measurements are now readily accessible due to pulsed Fourier transform NMR techniques (Vold et al, 1968; Freeman and Hill, 1969; Allerhand et al, 1971). Applications of this technique to nucleotide studies were initiated by several early ^{13}C line assignment studies (Dorman and Roberts, 1970; Jones et al, 1970; Mantsch and Smith, 1972). ^{13}C NMR study on adenosine-5'-monophosphate with Mn(II) ions has been reported (Kotowycz and Hayamizu, 1973).

In the present study, ^{13}C NMR results for both the spin-spin and spin-lattice relaxation times are obtained. From the spin-spin relaxation times, two types of Mn(II)-ATP complexes are shown to exist. These complexes, together with the unbound ATP molecule, form a three-site NMR exchange system. From the spin-lattice re-

laxation times, distances between the Mn(II) ion and the adenine carbons are worked out.

B. THEORY SECTION

As described in the introduction, Mn(II) ions may form one or two types of complexes with ATP molecules. Hence, the ATP nuclei may be involved in a two-site or a three-site NMR exchange system respectively. Relaxation rates for both systems are described in this section.

1. A Two-Site System

If ATP forms only one type of complex [$M_{(p)}ATP$ or $M_{(p+r)}ATP$] with Mn(II) ions, the unbound ATP and the complex, designated with symbols a and b respectively, comprise a two-site system:

$$a \underset{k_{ba}}{\overset{k_{ab}}{\rightleftharpoons}} b \qquad \text{(III-3)}$$

in which [a] >> [b] as the Mn(II) ion concentration used is very small. k_{ab} and k_{ba} are, respectively, the NMR exchange rate from species a to b and that from b to a. The principles and equations for the spin-lattice relaxation rates for a two-site system have been described and applied in the enzyme study in the previous chapter. For completeness, the equations for both spin-lattice and spin-spin relaxation are now described.

The contribution of the metal ion complex to the nuclear T_1 or T_2 relaxation rates is calculated from the experimental data using the following equation:

$$T_{jp}^{-1} = T_{j,metal}^{-1} - T_{j,blank}^{-1} \qquad \text{(III-4)}$$

where j stands for 1 and 2 for the T_1 and T_2 relaxation times, $T_{j,metal}$ is the T_j of the nucleus in the presence of metal ions and $T_{j,blank}$ is the T_j of the same nucleus in the absence of metal ions.

This contribution will be referred to either with the symbol T_{jp}^{-1} or " <u>paramagnetic</u> relaxation rate" from now on. For the T_1p^{-1}, the equation is given as Eq.(II-15) in the previous chapter. For the T_2p^{-1}, in the case of Mn(II) ion complexes where the chemical shift difference, $\Delta\omega_M$, between the bound and the unbound nuclei contributes very little to the relaxation, i.e. $(T_{2M}\cdot\tau_m)^{-1} >> T_{2M}^{-2}, \Delta\omega_M^2$ the equation of T_2p^{-1} also has a similar form as that of T_1p^{-1} (Swift and Connick, 1962). Therefore, in the two-site exchange system involving Mn(II) ions, the equations for both relaxation rates are summarized as

$$T_{jp}^{-1} = \frac{[b]}{[a]} \left(T_{j,b} + k_{ba}^{-1}\right)^{-1}$$

(III-5)

where [b] is the concentration of the complex, which is numerically equal to the initial Mn(II) ion concentration [m], since all the metal ions are bound under the experimental condition: [ATP]=0.3M and $[Mn^{+2}] \leq 3\times10^{-4}$M (Taqui Khan and Martell, 1962); $T_{j,b}$ is the nuclear relaxation time when the nucleus is in the complex b, and k_{ba} is the NMR exchange rate as previously defined.

Both $T_{j,b}$ and k_{ba} are functions of temperature. Therefore, the observed T_{jp}^{-1} may take two limiting forms (Swift and Connick, 1962; O'Reilley and Poole, 1963; Luz and Meiboom, 1964):

(i) At low temperatures, when the exchange rate is slow, $k_{ba} \ll T_{j,b}^{-1}$ the relaxation rate is controlled by the NMR exchange rate:

$$T_{jp}^{-1} = \frac{[b]}{[a]} k_{ba} \qquad \text{(III-6)}$$

(ii) At high temperatures, when the exchange rate is fast $k_{ba} >> T_{j,b}^{-1}$, the relaxation rate reflects the nuclear relaxation due to the metal ion complex:

$$T_{jp}^{-1} = \frac{[b]}{[a]} T_{j,b}^{-1} \qquad \text{(III-7)}$$

The details of $T_{j,b}$ and its temperature dependence will be described in a separate section(B-3).

2. A Three-Site Exchange System

When both $M_{(p)}ATP$ and $M_{(p+r)}ATP$ complexes are considered, the ATP nuclei are involved in a three-site system. Furthermore, the exchange processes among the three species (ATP; $M_{(p)}ATP$ and $M_{(p+r)}ATP$) may not be completely random. As described in the introduction, the phosphate groups of ATP are the primary metal-binding sites and the presence of these groups enhances the Mn(II)-adenine ring binding. In addition, both bindings are intramolecular (Sternlicht et al, 1965b). Therefore, the exchange between the unbound ATP and the backbound ATP complex is likely to proceed via an intermediate complex $M_{(p)}ATP$. The system is represented by a consecutive NMR exchange scheme:

$$ATP \rightleftharpoons M_{(p)}ATP \rightleftharpoons M_{(p+r)}ATP \qquad \text{(III-8)}$$

which is symbolically written as:

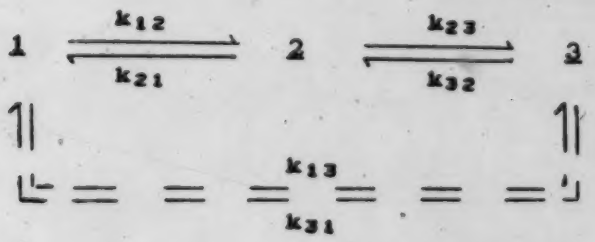

(III-9)

with the following conditions:

$$[1] >> [2]; [3],$$

and

$$k_{32} >> k_{31} \quad ; \quad k_{12} >> k_{13} \qquad \text{(III-10)}$$

Eq.(III-10) is used to express the consecutive nature of the present exchange scheme. Similar to the notations in the preceding scheme, the exchange rates are represented by symbols k_{xy} for the exchange from species x to another species y (x, y = 1, 2, 3). The temperature dependence of the exchange rates can be generalized in the following form (Eyring, 1935):

$$k_{xy} = \frac{RT}{Nh} \exp\left(\frac{-\Delta H^{\ddagger}_{xy}}{RT} + \frac{\Delta S^{\ddagger}_{xy}}{R}\right) \qquad \text{(III-11)}$$

where R is the gas constant, N is Avogadro's number, h is Planck's constant, T is the absolute temperature, $\Delta H^{\ddagger}_{xy}$ and $\Delta S^{\ddagger}_{xy}$ are, respectively, the activation enthalpy and entropy for the x to y exchange process.

The magnitude of the relaxation rate due to these metal ion complexes is calculated from experimental data as described by Eq.(III-4). The rate is now a function of the magnetic

properties of both complexes and the related NMR exchange rates. The details are described in the following subsections.

2A. The Spin-Spin Paramagnetic Relaxation Rate

From the modified Bloch equations (McConnell, 1958), several researchers have derived equations for the spin-spin relaxation rate for a three-site system and simplified the expressions in various forms (Swift and Connick, 1962; Angerman and Jordan, 1969; Hall et al, 1970).

In the case of Mn(II) ion complexes, the chemical shift contribution to the relaxation is very small when it is compared to the corresponding nuclear relaxation rate (Bernheim et al, 1959; Swift and Connick, 1962). In addition, the present scheme is a consecutive three site exchange with the constraints as defined in Eq.(III-10). Therefore, from the general expression derived by Angerman and Jordan(1969), the equation for the spin-spin relaxation rate can be simplified into the following form:

$$T_{2p}^{-1} = \frac{k_{12}F_{32} + k_{13}F_{23}}{(T_{2,2}^{-1}+k_{21})A_3 + k_{23}(T_{2,3}^{-1}+k_{31})} \qquad \text{(III-12)}$$

where

$$F_{32} = A_3T_{2,2}^{-1} + k_{23}T_{2,3}^{-1} \quad ,$$

$$F_{23} = A_2T_{2,3}^{-1} + k_{32}T_{2,2}^{-1} \quad ,$$

$$A_3 = T_{2,3}^{-1} + k_{32} \quad ,$$

$$A_2 = T_{2,2}^{-1} + k_{21} + k_{23} \quad .$$

In the above equation, the spin-spin relaxation time T_2 of the nucleus in species x (or site x) is denoted by $T_{2,x}$ [$x=1,2,3$ in the present scheme], and the NMR exchange rate, k_{xy}, has the same meaning as previously defined.

The above equation can also be simplified into two limiting forms, depending on the temperature:

(i) At low temperatures, the exchange rates are small:

$$k_{23} \ll T_{2,3}^{-1} \quad ,$$

$$k_{23} + k_{21} \ll T_{2,2}^{-1} \quad ,$$

Eq.(III-12) becomes

$$T_{2p}^{-1} = k_{12} = \frac{[2]}{[1]}k_{21} \qquad \text{(III-13)}$$

It is of interest to compare this equation with that for the two-site exchange [Eq.(III-6)]. Both

equations are of similar form. They are governed by a single exchange process and hence are independent of the magnetic properties of the ATP nuclei. For example, when species b is species 2, $k_{21} = k_{ba}$, and consequently the temperature dependence of a three-site system may appear similar to that of a two-site exchange.

(ii) At high temperatures when the exchange rates are large:

$$k_{32} \gg T_{2,3}^{-1},$$

$$k_{21} \gg T_{2,2}^{-1},$$

Eq.(III-12) becomes

$$T_{2p}^{-1} = \frac{[2]}{[1]} T_{2,2}^{-1} + \frac{[3]}{[1]} T_{2,3}^{-1} \qquad \text{(III-14)}$$

Furthermore, as the adenine carbon nuclei are located near the paramagnetic Mn(II) ion only in the $M_{(p+r)}ATP$ complex (species 3), at this site, the nuclear relaxation rate is much enhanced from that in the $M_{(p)}ATP$ complex. $T_{2,3}^{-1} \gg T_{2,2}^{-1}$ for the ^{13}C adenine carbon nuclei and Eq.(III-14) becomes:

$$T_{2p}^{-1}(^{13}C) = \frac{[3]}{[1]} T_{2,3}^{-1} \qquad \text{(III-15)}$$

However, for the ^{31}P nuclei, since the phosphate

groups are tightly bound to the Mn(II) ion in both complexes, then $T_{2,3} = T_{2,2}$.

Therefore, for the ^{31}P nuclei in ATP, Eq.(III-14) becomes:

$$T_{2P}^{-1}(^{31}P) = \frac{[2]+[3]}{[1]} T_{2,2}^{-1}$$

$$= \frac{[m]}{[ATP]} T_{2,2}^{-1} \qquad \text{(III-16)}$$

where [m] is the total initial Mn(II) ion concentration, since the affinity between ATP and the Mn(II) ions are so large that almost all the metal ions are bound (Taqui Kahn and Martell, 1962; Mohan and Rechnitz, 1974).

2B. The Spin-lattice Paramagnetic Relaxation Rate

In analogy to the T_2p^{-1} expressions, the spin-lattice relaxation rates for the three-site exchange system under study can be shown to have a form similar to Eq.(III-14). In the fast exchange region, the equation for T_1p^{-1} is

$$T_1p^{-1} = \frac{[2]}{[1]} T_{1,2}^{-1} + \frac{[3]}{[1]} T_{1,3}^{-1} \qquad \text{(III-17)}$$

where $T_{1,x}$ ($x=2,3$) is the T_1 relaxation time for metal complex x.

The equation has been generally accepted and used in the literature(e.g. Mildvan and Cohn, 1963; Reuben and Cohn, 1970). However, no derivation has been reported. The derivation of Eq.(III-17) is therefore included in Appendix B.

The equation for T_1p^{-1} can also be further simplified depending on the nuclei under observation. For the same reasons as given in section 2A, Eq.(III-17) then becomes

(A).

$$T_1p^{-1}(^{13}C) = \frac{[3]}{[1]}\, T_{1,3}{}^{-1} \qquad \text{(III-18)}$$

with $T_{1,3} \ll T_{1,2}$ for ^{13}C nuclei,

and

(B).

$$T_1p^{-1}(^{31}P) = \frac{[m]}{[1]}\, T_{1,2}{}^{-1} \qquad \text{(III-19)}$$

with $T_{1,2} = T_{1,3}$ for the ^{31}P nuclei.

3. Nuclear Relaxation Mechanisms Between the Mn(II) Ion and the ATP Nuclei

When a nucleus is in the proximity of the Mn(II) ion, the main nuclear relaxation is induced by the interaction between the nuclear spin and the unpaired electrons of the metal ion (Solomon, 1955; Solomon and Bloembergen, 1956). In the spin-lattice (T_1) relaxation, the dominant interaction is the dipolar coupling, which has been described in the previous chapter. Only the relevant equations for the present study are summarized here. For the present Mn(II)-ATP complexes which are quite small in size compared to the Mn(II)-enzyme complexes, the rotational motion of the complex is rapid and hence dominates the dipolar mechanism of the ATP nuclei (Sternlicht et al, 1965ab; Heller et al, 1970; Brown et al, 1974). Hence, $\tau_c = \tau_R$ from Eqs. (II-21) to (II-24), the spin-lattice relaxation rate is

$$T_{1,x}^{-1} = T_{1M}^{-1} = \frac{C_D}{R^6}\left(3 + \frac{7}{1+\omega_S^2\tau_R^2}\right)\tau_R \qquad \text{(III-20)}$$

where x stands for 2, 3, or b depending on the species and the exchange system, and the other symbols have been defined in Chapter II.

At the magnetic field strength (24KGauss or 25.5MHz for ^{13}C resonance) used in this study, $\omega_S^2 \tau_R^2 \gg 1$ (Sternlicht et al, 1965ab). Consequently, Eq.(III-20) can be further simplified into the following form:

$$T_{1,x}^{-1} = T_{1M}^{-1} = \frac{C_D}{R} \cdot 3\tau_R$$

$$= \frac{2}{5} S(S+1) g^2 \beta^2 \gamma_I^2 \cdot \frac{\tau_R}{R^6} \qquad \text{(III-21)}$$

From this equation, the distance R between the Mn(II) ion and the nucleus at site x can be evaluated.

In the spin-spin (T_2) relaxation, an additional scalar coupling also contributes to the nuclear relaxation. This interaction is induced by the overlapping of the wave functions of the nucleus in question and the unpaired electrons (Solomon and Bloembergen, 1956). Under the same conditions as for the T_{1M}^{-1} expression , the spin-spin relaxation rate is

$$T_{2,x}^{-1} = T_{2m}^{-1} = \frac{7}{15} S(S+1)\, g^2\beta^2\gamma_I^2 \cdot \frac{\tau_R}{R^6} + C_S\tau_e$$

(III-22)

where

$$C_S = \frac{1}{3} S(S+1) \left(\frac{A}{\hbar}\right)^2$$

In the equation, $T_{2,x}$ stands for the T_2 at species x (x = 2, 3, or b). All the other symbols (except A and τ_e) were defined previously. A is the scalar coupling constant which measures the extent of the coupling between the nucleus and the unpaired electrons of the Mn(II) ion. τ_e is the relevant correlation time of the scalar interaction. This scalar correlation time is related to the spin-lattice relaxation time of the electron and the NMR exchange rates (Bernheim *et al*, 1959).

For a two-site system [Eq.(III-3)], the scalar correlation time in the $T_{2,b}^{-1}$ relaxation is

$$\tau_e^{-1} = \tau_{1S}^{-1} + k_{ba}$$

(III-23)

By analogy, for a three-site system, the τ_e in the $T_{2,3}^{-1}$

relaxation is:

$$\tau_e^{-1} = \tau_{1S}^{-1} + k_{32} + k_{31} \qquad \text{(III-24)}$$

where the correlation times and the exchange rates are related to the three-site process.

Furthermore, in the present consecutive scheme, $k_{32} \gg k_{31}$, the scalar correlation time becomes:

$$\tau_e^{-1} \cong \tau_{1S}^{-1} + k_{32} \qquad \text{(III-25)}$$

In some cases [as was found in the present study and in the Mn(II)-inosine-5'-triphosphate study (Kuntz and Kotowycz, 1975)], the difference between the scalar correlation times given by Eqs. (III-23) and (III-25) may be useful in identifying the nature of the exchange system.

C. EXPERIMENTAL SECTION

1. Materials and Sample Preparation

ATP (disodium salt) of highest grade was obtained from Sigma Chemical Company. It was further purified to eliminate any metal ion impurities by the following procedure. First of all, a small aliquot (1ml) of 0.5M ATP solution (pH 7) was added on the top of a resin column (1cmx20cm; Dowex-50, Na^+ form), which had been cleaned and equilibrated in triply distilled water. Then, the ATP was eluted down the column slowly with triply distilled water. The collected eluate (about 1 litre) was freeze-dried at room temperature.

ATP solutions and stock Mn(II) ion solutions were prepared using deuterated water (D_2O) and triply distilled water as solvents:

(A). For all the ^{13}C T_2 measurements (1.0° to 90°C) and ^{13}C T_1 measurements at 30°C, D_2O was used as solvent, since it provides a strong deuterium resonance that can be used conveniently as a lock signal for stabilizing the magnetic field. Measurements on samples prepared in D_2O and H_2O were checked and the resultant T_{2p} values are found to be the same.

(B) For high temperature (60°C) T_1 measurements, D_2O can not be used as a solvent, because when samples in D_2O (type A sample) are heated at 60°C over a long period (>18 hrs), a significant portion of the H-8 protons of ATP is replaced by the deuterium from the D_2O solvent. The intensities of ^{13}C signals decrease gradually with time as a result of the diminishing nuclear Overhauser effect.

The deuteration rate, however, was not rapid enough to affect most of the measurements even at high temperatures. The ^{13}C linewidth measurements (T_2) took approximately two hours. But, for ^{13}C T_1 experiments, 16 to 20 hrs were required. Possible errors in using the decreasing ^{13}C intensities may exist. Hence, water was used as the solvent, and a coaxial capillary containing deuterated benzene was then used as a locking signal.

The ATP concentrations were determined by U.V. spectrometry (molar extinction coefficient = 1.572×10^4 at 260nm at a pH of 7). They were all 0.3M[ATP]. The metal ion solution was added with H.E. Pedersen micropipets. The pH values of all the solutions were rechecked after the last addition of Mn(II) ions and they remained constant. [i.e. The pH meter readings were 7 and 6.6 for the samples

in water and in D_2O respectively (Glasoe and Long, 1960)].

Stock solutions of Mn(II) ion were prepared by weighing out an appropriate amount of $MnCl_2.4H_2O$ crystals (Fisher Certified Grade), and dissolved in D_2O (or in H_2O) to a final volume of 25ml. The concentrations were also calibrated against a Fisher $Mn(NO_3)_2$ solution (standardized with atomic absorption). The calibrations were carried out by measuring the ^{31}P NMR linewidths on a pair of 5'-AMP (0.1M) solutions with the addition of the stock and the standard solutions respectively. The experimental uncertainty was ±5% in these measurements.

In all of the work, precaution was taken to prevent and detect any decomposition (hydrolysis of the terminal phosphate) in the ATP samples. Fresh samples were prepared for each measurement and the extent of hydrolysis was checked before and after the experiments using thin layer chromatography techniques (Randerath et al, 1964), or using ^{31}P NMR to measure the relative signal intensities of the inorganic phosphate (hydrolysis product) and the original ATP phosphates. Negligible hydrolysis was observed for all type (A) samples. Only in some type (B) samples, the ATP solutions containing Mn(II) ions hydrolyzed slightly (maximum detected $\leq$ 10%) due to many hours of heating at 60°C. However, the data were checked

for this effect. Measurements were first carried out at 32°, then 60°, and then again at 32°C. Results were reproducible within experimental error (±8%).

In all the ^{13}C and ^{1}H NMR studies, the relaxation rates of blank ATP solutions with the same ATP concentration as the Mn(II)-ATP solutions were used. The paramagnetic relaxation rates were then calculated with Eq.(III-4) using the results from both solutions.

2. ^{13}C NMR Measurements

Natural abundance proton decoupled ^{13}C NMR spectra were obtained in the Fourier transform mode on a Varian HA-100-15 NMR spectrometer (25.15 MHz) interfaced with a Digilab FTS/NMR-3 data system, the Nova 1200 computer and the pulse unit (FTS/NMR 400-2). For type (A) samples in deuterated water, the deuterium resonance of the solvent was used as the lock signal. For type (B) samples in water, the deuterium resonance of deuterated benzene in a coaxial capillary was used. All measurements were carried out under controlled temperatures using the Varian temperature control unit and were calibrated with a thermocouple before and after each run. Samples were put in the probe at least 20 minutes before the measurements

were begun.

Spin-spin relaxation times were measured from the linewidths at half height from the Fourier transformed spectra. For each spectrum, 2,000 free induction decay (FID) signals were stored in 16K (16384 bytes) over a corresponding frequency domain of 4000 Hz. The Digilab system yields 16K data points in the transformed real spectrum by zero filling and carrying out a 32K transform (0.25 Hz per byte over 4000 Hz). The pulse widths and noise-decoupler offset values were optimized by maximizing the signal intensities at a reduced power level of the noise-decoupler.

Spin-lattice relaxation times were evaluated from proton decoupled partially relaxed Fourier transform spectra obtained using the $(180^\circ - \tau - 90^\circ - 5T_1 -)_n$ pulse sequence (Vold et al, 1968; Freeman and Hill, 1969; Allerhand et al, 1971). For each spectrum, 500 FID signals were accumulated. For short values of T_1 (<0.2sec), a triple pulse sequence, $(90^\circ - 5T_1 - 180^\circ - \tau - 90^\circ - 5T_1)_n$, was used (Freeman and Hill, 1971) to improve the accuracy of the measurements. Each spectrum was obtained from 5,000 FID signals and each experiment was repeated twice.

A typical set of partially relaxed F.T. spectra

for the adenine carbons with different τ values is shown in Fig. III-2. Least squares analyses (Appendix A) were carried out on the data from fourteen different τ settings, which yielded T_1 values with standard deviations of less than 8%.

In all these experiments, the pulse widths used were 100 microseconds and 50 microseconds for the 180° and 90° pulses respectively. The ^{13}C pulse frequency was offset in a way such that the signals to be observed were within 1500 Hz from the carrier (Jones, 1972). Therefore, for ATP, the carbon signals in the adenine base region and the sugar region were measured separately.

FIGURE III-2. A sample set of ^{13}C NMR spectra of the adenine carbons of ATP, obtained in a $180^{\circ}-\tau-90^{\circ}$ pulse experiment. The experiment was carried out at 25.15MHz, 30°C and proton-noise decoupled. The sample contained 0.3M ATP in D_2O at a pD of 7.0. The top spectrum is a normal Fourier transformed spectrum at $\tau >> 5T_1$. The other spectra are the partially-relaxed F.T. spectra at various τ settings. Each spectrum was obtained by Fourier transformation of 500 free induction decays.

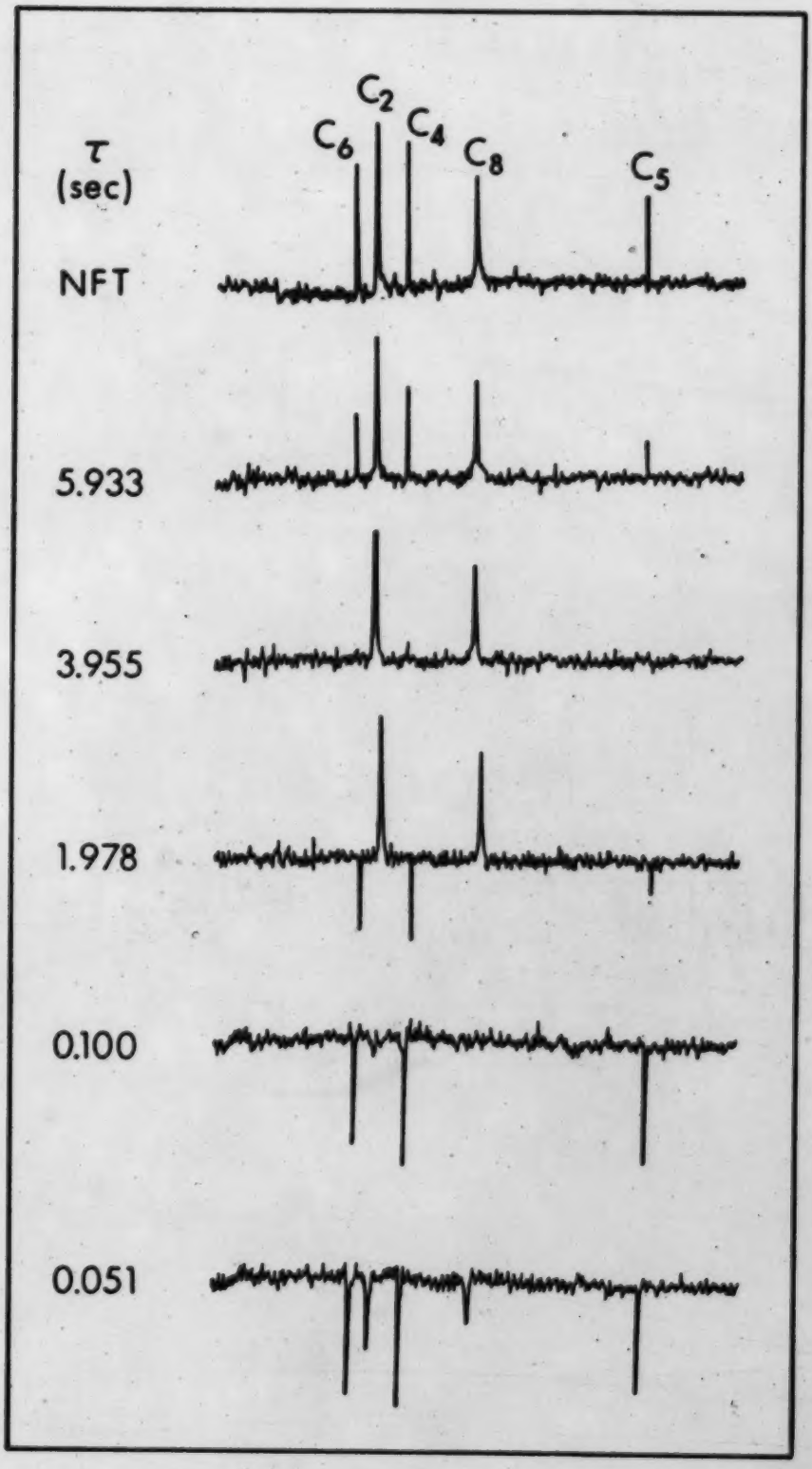
τ
(sec)
C6
C2
C4
C8
C5
NFT
5.933
3.955
1.978
0.100
0.051

3. ^{1}H NMR Measurements

The water proton linewidth measurements were made on a Mn(II)-ATP and a blank ATP solutions. Both solutions contained 0.27M of ATP and the [Mn^{+2}] in the Mn(II)-ATP sample was 9.9×10^{-4}M. The experiments were carried out in the continuous wave mode using a Varian HA-100-12 NMR spectrometer (100.0 MHz). A trace of DSS (sodium 2,2-dimethyl-2-silapentane-5-sulfonate) was used as an internal lock. The temperature was also calibrated using a thermocouple.

The T_1 experiments for the ATP protons were carried out in Fourier transform mode using a Varian HA-100-15 NMR spectrometer (100.0MHz). The specifications of the spectrometer have been described in the previous section (C-2). The $180^{\circ}- \tau -90^{\circ}$ pulse sequence was also used, but only one scan (FID) was sufficient for a good signal to noise ATP proton spectrum.

D. RESULTS

The ^{13}C NMR spectrum of ATP is shown in Fig. III-3. The adenine ring carbon signals were assigned on the basis of the earlier work on nucleotides and nucleosides (Dorman and Roberts, 1970; Jones *et al*, 1970). The ribose carbon resonances were assigned according to the work of Mantsch and Smith (1972).

On progressive addition of Mn(II) ions, the ^{13}C signals for the ribose carbons were not affected. However, the adenine ring ^{13}C resonances showed specific effects. The results (reported as T_1p^{-1} and T_2p^{-1}) are plotted vs the total Mn(II) ion concentration in Fig. III-4 and Fig. III-5 respectively. From the figures, it is seen that the C-5 and C-8 resonances were most strongly affected on the addition of Mn(II) ions. The data in these figures are normalized to a constant $[Mn^{+2}]$ /[ATP] ratio and are summarized in Table III-1.

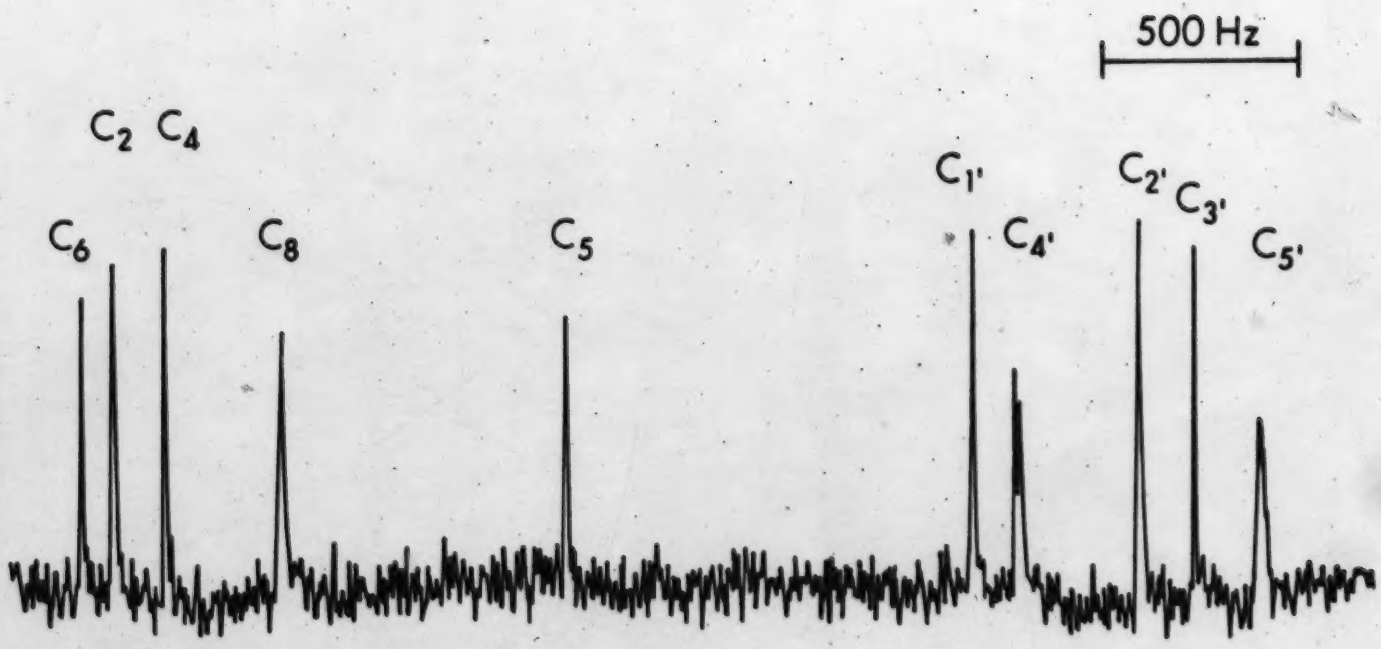

FIGURE III-3. Proton-decoupled natural abundance ^{13}C FT NMR spectrum of ATP. The measurement was carried out at 25.15MHz (^{13}C) and 30°C on a 0.3M ATP solution in D_2O at a pD of 7.0. The spectra were obtained by Fourier transformation of 2,000 free induction decays.

FIGURE III-4. The effect of Mn(II) ions on the ^{13}C longitudinal relaxation rates of the adenine base nuclei of ATP. The measurements were carried out in D_2O at a pD of 7.0 at 30°C. The ATP concentration is 0.30 M.

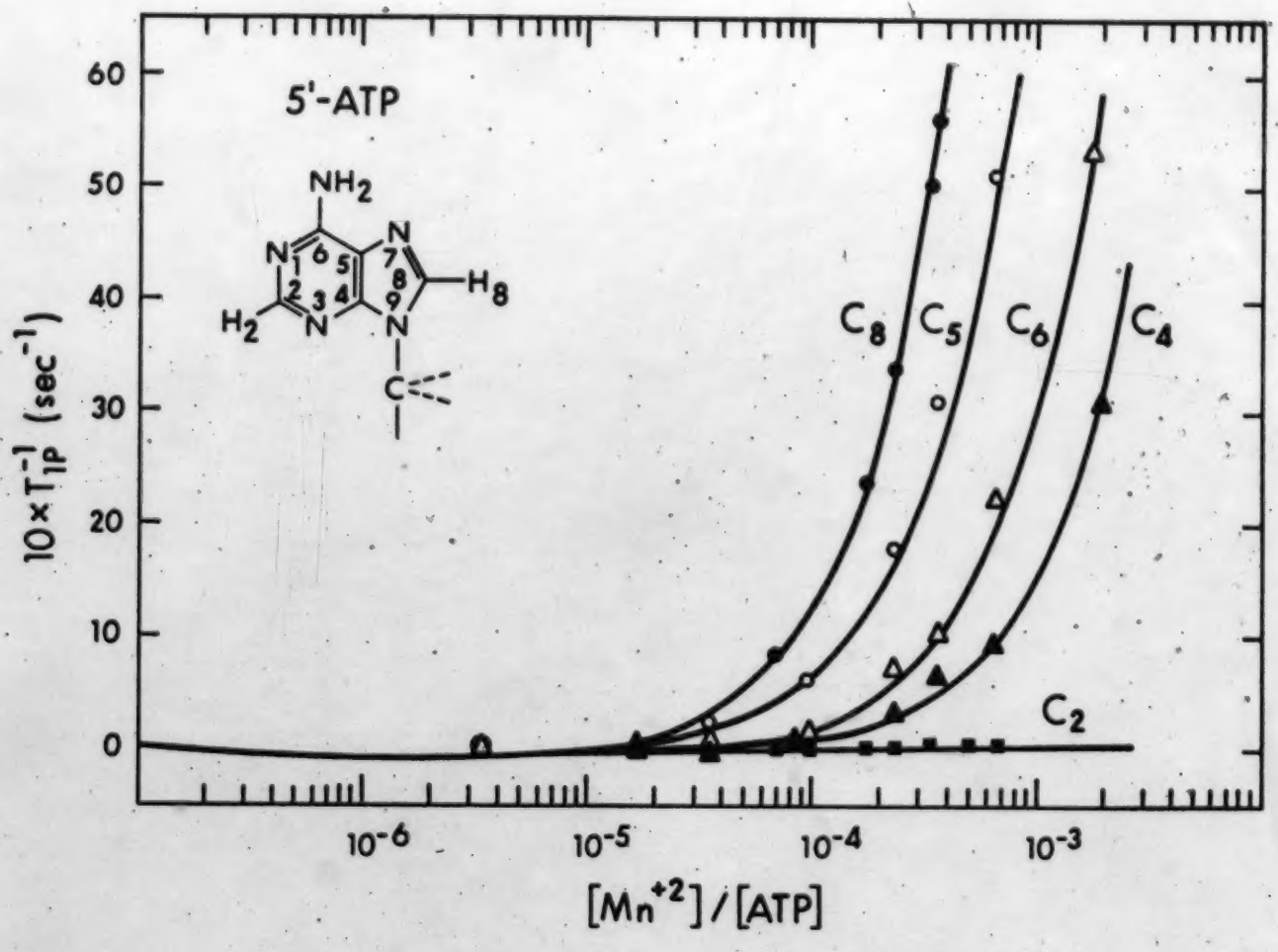
5'-ATP
NH2
H2
H8
C8
C5
C6
C4
C2
60
50
40
30
20
10
0
10×T1P-1 (sec-1)
10-6
10-5
10-4
10-3
[Mn+2] / [ATP]

FIGURE III-5. The effect of Mn(II) ions on the ^{13}C transverse relaxation rates of the adenine base nuclei of ATP. The measurements were carried out in D_2O at a pD of 7.0 at 30°C. The ATP concentration is 0.30 M.

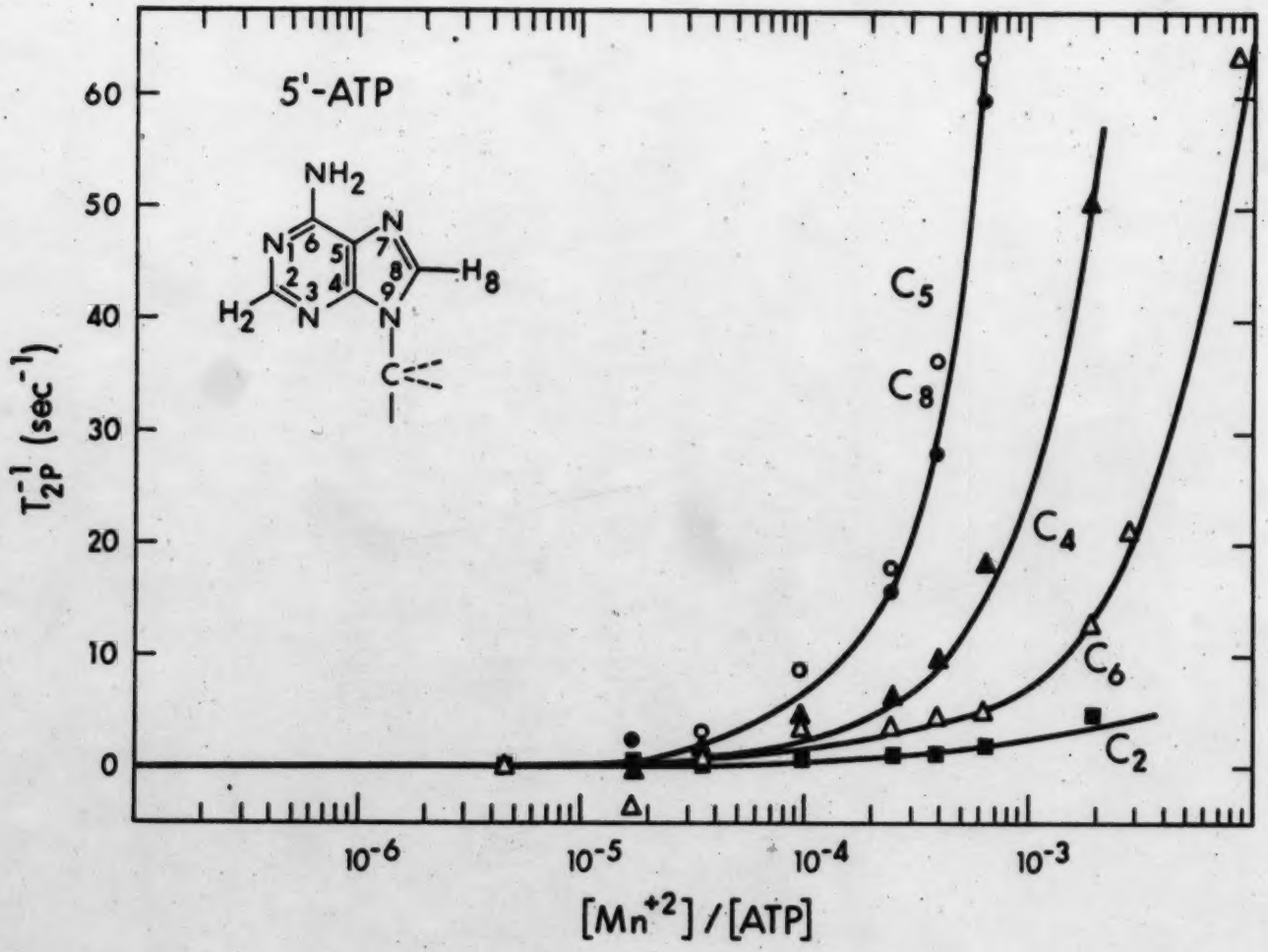
5'-ATP
NH2
N
N1 6 5 7
2 4 8
H2 3 N 9 N H8
C
60
50
40
30
20
10
0
T2P-1 (sec-1)
C5
C8
C4
C6
C2
10-6
10-5
10-4
10-3
[Mn+2] / [ATP]

TABLE III-1 . Summary of ^{13}C T_1p^{-1} and T_2p^{-1} Values for Mn(II)-ATP Solutions ‡.

	C-6	C-2	C-4	C-8	C-5
T_1^{-1} (sec^{-1}) [0.3M ATP]	0.158 ±0.006	5.88 ±0.35	0.169 ±0.007	7.69 ±0.59	0.153 ±0.006
T_1p^{-1}(sec^{-1})*	1.1±0.15	N.O.**	0.59±0.07	5.0±0.2	2.8±0.3
T_2p^{-1}(sec^{-1})*	4.1±0.8	0.03	10.7±0.5	28.6±2.4	33.4±2.6

‡ Experiments were carried out in D_2O at a pD of 7.0 at 30°C. [ATP] = 0.30 M; $[Mn^{+2}]/[ATP] = 3.7x10^{-4}$.

* Average values from five measurements scaled to a $[Mn^{+2}]/[ATP]$ ratio of $3.7x10^{-4}$.

** No change observed.

D. RESULTS (CONTINUED)

Spin-spin relaxation rates, T_2p^{-1}, were studied as a function of temperature. In Fig. III-6, the values of T_2p^{-1} for carbons C-5, C-8, C-6 and C-4 are plotted against the reciprocal of the absolute temperature. Carbon C-2 and the ribose carbon resonances remained unaffected by Mn(II) ions throughout the temperature range studied.

Spin-lattice relaxation rates, T_1p^{-1}, for carbons C-6, C-4, C-8 and C-5 were also measured at a higher temperature (60°C). These T_1p^{-1} values are tabulated in Table III-2 together with the data at 32°C for comparison purposes.

The T_1p^{-1} values for protons H-8 and H-2 were measured using ^1H NMR techniques at both of these temperatures. The results are in agreement with those of Sternlicht *et al* (1965b). The proton data as well as the ^{31}P T_1p^{-1} data for the α and γ ^{31}P nuclei obtained by Sternlicht *et al* (1965a) are tabulated in Table III-3. Finally, T_2p^{-1} values for the water protons in the Mn(II)-ATP solutions were measured over the same temperature ranges. The results are plotted in Fig. III-7.

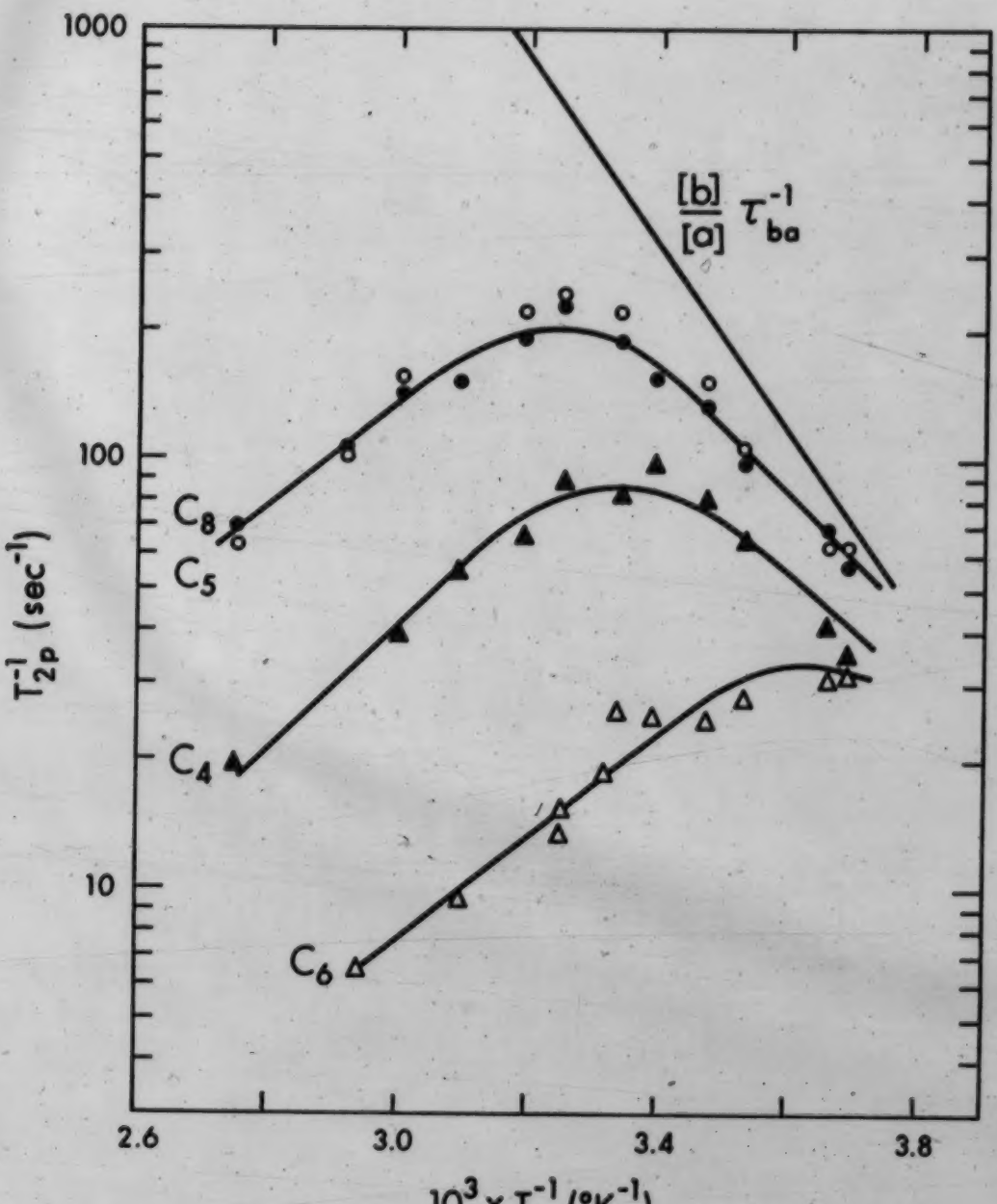

FIGURE III-6. The temperature dependence of T_{2p}^{-1} of the ATP ^{13}C nuclei. The values are scaled to the same $[Mn^{+2}]/[ATP]$ ratio of 2.5×10^{-3}. The figure shows only those carbons that are affected by the Mn(II) ion.

TABLE III-2. The T_1p^{-1} Temperature Dependence of the ^{13}C Nuclei in ATP.‡

	C-6	C-2	C-4	C-8	C-5
(A) At 32°C					
T_1[pure ATP](sec)	2.10±0.05	0.16±0.01	4.05±0.30	0.15±0.01	3.80±0.05
T_1p^{-1}(sec^{-1})	0.41±0.04	N.O.**	0.29±0.03	2.2±0.2	1.5±0.3
(B) At 60°C					
T_1[pure ATP](sec)	3.3±0.2	0.44±0.01	6.5±0.3	0.38±0.01	5.8±0.2
T_1p^{-1}(sec^{-1})	0.17±0.03	N.O.**	0.13±0.02	0.94±0.10	0.63±0.02
$T_1p^{-1}(32°)$ / $T_1p^{-1}(60°)$ ratio	2.4		2.2	2.3	2.4

‡ Experiments were carried out in H_2O at a pH of 7.0.

[ATP] = 0.30 M; $[Mn^{+2}]/[ATP] = 2.0 \times 10^{-4}$.

** No change observed.

TABLE III-3. The T_1p^{-1} Temperature Dependence of the ^1H and ^{31}P Nuclei in ATP.

	T(°C)	$T_1p^{-1}(sec^{-1})$		
		H-8‡	H-2‡	α,γ-^{31}P *
	32	41.0±4	9.8±1.0	12
	60	19.0±2	4.2±0.5	5.9
$\frac{T_1p^{-1}(32°)}{T_1p^{-1}(60°)}$	ratio	2.2	2.3	2.0

‡ The ^1H nmr experiments were carried out in H_2O at a pH of 7.0. [ATP] = 0.30 M; $[Mn^{+2}]/[ATP] = 3.9 \times 10^{-4}$ for H-8 and 9.2×10^{-4} for H-2. Different Mn(II) ion concentrations were used in studies of the two protons to increase the accuracy of the measurements.

* The ^{31}P data is from Sternlicht et al (1965a). The experiments were carried out in H_2O at a pH of 9.0, [ATP] = 0.35M and $[Mn^{+2}]/[ATP] = 1.1 \times 10^{-4}$.

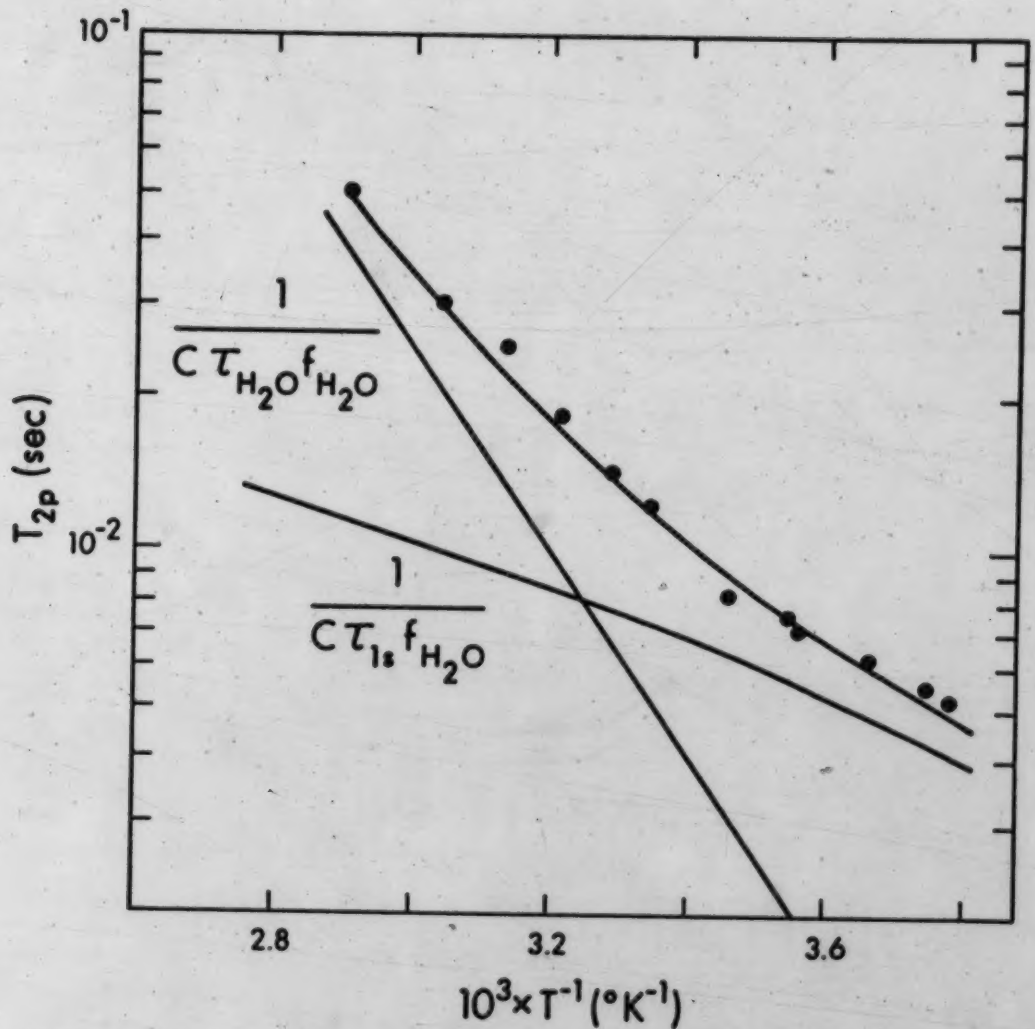

FIGURE III-7. The temperature dependence of the water proton transverse relaxation times in a Mn-ATP solution. The experiment was carried out at 100.0MHz in continuous wave mode. The solution (pH7.0) contained 0.27M ATP and 9.9×10^{-6}M $MnCl_2$ in triply distilled water. The curve is the calculated sum of the two straight lines evaluated using Eq. (III-29). The f_{H_2O} and C are defined in Eq. (III-29).

E. DISCUSSION

1. The Dominant Relaxation Mechanism of the ^{13}C T_2p^{-1} in the Present Study

The ribose carbon nuclei of ATP were not affected by Mn(II) ions, but those of the adenine base showed selective effects [Figs. (III-4) and (III-5)]. Qualitatively, the data suggest that the adenine ring of the ATP molecule is interacting with the metal ion, and the ribose carbon nuclei are not involved. Similar changes were also observed in adenosine-5'-monophosphate in the presence of Mn(II) ions (Kotowycz and Hayamizu, 1973).

As described in the theory, the observed relaxation rates (T_1p^{-1} and T_2p^{-1}) may be the results from either the two-site or the three-site system. Before the calculations of metal-carbon distances can be carried out from the T_1p results, the temperature dependence of T_2p^{-1} has to be considered in order to determine the appropriate exchange scheme for the Mn(II)-ATP system.

The results of the spin-spin relaxation rates shown in Fig. (III-6) fall into two regions:

(1) A high temperature region ($1/T<3.4\times10^{-3}$) in which

different carbons have their characteristic relaxation rates.

(ii) A low temperature region ($1/T > 3.4 \times 10^3$) in which the T_{2p}^{-1} rates show a change in slope and begin to converge to a constant value at low temperatures. As these carbon nuclei are in the same adenine ring, this dependence indicates that the observed T_{2p}^{-1} rates are approaching the slow exchange limit which is governed by a characteristic exchange rate [Eq.(III-6) or Eq.(III-13)].

In the low temperature region, a similar temperature dependence of T_{2p}^{-1} relaxation rates was observed for the adenine protons and the phosphorus nuclei of the phosphate groups (Sternlicht et al, 1965ab). These workers then suggested that a two-site exchange is adequate for the Mn(II)-ATP system and that one type of metal complex in the form of $M_{(p+r)}^{ATP}$ exists (Sternlicht et al, 1965b). However, the low temperature data are not conclusive as suggested in the theory section [Eq.(III-6) and (III-13)], since the relaxation rates may just be controlled by a certain NMR exchange rate. To show this feature, the ^{31}P T_{2p}^{-1} data obtained by Sternlicht et al (1965a) are plotted as the solid straight line in Fig. (III-6). It is seen that the ^{13}C relaxation rates also behave in the same

manner in this low temperature region.

At higher temperatures, the ^{31}P T_2p^{-1} relaxation rates are still in the slow exchange region (Sternlicht *et al*, 1965a), and the ^{1}H T_2p^{-1} relaxation rates are controlled by the dipolar interaction whose temperature dependence is dominated by the rotational motion of the whole Mn(II)-ATP complex (Sternlicht *et al*, 1965b). Therefore, no further information on the exchange processes can be obtained. However, the ^{13}C T_2p^{-1} relaxation rates are different.

Inspection of Eqs. (III-21) and (III-22) shows that the contribution of the dipolar interaction to T_2p^{-1} relaxation can be estimated from the magnitude of the T_1p^{-1} relaxation (Bernheim *et al*, 1959), namely, the first term in Eq.(III-22) is 7/6 of the T_1p^{-1} value. From the ^{13}C results (Table III-1), it is seen that the magnitudes of T_2p^{-1} are always larger than those of T_1p^{-1} , especially for carbons C-5 and C-8. Therefore, to a good approximation, the observed ^{13}C T_2p^{-1} in the high temperature region (Fig. (III-6); $1/T<3.4\times10^{3}$) are controlled mainly by the scalar mechanism.

2. The Temperature Dependence of T_{2p}^{-1}

The analysis will be started first in terms of a two-site exchange process and it will be shown that a three-site exchange process is most consistent with the data. In the case of a two-site exchange, since the scalar mechanism dominates the nuclear spin-spin relaxation, in the high temperature region, the observed relaxation rate T_{2p}^{-1} [Eqs. (III-7) and (III-22)] becomes:

$$T_{2p}^{-1} = \frac{[b]}{[a]} T_{2,b}^{-1} = \frac{[m]}{[ATP]} \left[\frac{1}{3} S(S+1) \left(\frac{A}{\hbar} \right)^2 \right] \tau_e$$

where $$\tau_e^{-1} = k_{ba} + \tau_{1S}^{-1} \qquad \text{(III-26)}$$

The magnitude of the exchange rate k_{ba} has been determined from the phosphorus exchange study and is about $2.3 \times 10^5 sec^{-1}$ at 27°C (Sternlicht *et al*, 1965a). The electronic spin-lattice relaxation rate τ_{1S}^{-1} is in the order of 10^7 sec^{-1} at the same temperature (Reed *et al*, 1971). Therefore, $\tau_e = \tau_{1S}$, and the observed T_{2p}^{-1} relaxation rate becomes:

$$T_{2p}^{-1} = \frac{[m]}{[ATP]} \left[\frac{1}{3} S(S+1) \left(\frac{A}{\hbar} \right)^2 \right] \tau_{1S} \qquad \text{(III-27)}$$

The principles of electronic relaxation have been described in the previous chapter. According to Bloembergen and Morgan (1961), τ_{1S} is governed by:

$$\tau_{1S}^{-1} = \frac{2}{50} \Delta^2 [4(S+1)S - 3] \left\{ \frac{\tau_V}{1 + \omega_S^2 \tau_V^2} + \frac{4\tau_V}{1 + 4\omega_S^2 \tau_V^2} \right\}$$

where $$\tau_V = \tau_V^{\circ} \exp (E_V / RT) \qquad \text{(III-28)}$$

Δ is the zero field splitting energy (in Gauss) and the other symbols were defined previously. In the above equation, only the Δ of 195 Gauss and τ_V of 8.5×10^{-12} sec (27°C) have been reported from EPR studies on Mn(II)-ATP solutions (Reed et al, 1971). In order to determine the temperature dependence of the electronic relaxation time over the temperature range used in the present study, water proton experiments were carried out. The T_{2p}^{-1} relaxation rates of the water protons in the Mn(II)-ATP solution are now considered.

In an early study on water protons in dilute Mn(II) ion solutions, Bernheim et al (1959) showed that the proton relaxation rates T_{2p}^{-1} are always in the rapid exchange region and are dominated by the scalar mechanism. By taking the reciprocal of Eq.(III-26), these researchers

showed that the data can be conveniently analysed in terms of the exchange rate and the electronic relaxation rate using the following equation:

$$T_{2p} = \frac{1}{C\ f_{H_2O}} \cdot \tau_{H_2O}^{-1} + \frac{1}{C\ f_{H_2O}} \cdot \tau_{1S}^{-1} \qquad \text{(III-29)}$$

where $f_{H_2O} = \frac{n\,[Mn]}{[H_2O]}$; $C = \frac{1}{3} S(S+1) \left(\frac{A}{\hbar}\right)^2_{H_2O}$

In the last term f_{H_2O}, n is equal to 3 as the number of exchangeable water molecules in the first coordination sphere of the Mn(II) ion is close to three in the presence of ATP (Heller et al, 1970; Zetter et al, 1973).

The individual temperature dependence of τ_{H_2O} and τ_{1S} is governed by equations (III-11) and (III-28) as described previously. By means of these equations, together with an appropriate set of trial parameters, the magnitudes of the two terms in Eq.(III-29) were evaluated and are shown as straight lines in Fig. (III-7). The best fit to the data was obtained by adding the two lines and it is shown as the solid curve in the figure. The parameters used are listed in Table III-4, together with those obtained from dilute Mn(II) aqueous solutions.

TABLE III-4. Parameters obtained in the Water Proton T_2p Analysis‡.

		Mn(II)-ATP Solution‡	Mn(II)-H_2O Solution
$\Delta H^{\ddagger}$	kcal/mole .	8.4	7.5^{ω} ; 7.82^{δ}
$\Delta S^{\ddagger}$	cal/deg ..	2.3	1.3^{ω} ; 1.38^{δ}
A/h	Hz	4.6×10^{5}	$2.0\times10^{5}{}^{\beta}$; $1.0\times10^{6}{}^{\omega}$
$\tau_v(27^{\circ})$	sec	8.5×10^{-12} *	$3.2\times10^{-12}{}^{\zeta}$; $2.4\times10^{-12}{}^{\omega}$
E_v	kcal/mole .	2.6	3.9^{ω}

‡ Experiments were carried out on a solution with [ATP] = 0.3M and $f_{H_2O} = 1.1\times10^{-4}$. The proton frequency is 100.0MHz.

* Value from Reed et al (1971).

β Value from Bernheim et al (1959).

δ Value from ^{17}C NMR study (Zetter, et al, 1972).

ω Value from Bloembergen and Morgan (1961).

ζ Value from Rubinstein et al (1971).

After determining the temperature dependence of the electronic relaxation time, the high temperature dependence of ^{13}C T_{2p}^{-1} can be evaluated from Eq.(III-28) [by varying the term A/h]. A typical trial to fit carbons C-8 and C-5 is shown as the "dashed" line in Fig. III-8. The low temperature dependence of T_{2p}^{-1} is shown as the line labelled with k_{21} [2]/[1] in the figure. The slope of this line is taken from Sternlicht et al (1965a) for reasons explained in the previous section (E-1). Then, by using Eq.(III-5), the resultant (overall) temperature profile of T_{2p}^{-1} can be evaluated. It was found that no matter how we changed the magnitudes of the two lines, the predicted profiles all had, in the high temperature region ($\gtrsim 40^{\circ}C$), a slope similar to that of the dashed line. Similar trials to fit other carbons failed due to the same reasons.

Another possible explanation for the peculiar ^{13}C T_{2p}^{-1} temperature dependence may be due to the contribution of the chemical shift effect which has been generally negligible in most Mn(II) ion complexes. In other words, the validity of using Eqs.(III-5) and hence (III-26,27) for analyzing the observed data requires the following condition (Swift and Connick, 1962): $(T_{2M} \cdot \tau_m)^{-1} >> \Delta\omega_M^2$

FIGURE III-8. The analysis of the temperature dependence of T_2p^{-1} for the carbon nuclei C-5 and C-8 [C-5 open circles, C-8 solid circles]. The limiting values to the curve are represented with the straight lines as discussed in the text.

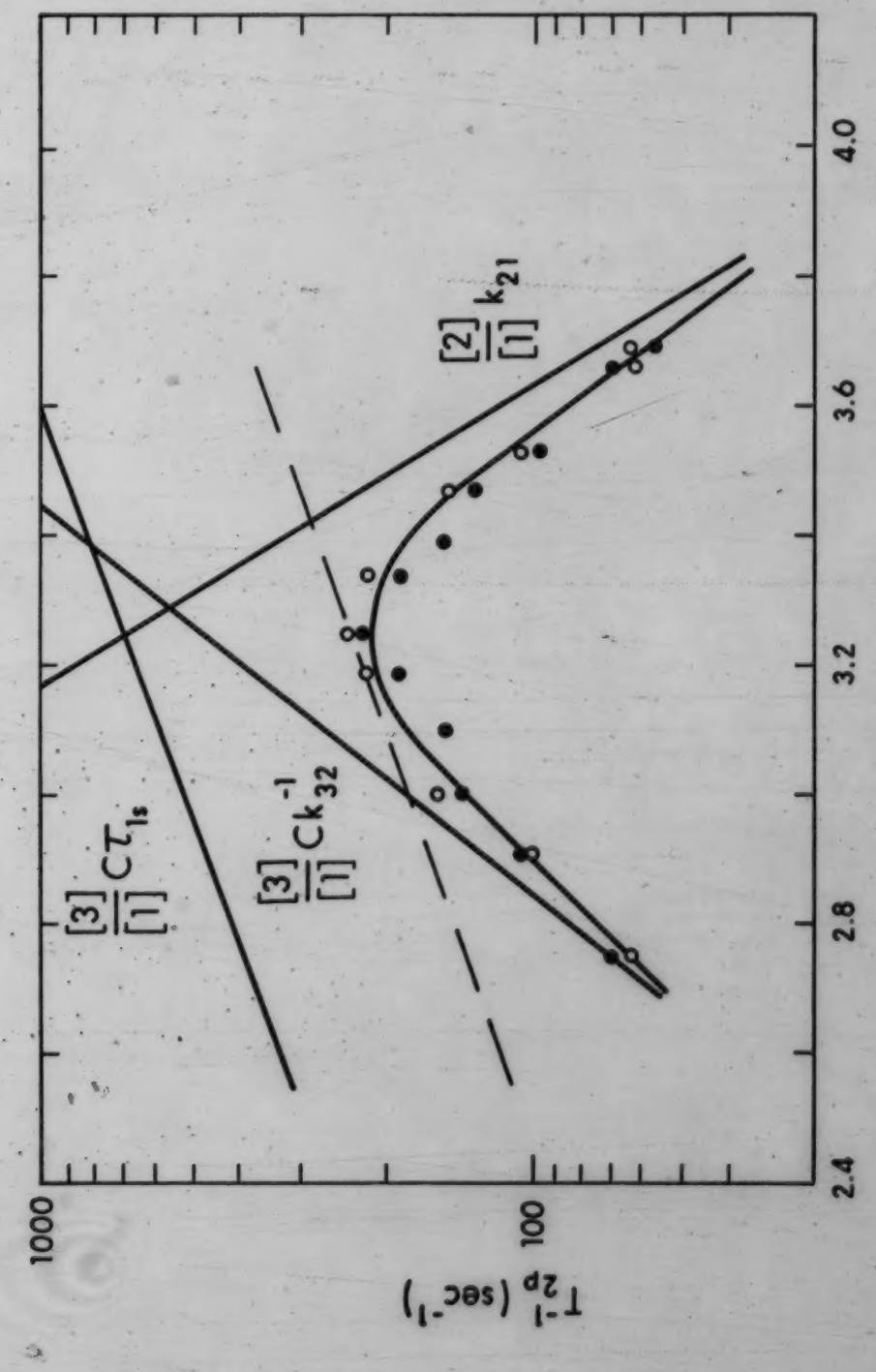
1000
100
T_{2p}^{-1} (sec^{-1})
2.4
2.8
3.2
3.6
4.0
$10^3 \times T^{-1}(°K^{-1})$
$\frac{[3]}{[1]} C\tau_{1s}$
$\frac{[3]}{[1]} Ck_{32}^{-1}$
$\frac{[2]}{[1]} k_{21}$

in which the $\Delta\omega_M$ term is given by Bloembergen (1957) as:

$$\Delta\omega_M = -\frac{A}{\hbar}\frac{g\beta\, S(S+1)}{\gamma_I\, 3\,k\,T}\cdot\omega_I$$

where k is Boltzman's constant, A/h is the scalar coupling constant (Hz) and other symbols have been defined previously. To justify the above condition, the magnitudes of these parameters ($\Delta\omega_M$, T_{2M} , τ_m) were estimated under the present experimental conditions [25.15MHz for the ^{13}C and in the high temperature regions ($\geq 30^{\circ}C$)]. Assuming that the scalar coupling constant for the ^{13}C nuclei may take the maximum value of 10^6 Hz as observed in the coupling between the Mn(II) electrons and the ^{31}P nuclei of ATP (Sternlicht et al, 1965a) [Subsequent results (Table III-5) show that the constants are about 5×10^5 Hz], the $\Delta\omega_M^2$ is 9×10^8 Hz^2, calculated with the preceding equation at 25.15MHz and at 40.0°C. At this temperature, T_{2M}^{-1} is $5\times10^6 sec^{-1}$, calculated from the scalar term in Eq.(III-26) in which the value of τ_e is 4.3×10^{-8}sec [calculated from the results in Table III-4]. Finally, at the same temperature, the NMR exchange rate is 10^6 sec^{-1} calculated from Sternlicht et al ^{31}P data (1965a). Hence, the product $(T_{2M}\cdot\tau_m)^{-1}$ is 5×10^{12} sec^{-2}, which is much bigger than the $\Delta\omega_M^2$ (9×10^8 Hz^2). Therefore, Eqs.(III-5,26 and 27) are valid for the present case and the chemical shift effect also does not affect the ^{13}C

relaxations. In summary, a two-site exchange is not likely from the present findings.

3. The Three-Site Scheme

3A. The T_2p^{-1} Temperature Dependence

In the three-site scheme presented in the theory section, the ^{13}C T_2p^{-1} relaxation rates may be in the following regions:

(i) In the high temperature region, from Eq.(III-15), the rate is:

$$T_2p^{-1} = \frac{[2]}{[1]} \cdot T_{2,3}^{-1} = \frac{[M_{(p+r)}ATP]}{[ATP]} \cdot \frac{S(S+1)}{3\hbar^2} A^2 \tau_e$$

where $$\tau_e^{-1} = \tau_{1S}^{-1} + k_{32} \qquad \text{(III-30)}$$

(ii) In the low temperature region, from Eq.(III-13), the rate is:

$$T_2p^{-1} = \frac{[2]}{[1]} \cdot k_{21} = \frac{[M_{(p)}ATP]}{[ATP]} \cdot k_{21} \qquad \text{(III-31)}$$

The overall paramagnetic relaxation rate at every temperature may be approximated by adding the reciprocals of the limiting values from these equations. Therefore, the tem-

perature dependence of T_{2p}^{-1} is then a function of the exchange rates k_{21}, k_{32} and the electronic relaxation time. Inspection of the related equations shows that there are several parameters that govern the temperature dependence. Nevertheless, some of them have been determined. As shown previously [section E1], the values of T_{2p}^{-1} for the ^{31}P, ^{1}H and ^{13}C nuclei in the low temperature region actually reflect the same exchange process. Hence, part of the temperature variation of T_{2p}^{-1}, i.e. that of k_{21} in Eq.(III-31), is the same as that obtained from the previous ^{31}P NMR observations (Sternlicht et al, 1965a). Furthermore, the temperature dependence of the electronic relaxation time can now be evaluated from the parameters obtained from the water proton experiment (Table III-4). Consequently, the parameters to be determined reduce to the following:

(i) The concentration of complexes [2] and [3];

(ii) The individual coupling constants A/h(Hz);

(iii) The activation parameters that govern The k_{23} exchange rate.

Using the above procedures and varying the three groups of parameters, a fit to the carbon C-8 and C-5 data is plotted in Fig. III-8. In the figure, the labelled straight lines represent the limiting values of the corresponding relaxation rates for k_{32}, k_{21} and T_{1S}^{-1}

individually. The calculated results on the basis of this analysis are shown as the solid curve in the figure. A satisfactory fitting to the data for the other carbons was similarly obtained and these results are plotted as solid curves in Fig. III-6. The parameters used in the analysis are as follows:

(i) The distribution of the Mn(II) ions in ATP is $[\underline{2}] = 0.80[Mn^{+2}]$ and $[\underline{3}] = 0.2[Mn^{+2}]$. The uncertainty is estimated as $\pm 0.06[Mn^{+2}]$.

(ii) The coupling constants A/h for the carbon nuclei are listed in Table III-5. The magnitude of these constants are comparable to those observed in Mn(II) ions with ^{13}C of pyruvate (Fung et al, 1973), ^{17}O and ^{1}H of water (Swift and Connick, 1962), and ^{31}P of ATP (Sternlicht et al, 1965a).

TABLE III-5. Scalar Coupling Constants‡ between the Adenine Base Carbon Nuclei of ATP and Mn(II) ion.

	C-8	C-5	C-4	C-6
A/h (Hz)	4.9×10^5	4.9×10^5	2.8×10^5	1.2×10^5

‡ The values are obtained from the fitting of the data in Fig. III-6.

(iii) The activation parameters and the resultant NMR exchange rate k_{32} at 27°C are listed in Table III-6.

TABLE III-6. The Activation Parameters and the NMR Exchange Rate for the 3 $\rightleftharpoons$ 2 Process in the Mn(II)-ATP System.‡

$\Delta H^{\mp}$ (Kcal/mole)	$\Delta S^{\mp}$ (cal/deg)	$k_{32}(sec^{-1})$
7.1	-1.2	2.7×10^{7} (27°C)

‡ The solution composition is [ATP] = 0.3 M; $[Mn^{+2}] = 7.6 \times 10^{-4}$ M; [2] = 0.8 $[Mn^{+2}]$; [3] = 0.2 $[Mn^{+2}]$.

3B. The T_1p^{-1} Temperature Dependence

Further information can be obtained from the comparison of the spin-lattice relaxation rates as a function of temperature for different ATP nuclei. The ^{31}P T_1p^{-1} values decrease two-fold when the temperature increases from 32°C to 60°C (Table III-3). In this high temperature region, the rate is governed by Eqs. (III-19) and (III-21) which are summarized as:

$$T_1p^{-1}(^{31}P) = \frac{[m]}{[ATP]} \cdot \left[\frac{2S(S+1)\ g^2\beta^2\gamma_I^2}{5\ R^6}\right] \cdot \tau_R \qquad \text{(III-32)}$$

In this equation, the possible variables which can change with temperature are the concentration of the metal complexes [m] and the rotational correlation time τ_R. Since the binding between the metal ions and ATP is very strong, the former term [m] is invariant with temperature. This property is indicated by the large overall formation constant and the small enthalpy of formation for the complexes [$K_f = 3.1\times10^6 M^{-1}$(25°C) and $\Delta H = -3.0$Kcal mole^{-1} (Mohan and Rechnitz, 1974; Taqui Khan and Martell, 1966)]. Thus, the temperature dependence is due to the rotational correlation time τ_R.

A similar decrease in the relaxation rates with temperature was observed for the ^{13}C and ^1H nuclei (Tables III-2 and III-3). For these nuclei, their relaxation is governed by Eqs. (III-18) and (III-21) which are summarized as follows:

$$T_1p^{-1}(^{13}C \text{ or } ^1H) = \frac{[\underline{3}]}{[ATP]} \cdot \left[\frac{2S(S+1)\ g^2\beta^2\gamma_I^2}{5\ R^6}\right] \cdot \tau_R \qquad \text{(III-33)}$$

Similarly, the temperature dependence may be due to τ_R or the concentration of species [$\underline{3}$]. The latter term could vary if a redistribution of the Mn(II)-ATP complexes in the

$\underline{2} \rightleftharpoons \underline{3}$ equilibrium occurs with temperature. Nevertheless, from the preceding analysis of the T_2p^{-1} data, the concentration of species $\underline{3}$, $[\underline{3}]$, is equal to $0.2[m]$ over the whole temperature range and therefore is a constant. Thus, the consistent explanation to the present comparison is that all the ATP nuclei have a very similar correlation time τ_R and hence exhibit the same temperature dependence. This result further supports the presence of the backbound complex in which the phosphates and the adenine ring nuclei are intramolecularly bound to the same Mn(II) ion (Sternlicht et al, 1965b).

4. Geometry of the Backbound Mn(II)-ATP Complex

According to Eq.(III-33), the observed spin-lattice relaxation rate T_1p^{-1} is a function of the nuclear relaxation in the backbound complex. The data in Table III-1 can therefore be used to estimate the Mn(II) ion to carbon distances. From the preceeding discussion, τ_R of the phosphorus nuclei gives a consistent explanation for both ^{13}C and ^{1}H relaxation rates. Furthermore, the use of τ_R to stand for the overall dipolar correlation time, τ_C, is justified by considering the relative magnitudes of all the relevant correlation times (at 27°C):

(i) The rotational rate, τ_R^{-1}, is $1\times10^9 sec^{-1}$ (Sternlicht et al, 1965a).

(ii) The exchange rate, k_{32}, is $2.7\times10^7 sec^{-1}$ (Table III-6).

(iii) The electronic relaxation rate, τ_{1S}^{-1}, is $2\times10^7 sec^{-1}$ (24KGauss), calculated with Eq.(III-28) and using the relevant parameters listed in Table III-4.

Since

$$\tau_c^{-1} = \tau_R^{-1} + k_{32} + \tau_{1S}^{-1}$$

therefore, the value of τ_R (1×10^{-9}sec) can be used in Eq.(III-33) for the calculations. In addition, another value of 3×10^{-10}sec, corresponding to the rotational time of the water protons in a hexaquo-Mn(II) ion complex, was used in the early ^1H NMR studies (Sternlicht et al, 1965b). Therefore, both values of τ_R were used to calculate the distances and the results are summarized in Table III-7.

In Row I of the table where τ_R of the water protons is used, the distances are so short that the Mn(II) ion cannot be located properly. For example, the distance from the C-8 carbon to the Mn(II) ion is 2.5A which is even shorter than that between the water protons and the Mn(II) ion where there is direct coordination (Reuben and Cohn, 1970). However, when τ_R of the phosphorus nuclei is used,

TABLE III-7. Metal-Nuclei Distances (A) for the Mn(II)-ATP Backbound Complex.

	C-6	C-4	C-5	C-8	H-8	H-2	H-1'
I. $3x10^{-10}$(sec)	3.2±.2	3.6±.2	2.8±.2	2.5±.2	2.7*	3.5*	4.5*
II. $1x10^{-9}$(sec)	4.0±.2	4.4±.2	3.4±.2	3.1±.2	3.4*	4.4*	5.7*
III. Model Study** $M_{(p+r)}ATP$	4.0±.3	4.6±.3	3.4±.3	3.2±.3	3.3±.3 3.5±.3+	6.9±.3 6.8±.3+	6.5±.3+
IV. Model Study‡ $M_{(p)}ATP$	7.1±.3	8.1±.3	6.8±.3	6.6±.3			

* Proton-metal ion distances recalculated from the data of Sternlicht et al (1965b), using [3]/[ATP] instead of $[Mn^{+2}]/[ATP]$.

+ Distances for the proposed Mn-ATP complex (Sundaralingam, 1969).

** Predicted distances from the model backbound complex as discussed in the text.

‡ Calculated minimum distances for the $M_{(p)}ATP$ model complex, as discussed in the text.

the results (Row II) give a set of distances which suitably locates the Mn(II) ion close to the N-7 nitrogen. Also with this value, the proton to Mn(II) ion distances were recalculated from the data of Sternlicht et al (1965b), using the concentration factor [3] /[ATP] instead of $[Mn^{+2}]/[ATP]$. All these distances agree very well with those (Row III) predicted from a model backbound complex (Fig. III-9). In the model, the predicted distances were calculated by placing the Mn(II) ion 2.3A from the nitrogen N-7 and in the same plane as the adenine ring. The bond angles and bond lengths of ATP used in the calculations were obtained from earlier X-ray studies (Kraut and Jensen, 1963; Kennard et al, 1971). According to the geometry (Fig. III-9), a "bridging" water molecule is not present between the Mn(II) ion and the N-7 nitrogen in the backbound complex.

Finally, the question of whether the nuclear relaxation rate $T_{1,2}^{-1}$ due to the Mn(II) ion in the $M_{(p)}ATP$ complex can be neglected with respect to the $T_{1,3}^{-1}$ relaxation rate must be answered. First of all, the distance between the Mn(II) ion and the N-7 nitrogen of the adenine base for the $M_{(p)}ATP$ complex is estimated. As there are nearly three (kinetically equivalent) mobile water molecules exchanging between the solvent and the

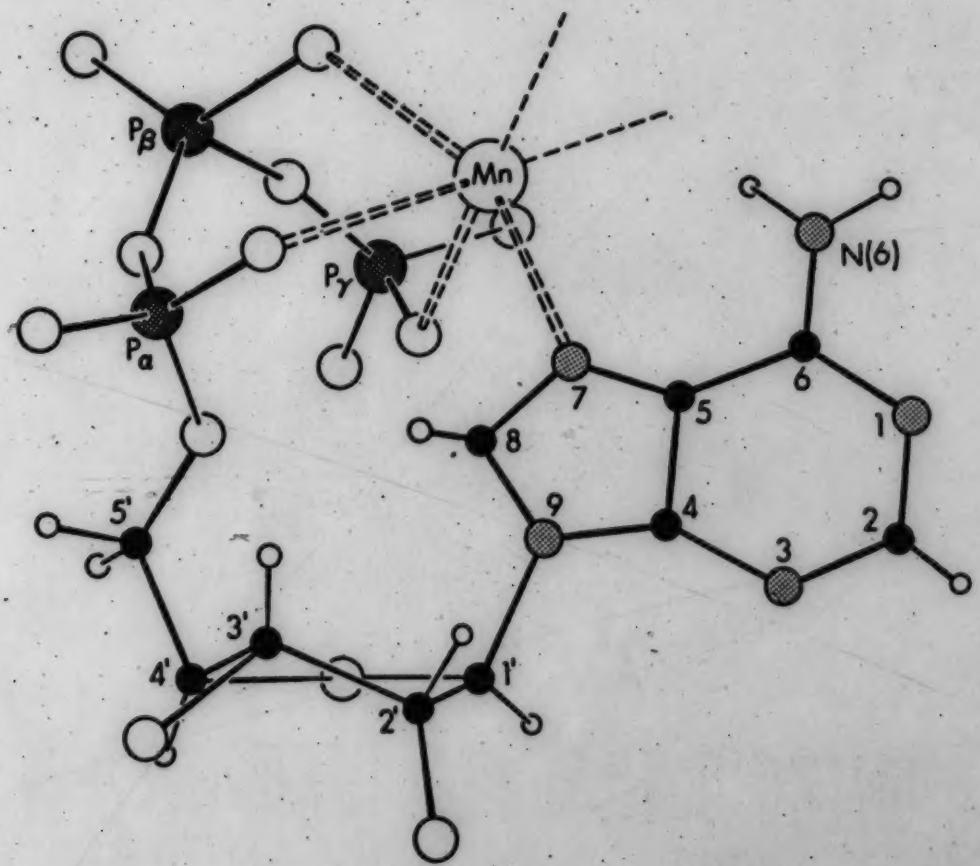

FIGURE III-9. Proposed structure for the Mn(II)-ATP backbound complex in solution.

coordination sphere of the complex (Zetter et al, 1973), hence, the closest separation between the Mn(II) ion and the N-7 must be large enough at least to insert a water molecule. Also, the distance between N-7 and the proton of this water molecule cannot be shorter than the length of a hydrogen bond, otherwise, a slowly exchanging or non-equivalent water molecule should be detected for the Mn(II)-ATP system. This distance is therefore chosen as 3A, since the hydrogen bond length is as large as 3A between the water protons and the ATP nuclei in the solid state (Kennard et al, 1971). The average distance between a Mn(II) ion and the water protons in the first coordination sphere is 2.8A, as described in the previous chapter. Therefore, the Mn(II) ion to N-7 nitrogen distance is taken as 5.8A, assuming that the metal ion, the hydrogen of the water and the N-7 nitrogen of the adenine base are colinear.

Then, following the same approach as was used for the preceeding model calculation except now the Mn(II) ion to N-7 distance is 5.8A instead of 2.3A, the Mn(II) ion to the adenine carbon distances are calculated and are also listed in Table III-7 (Row IV). These distances are much longer than those of the backbound complex (Row II). Furthermore, the relative magnitudes of the paramagnetic

nuclear relaxation rates for the two complexes, $T_{1,2}^{-1}$ / $T_{1,3}^{-1}$, can be estmated by taking the ratio of these distances [Eq.(III-33)],i.e. [R (Row II) / R (Row IV)]^6. This assumes that the other parameters in Eq.(III-33) for both complexes are the same. The ratios are 0.032, 0.025, 0.016 and 0.011 respectively for C-6, C-4, C-5 and C-8. Hence, the maximum contribution from $T_{1,2}^{-1}$ estimated from the $M_{(p)}ATP$ model is only about 1% to 3% of the $T_{1,3}^{-1}$ values for the backbound complex. Therefore, the contribution from $T_{1,2}^{-1}$ is neglected in the present data analysis.

F. CONCLUSIONS

A consecutive three-site NMR exchange mechanism is used to interpret the ^{13}C data. The results suggest the co-existence of two Mn(II)-ATP complexes in a ratio of 80% to 20%. Other minor complexes may exist as a result of bindings at other adenine nitrogens or even the ribose oxygens. Nevertheless, the fraction of these complexes, if present, is much less than 5%, and hence very difficult to detect using NMR paramagnetic relaxation techniques.

The formation of the backbound complex, $M_{(p+r)}ATP$, proceeds via an intermediate complex $M_{(p)}ATP$

in which only the phosphates are bound to the Mn(II) ion. The NMR exchange rate between the two complexes is very fast ($k_{32} = 2.7 \times 10^7 sec^{-1}$ at 27°C) when compared to that between $M_{(p)}ATP$ and the unbound ATP ($k_{21} = 2.3 \times 10^5 sec^{-1}$ at 27°C) (Sternlicht et al, 1965a). The presence of the phosphate-Mn(II) ion binding facilitates the secondary ring-Mn(II) ion binding. This is in agreement with the fact that adenosine does not bind Mn(II) ions (Schneider et al, 1964).

The intermediate complex accounts for 80% of the Mn(II)-ATP complexes. Consequently, most of the Mn(II) ions have three coordination sites for the water solvent molecules (the three phosphates account for the other three sites). This number agrees with other indirect studies based on ^{17}O NMR (Zetter et al, 1973) and ^{1}H NMR (Heller et al, 1970). The remainder (20%) is the backbound complex. Hence, the adenine-ring-Mn(II) ion interaction may not be large enough to be detected by the kinetic study (Hammes and Miller, 1967). Nevertheless, the presence of both complexes may explain the similar yet not identical properties of Mn(II) and Mg(II) ions in the presence of ATP, since for the Mg(II)-ATP complex, there is no ring interaction as described in the introduction.

CHAPTER IV

SELF ASSOCIATION OF FOLIC ACID IN AQUEOUS SOLUTION BY PROTON MAGNETIC RESONANCE

A. INTRODUCTION

Folic acid (Latin, folium, leaf) is a widely distributed vitamin which was first extracted from spinach leaves (Mitchell *et al*, 1941; Angier *et al*, 1946). In aqueous solutions at neutral pH, folic acid exists as a divalent anion, folate, as shown in Fig. IV-1-(A) (Albert, 1953; Pastore, 1971). It consists of three characteristic building units: (1) a substituted pterine, (2) p-amino-benzoic acid, and (3) glutamic acid.

Folic acid can undergo a variety of reactions and the resultant derivatives have different biological activities (Rabinowitz, 1960). For example, the addition of hydrogen atoms at the 7 and 8 positions produces a dihydro-folic acid; further hydrogenation at the 5 and 6 positions gives a tetrahydro-folic acid. These two folic derivatives are the active forms of folic acid in most biological systems (Sauberlich and Baumann, 1948; Bond *et al*, 1949).

A. Folate (pD 7.1)

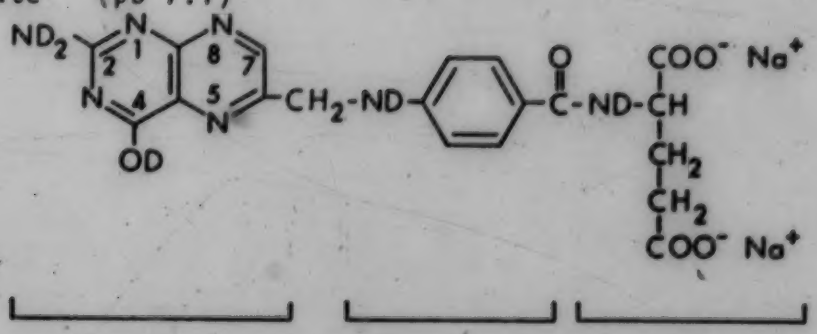

2-Amino-4-hydroxyl-6-methylpterin unit | p-Aminobenzoic acid unit | Glutamic acid unit

B. Model Compound I (pD 12.5)

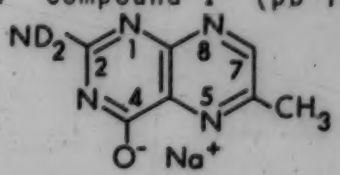

2-Amino-4-hydroxyl-6-methyl pterin

C. Model Compound II (pD 7.1)

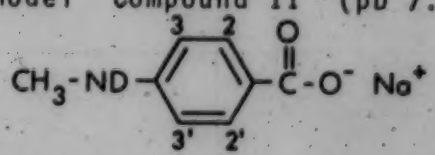

Sodium p-(N-methy)-amino-benzoate

FIGURE IV-1. Formula structures of folic acid and the two model compounds. All labile protons in the structures are denoted with "D".

However, halogenation of the aromatic benzoic acid unit deactivates the folic acid (Consulich et al, 1951). Some folic acid analogues, such as N^{10}-methyl-folate and N^{10}-methyl-C^4-amino-folate (Methotrexate), may even have inhibitory effects on the folate enzyme systems.

Metabolically, the most important role of folic acid is its function as a one carbon unit carrier (Shive et al , 1947) in a number of biosyntheses, for example, of the purines (Greenberg, 1954), serine (Blakley, 1954) and thymidylate (Wahba and Friedkin, 1962; Pastore and Friedkin, 1962). A deficiency of folic acid induces the failure of these biosyntheses in organisms and mammals (Jaenicke, 1964; Lukby and Cooperman, 1964). The biological functions and the chemistry of folic acid and its various derivatives have been the subject of extensive research (Rabinowitz, 1960; Brown and Reynolds, 1963; Whiteley, 1971).

In an earlier NMR study, Pastore(1971) observed different temperature dependences in the proton chemical shifts of folic acid and its analogues. The researcher proposed that folic acid is different from its analogues by forming complexes through self-association. The nature of these complexes , however, has not been worked out. Inspection of the molecular model of folic acid indicates that it can exist either in an extended conformation or in

a partly-folded conformation in which the pterine ring lies partially over the benzoic acid fragment of the same molecule. Several coenzymes have been shown to exist in a completely folded conformation in aqueous solutions, for example, the pyridine dinucleotides (Sarma and Kaplan, 1969 and 1970a,b), and flavin adenine dinucleotide FAD (Sarma et al, 1968; Kotowycz et al, 1969).

In addition, for large molecules with aromatic and aliphatic groups in aqueous solutions, intermolecular association may also exist, as has been observed in purine nucleosides and nucleotides from osmotic-pressure studies (Ts'O et al, 1963; Ts'O and Chan, 1964) as well as in aliphatic fatty acids from NMR studies (Inoue and Nakagawa, 1966; Muller and Birkhahn, 1967).

To distinguish the most probable conformation for folic acid and its mode of association, ^{1}H NMR techniques were employed since the proton resonances corresponding to the two characteristic aromatic units in the folate molecule [Fig. IV-1-(A)] are clearly resolved (Fig. IV-2).

In the presence of a magnetic field, a diamagnetic current of the mobile π electrons is induced in the aromatic ring. This gives rise to a small secondary magnetic field which, in turn, affects the magnetic pro-

perties of the surrounding nuclei (Waugh and Fessenden, 1957; Johnson and Bovey, 1958). Consequently, in the space directly above or below the ring, the two fields are opposed. A proton in this space is then shielded and experiences a high-field shift. However, when the proton is in the periphery of the ring, where the magnetic fields are reinforced, a low-field shift of the proton results. Therefore, the proton chemical shifts of folate can be used to monitor the regional magnetic environment, which in turn can give further information on the conformation and intermolecular association of folic acid. This principle of "diamagnetic ring-current effect" (Johnson and Bovey, 1958) has been employed to interpret the data in the conformational studies of purine nucleosides and nucleotides in aqueous solutions (Jardetzky, 1960; Ts'O et al ,1969).

By measuring the ^1H chemical shifts, a comparative study between folate and the model compounds was carried out. Two model compounds for this study were chosen [Fig. IV-1-(B) and-(C)]. The first one is 2-amino-4-hydroxy-6-methyl pterine. This compound will be refered to as model compound I from now on. It is the model for the pterine unit of the folate molecule. The second compound is sodium p-(N-methyl)-amino-benzoate, refered to

as model compound II from now on. It is the model for the benzene region of folate. Comparison of the proton chemical shifts of the model compounds with that of folic acid shows that folic acid exists in solution in an extended conformation (unfolded). In addition, the chemical shifts of the folate protons were studied as a function of temperature and folate concentration. On the basis of these dependences, the folate molecules are shown to associate intermolecularly. A model for the stacking is proposed.

B. EXPERIMENTAL SECTION

1. Materials and Sample Preparation

Folic acid (acid form) was purchased from Calbiochem, California. As the acid form does not dissolve in water, it was dissolved in a very dilute aqueous sodium hydroxide solution and the pH was adjusted to about 6 to form the divalent anion (folate) (Albert, 1953).

The folate solution (pH about 6) was passed through a cation-exchange resin to eliminate any possible heavy metal ion impurities (Albert, 1953). The effluent was then adjusted to a pH of 7 and concentrated by freeze-drying. A yellow powdery salt, disodium folate (M.W. 485.4), was obtained.

The salt was redissolved in D_2O and the solution was freeze-dried again. By repeating this procedure three times, most of the labile protons [Fig. IV-1-(A)] were replaced by deuterium so that the original proton signals were eliminated and would not obstruct the appearance of the other folate proton resonances.

Model compound I, 2-amino-4-hydroxy-6-methyl pterine (M.W.180.2), was obtained from Dr. R.B. Angier, Lederle Labs., American Cyanamid Company. It was

synthesized using the procedure developed by Angier et al (1952). This compound would dissolve in D_2O only at a pD of 12.9. Hence, a series of folic acid samples were also studied at this value of the pD so that the results can be compared with that in the model compound.

Model compound II, sodium-p-(N-methyl)-benzoate (M.W.173.2), was purchased from K.and K. Labs., California.

The internal reference, sodium-2,2-dimethyl-2-silapentane-5-sulfonate (DSS), was from Merck, Sharp and Dohme of Canada Ltd., Quebec.

For the NMR experiments, all solutions were prepared by weighing both the solutes and the D_2O solvent, hence the concentrations are expressed in molalities. The quantity of DSS used was kept to a minimum (0.8 mg/gm D_2O), so that its influence on the compound under study was minimal. All solutions used were in D_2O and at a pD of 7.1±0.1, obtained by adding 0.4 units to the observed pH meter readings (Glasoe and Long, 1960).

2. Instrumental Techniques

Proton NMR experiments were carried out on the Varian HA-100-15 (100.0 MHz) and the Bruker HFX-90 (90.0 MHz) NMR spectrometers in the continuous wave mode. The first part of the experiments was carried out on the Varian spectrometer. The remainder of the experiments were carried out on the Bruker spectrometer after it was installed since the latter spectrometer is equipped with a heteronuclear lock system.

For measurements on the Varian spectrometer, a 5% tetramethyl-silane (TMS) solution in deuterated acetone was sealed in a small capillary and placed into the NMR tube containing the sample. The proton resonance of TMS was thus used as a lock signal. For the measurements on the Bruker spectrometer, the deuterium resonance of the solvent D_2O was used for the heteronuclear lock signal. Several measurements at various temperatures were repeated on both spectrometers and the results were reproducible.

The temperature was calibrated and rechecked every one and a half hours, using an ethylene glycol standard sample. The difference in chemical shifts between the hydroxyl protons and the ethyl protons was used to evaluate the temperature. The calibration chart was

obtained from Dr. O. Yamamoto, National Chemical Laboratory for Industry, Tokyo, Japan (Yamamoto and Yanagisawa, 1970). All samples were placed in the NMR probe 20 minutes before taking the measurements.

All chemical shifts were calibrated with respect to the internal DSS signal. The use of an internal reference avoids the ambiguity that may arise from the variation of the bulk magnetic susceptibility when an external reference is used (Blackburn et al, 1969). All the chemical shifts reported in this chapter represent the average of three measurements. Their values are reported in ppm. Hence, a low field shift corresponds to a large ppm value.

C. RESULTS

1. Proton NMR Spectra

The 100.0 MHz ^1H NMR spectrum of folate in D_2O at 30.5°C is shown in Fig. IV-2. The resonances were previously assigned by Pastore *et al* (1963). In the spectrum, H-2 and H-3 designate the resonances corresponding to the four benzene ring protons. H-1 and H-4 are those from the protons in the pterine ring and the methylene bridge, $-CH_2-ND-$, between the pterine and benzoic acid units. The multiplet at 4.4 ppm adjacent to low field of the H-4 resonance corresponds to the α-CH proton resonance of the glutamate unit, and H-5 represents the resonances for the four remaining protons in the same unit. The latter resonances remained unchanged when either the temperature or the concentration of the folic acid was varied. Therefore, the most intense peak of the resonances was used to denote the chemical shifts for these protons.

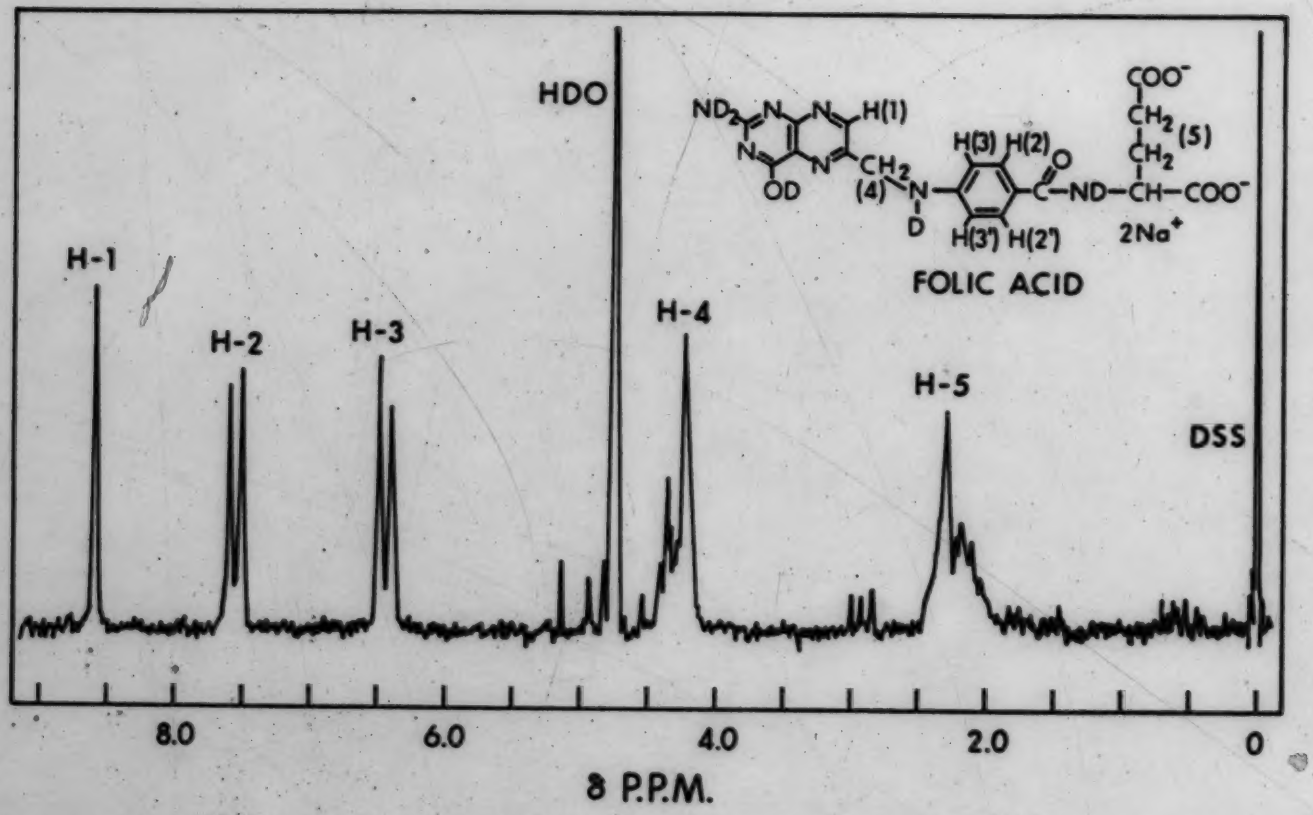

FIGURE IV-2. The 100.0 MHz NMR spectrum of 0.049m disodium folate in D_2O (pD 7.1; 30.5°C). The chemical shifts are measured with respect to internal DSS.

The ^{1}H NMR spectra of model compound I and model compound II are shown in Fig. IV-3-(A) and Fig. IV-3-(B) respectively. Model compound I shows two proton signals which are assigned to the -CH- and $-CH_3$ protons (Whiteley and Huennekens, 1967). In the present study, the signal at 8.5 ppm was used in the comparative study with the H-1 proton shifts of folate (Fig. IV-2).

Model compound II shows a singlet corresponding to the N-methyl protons (2.8ppm) and the doublet for the aromatic ring protons. The aromatic resonances were assigned according to the studies on disubstituted benzene derivatives (Martin and Dailey, 1963; Smith, 1964). Chemical shifts of these protons, denoted by H-2 and H-3 in Fig. IV-3-(B), were compared with those of the corresponding folate protons (Fig. IV-2).

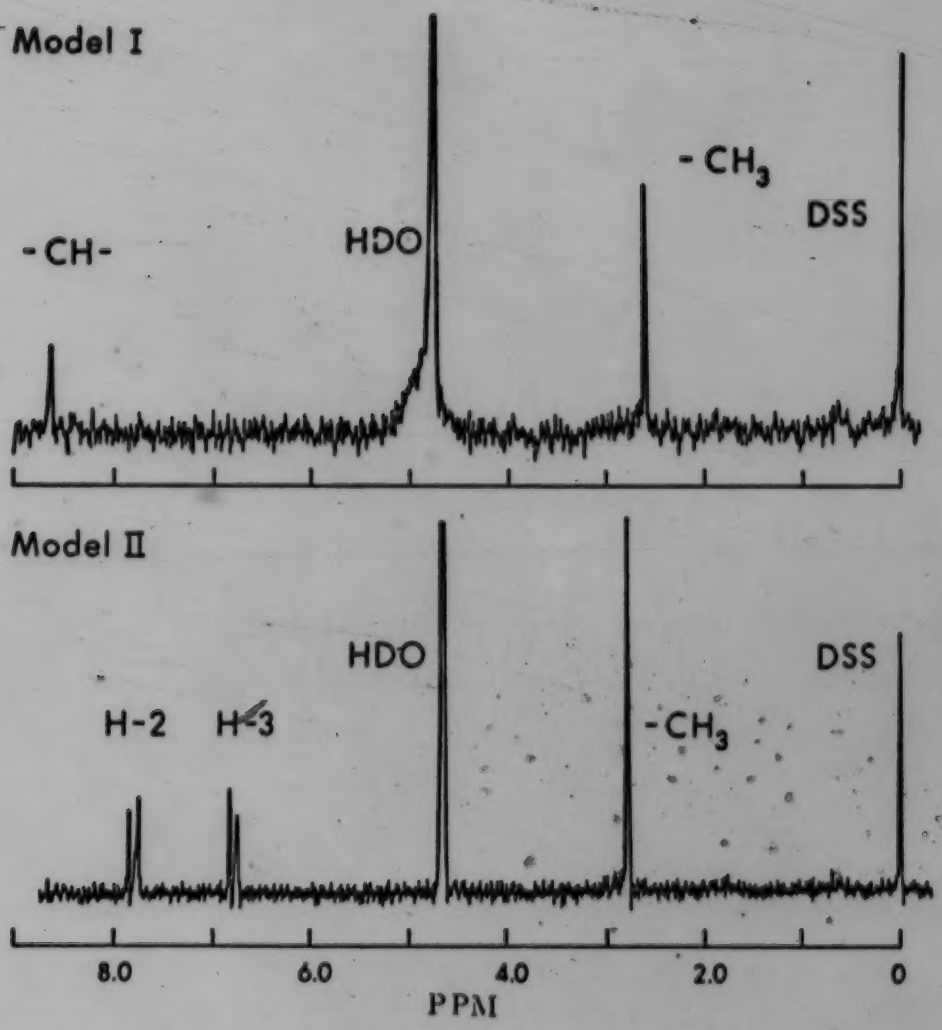

FIGURE IV-3. The 100.0 MHz ^1H NMR spectrum of the model compounds in D_2O at 30.5°C.

(A) Model Compound I (0.035mM at pD 12.9), and

(B) Model Compound II (0.060mM at pD 7.1).

2. The Concentration Dependence of the Chemical Shifts

The chemical shifts of folate protons were measured at 30.5°C as a function of the folate concentration. The results are shown in Fig. IV-4. The concentration ranged between 0.0091m (the lower concentration limit of the instrument) and 0.094m (the upper solubility limit of folate in D_2O). Protons H-1 and H-4 experience the largest shift (to low field) with the decrease in concentration. However, protons H-5 remained unchanged. By extrapolating the data to infinite dilution using a least-squares analysis, the limiting shifts were obtained. These results are summarized in Table IV-1, together with the proton chemical shifts for the most concentrated folate solution for comparison purpose.

Similar experiments were carried out at 30.5°C for both the folate solution at a pD of 12.9, and the model compound I solution also at this pD. The chemical shifts for the folate proton H-1 and the -CH- proton of model compound I are tabulated in Table IV-2 as a function of concentration. The limiting shifts for these protons were obtained by extrapolation as described above.

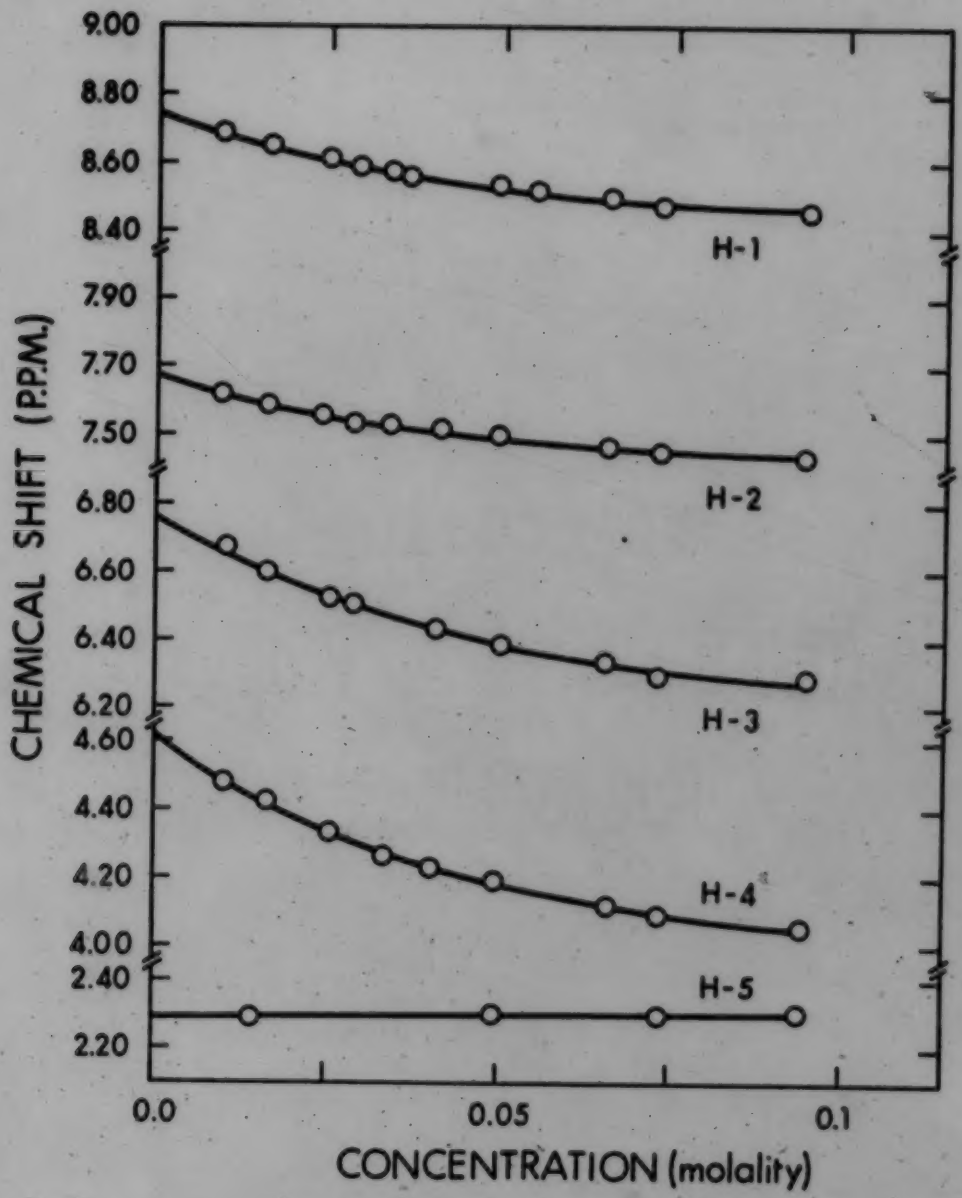

FIGURE IV-4. The concentration dependence of the proton chemical shifts of disodium folate in D_2O (pD7.1; 30.5°C).

TABLE IV-1. The Concentration Dependence of Proton Chemical Shifts of Disodium Folate in D_2O at 30.5°C and a pD of 7.1.

Concentration (m)	Shift* (ppm)				
	H-1	H-2	H-3	H-4	H-5
0.094	8.457	7.438	6.271	4.054	2.308
0.00 **	8.73	7.66	6.74	4.57	2.29
difference	0.27	0.22	0.47	0.52	0.02

* The chemical shifts are to low field of DSS. The error limits are ± 0.002 ppm.

** The limiting shifts are obtained from extrapolation of the data (Fig. IV-4) to infinite dilution. The error limits are ± 0.01 obtained from the standard deviations of least-squares analysis.

TABLE IV-2. The Concentration Dependence of Proton Chemical Shifts of Folate Solution and Model Compound-I Solution at 12.9 pD and 30.5°C.

(A) Folate	H-1
Concentration (m)	Chemical Shift* (ppm)
0.087	8.567
0.064	8.580
0.045	8.590
0.031	8.599
0.0082	8.606
0.00 **	8.61±0.01

(B) Model Compound I	—CH—
Concentration (m)	Chemical Shift*(ppm)
0.150	8.403
0.092	8.422
0.062	8.457
0.027	8.476
0.00**	8.51±0.02

* The chemical shifts are to low field of DSS, error limits are ±0.002 ppm.

** Limiting shifts are obtained from extrapolation of the data to infinite dilution using least-squares analysis.

The chemical shifts for protons H-2 and H-3 for model compound II at 30.5°C were measured over a concentration range between 0.24m and 0.023. These shifts are independent of concentration. The H-2 and H-3 proton shifts for 0.023 solution are listed in Table IV-3. Also, the limiting shift of the corresponding protons of folate (from Table IV-1) are included for comparison.

TABLE IV-3. The Comparison of Chemical Shifts* between the Protons in Folate and those in Model Compound-II.

Compound	Proton Chemical Shift (ppm)	
	H-2	H-3
Folate**	7.66±0.01	6.74±0.01
Model II‡	7.766±0.002	6.768±0.002
difference	0.10	0.03

*The experiments were carried out in D_2O at 30.5°C and a pD of 7.1.

** The limiting shifts at infinite dilution are obtained from Table IV-2.

‡ The shifts are independent of concentration over a large range (0.23m to 0.024m).

3. The Temperature Dependence of Chemical Shifts of the Folate Protons

The chemical shifts of all the folate protons were studied as a function of temperature (5.8° to 60.0°C) at two folate concentrations (0.049m and 0.009m). The temperature dependences are plotted in Fig. IV-5.

As observed in the concentration dependence studies, protons H-1 and H-4 shift the most with temperature, whereas proton H-5 resonances remained unchanged. This result was observed for experiments carried out at both concentrations.

To summarize the temperature dependence of the folate proton shifts, data at the highest temperature (60°C) and at the lowest temperature (5.8°C) are compared in Table IV-4 for solutions at both folate concentrations.

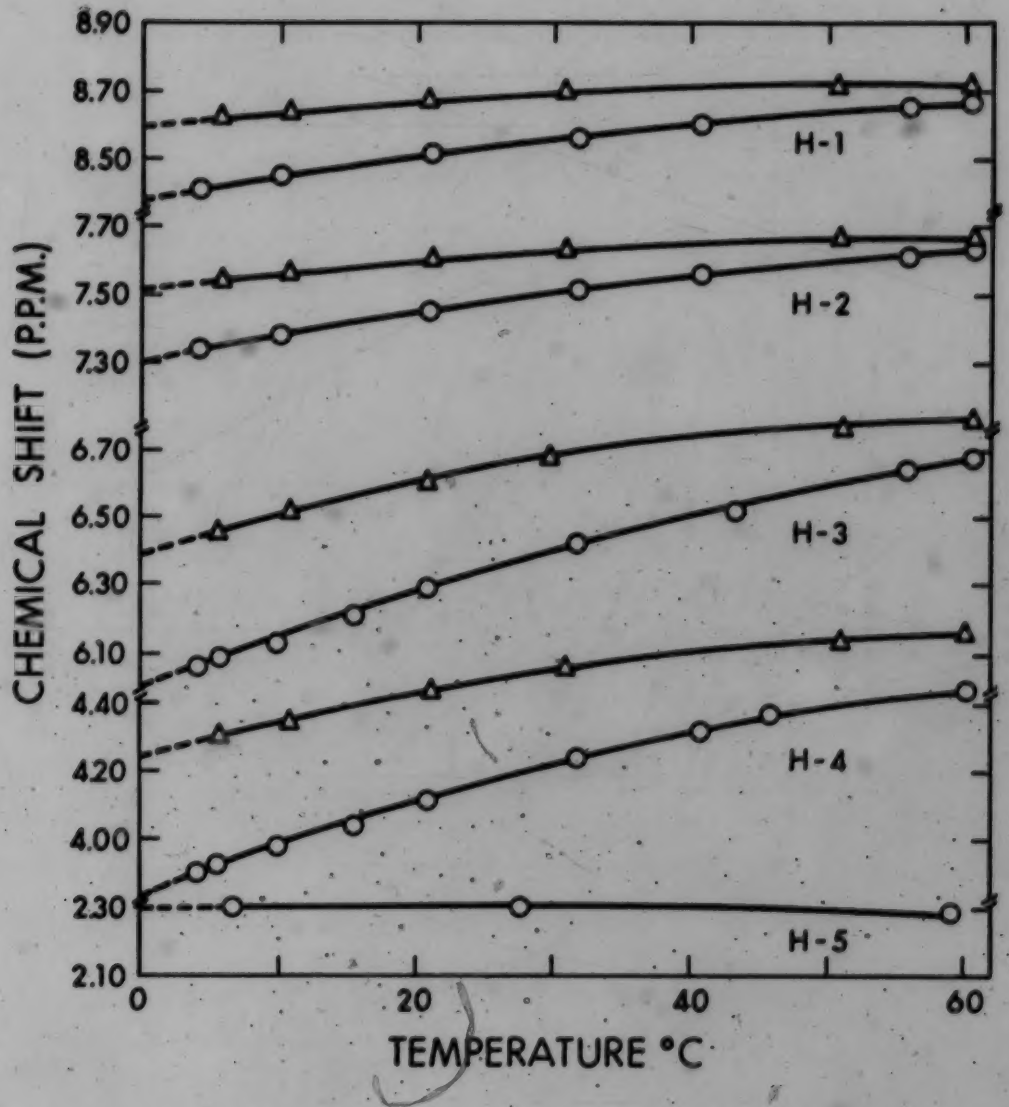

FIGURE IV-5. The temperature dependence of the proton chemical shifts of disodium folate in D_2O (pD 7.1; 30.5°C). The measurements are carried out at two concentrations, namely : O 0.049m and Δ 0.009m.

TABLE IV-4. The Temperature Dependence of the Proton Chemical Shifts of Disodium Folate in D_2O at 7.1 pD, in Two Different Concentrations.

(A) 0.049m folate.

Temperature (°C)	Shift* (ppm)				
	H-1	H-2	H-3	H-4	H-5
60	8.660	7.626	6.667	4.420	2.290
5.8	8.422	7.348	6.078	3.927	2.300
difference	0.24	0.27	0.59	0.49	0.01

(B) 0.009m folate.

60	8.732	7.668	6.787	4.616	2.290
5.8	8.624	7.538	6.448	4.301	2.290
difference	0.11	0.13	0.34	0.32	0.00

* The chemical shifts are to low field of internal DSS, error limits are ± 0.002 ppm.

D. DISCUSSION

1. The Folate Conformation in Aqueous Solution

As described in the introduction, folate may exist in solution in an extended conformation or in a partly folded conformation with the pterine unit either above or below the benzoic acid unit. This intramolecular folding may be studied by comparing the proton chemical shifts of folate at infinite dilution, when the intermolecular shielding effects are negligible (Kotowycz et al, 1969), with the shifts observed for the corresponding protons in the model compounds. The two model compounds are (I) 2-amino-4-hydroxyl-6-methyl pteridine, and (II) sodium p-(methyl-amino) benzoate. These model compounds were chosen because they are not only similar to parts of the folate molecule in structure, but they also possess a planar aromatic molecular skeleton. Hence, the protons in these models do not experience any intramolecular shifting effect.

In model compound I, the chemical shift of the -CH- proton is slightly concentration dependent [Table IV-2-(B)]. Therefore, the limiting shift was calculated by extrapolation to infinite dilution and compared with that of folate at the same value of pD (Table IV-2A). The

difference is 0.09ppm In model compound II, the proton chemical shifts are independent of concentration and temperature(Table IV-3). The data in Table IV-3 indicates that these chemical shifts are very similar to the limiting shifts for protons H-2 and H-3 of folate at infinite dilution: the difference is 0.03 ppm for the H-3 protons, and 0.10 ppm for the H-2 protons. The latter difference may partly be due to the fact that the H-2 protons are near an amide group in folate but near a carboxyl group in model compound II.

In both comparisons, the differences in chemical shift between these protons are much smaller than those arising from diamagnetic ring current shielding effects in molecules such as FAD (Sarma et al, 1968; Kotowycz et al, 1969), and the purine nucleosides (Broom et al, 1967). The present results indicate that the folate protons do not experience the diamagnetic ring-current shielding effect from intramolecular interaction. Therefore, the folate molecules exist in an extended conformation in aqueous solutions. In this stretched-out conformation, the ionized groups of the glutamic acid units of the neigbouring molecules are far apart from each other so that the electrostatic repulsion is minimized. Also, inspection of the CPK model of folic acid indicates that the folded conforma-

tion may lead to considerable strain in the middle parts of the molecule.

2. The Intermolecular Association of Folates

In most aromatic compounds, the proton chemical shifts only vary slightly with concentration or temperature (Zimmerman and Foster, 1957; Bothner-By and Glick, 1957). For example, a 0.1ppm shift was observed for the five ring protons in azulene in dioxane solution over a concentration range of 17 mole% (Schneider et al, 1958). In contrast, 0.2 to 0.5ppm shifts were observed for the folate protons just over a 0.2 mole% change in concentration [0.094m to 0m in Table IV-1]. Similar pronounced temperature dependence in the chemical shifts of the folate protons was observed [Table IV-4 and Pastore (1971)]. For a comparison, a 0.16ppm shift of proton H-3 in methotrexate (a folate analogue) was observed over a 50°C change in temperature, whereas a corresponding 0.48ppm shift was observed in folate (Pastore, 1971). Therefore, these characteristic

dependences indicate that the folate molecules are intermolecularly associated.

In large molecules with aromatic and aliphatic fragments, two types of intermolecular association are often encountered:

(i) Vertical stacking, in which the molecules are packed with the aromatic rings one above the other, forming molecular coplanar stacks. This type of stacking has been proposed for most nucleosides and nucleotides (Ts'O et al, 1969 and references therein).

(ii) Micelle formation, in which the aromatic (hydrophobic) regions of the molecules associate, yet the aliphatic groups with ionizable terminal groups extend outwards into the water solvent. Micelle formation has been observed for most long chain aliphatic acids (Inoue and Nakagawa, 1966; Muller and Birkhahn, 1967) as well as for benzyl penicillin (Thakkar and Wilham, 1971).

If the folate molecules formed micelles, the pterine units would be in the interior of the micelle, whereas the glutamic acid fragment would form the spherical surface. This symmetrical arrangement implies that the H-1 proton should be most sensitive with respect to the folate concentration and temperature. However, the data in Table

IV-1 and Table IV-4 indicate that protons H-3 and H-4 have the largest concentration and temperature dependence. Furthermore, in the concentration dependence study (Fig. IV-4), a sharp discontinuity in the curves would have occurred if the folate molecules formed a micelle (Muller and Birkhahn, 1967). However, the chemical shifts vary monotonically.

In both studies shown in Figs. IV-4 and IV-5, when the concentration is increased or the temperature is decreased, all the folate protons (except the H-5 protons which are constant) are shifted to high field. This indicates that the intermolecular association is not due to hydrogen-bonding which induces low field shifts on the related protons (Arnold and Packard, 1951; Schneider et al, 1958). Therefore, the association most likely arises from the interactions between the neighbouring aromatic groups in a vertical stacking manner. In the stacks, the folate protons are either above or below the nearby aromatic units. Consequently, a pronounced diamagnetic-ring-current effect on the proton shifts is observed.

Finally, the relative orientation of folate molecules in the vertical stacks is considered. The molecule may orient itself with its aromatic pteridine unit (the head) and its glutamic acid unit (the tail) above or

below the corresponding units of the neighboring folate molecules [a head to head arrangement]. Another possibility is that the aromatic unit (the head) is above or below the neighboring glutamic acid unit (the tail) [a head to tail arrangement]. In the former arrangement, similar temperature and concentration dependences would be expected for the pair of protons H-1 and H-4, as well as for the pair of protons H-2 and H-3. From the results listed in Tables IV-1 and IV-4, the chemical shift differences of prons H-3 and H-4 resemble more each other in magnitude, instead of that of protons H-3 and H-1. The similarity is also observed for the H-2 and H-1 protons.

From the magnitudes of the diamagnetic shifts, i.e. H-3, H-4 >> H-1; H-2 >> H-5, the most consistent mode for association is shown in Fig. IV-6. In the figure, the folates are partially overlapping in a head-to-tail manner. From this model, it is seen that the protons H-3 and H-4 are the closest to the neighboring pterine units. Protons H-2 and H-1 are a little further removed from the nearby benzoic acid units, whereas the glutamic acid protons H-5 are away from both units and hence they are completely insensitive towards the changes in temperature and concentration. The same head-to-tail model is supported by a

subsequent pH and concentration study (Poe, 1973), after the publication of the present result (Lam and Kotowycz, 1972).

The model also shows a uniform distribution of ionized groups of the folate molecules towards the polar water solvent, while the aromatic groups attain significant hydrophobic interactions. Similar partially-overlapping models have been observed in many heterocyclic compounds in the crystalline state (Bugg et al, 1971) and in solution as described in the introduction.

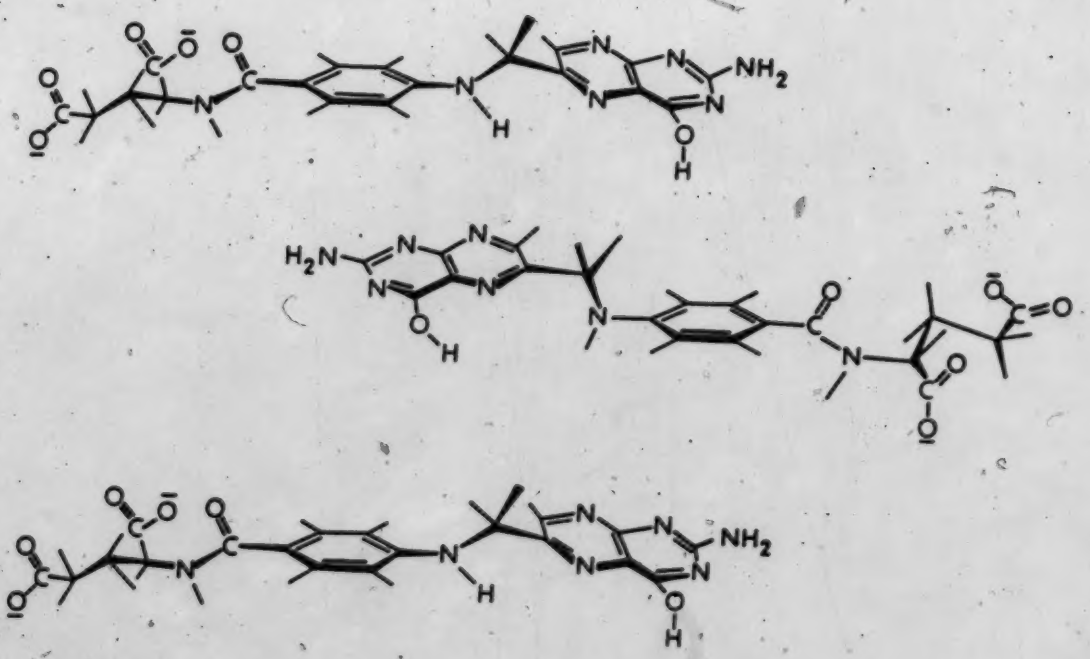

FIGURE IV-6. The proposed, alternating, head to tail intermolecular stacking model for folate ions in aqueous solution (pD 7.1).

E. CONCLUSIONS

The ^1H NMR experiments on disodium folate in aqueous solution (pD 7.1) indicate that the folate ion exists in an unfolded, extended conformation. Folate ions, however, are involved in strong intermolecular association. This property is quite characteristic when compared to the much weaker associations in other folic analogues, such as N^{10}-methyl folate, Methotrexate and dihydro-folate (Pastore, 1971; Poe, 1973). The difference may be one of the factors for the diverse biological effects of folic acid and these folate derivatives. Furthermore, the data show that the folate ions associate in vertical stacks. From the variations of the chemical shifts with temperature and concentration, a head-to-tail vertical stacking model is proposed with the hydrophilic ends of the molecule alternating in orientation with respect to the hydrophobic portion of the neighboring molecules.

BIBLIOGRAPHY

Albert, A. (1953) Biochem.J. 54, 646.

Alberty, N.J. (1967) Progr.Reaction Kinetics 4, 353.

Allerhand, A., Doddrell, D., Glushko, V., Cochran, D.W., Wenkert, E., Lawson, P.J. and Gurd, F.R.N. (1971) J.Amer.Chem.Soc. 93, 544.

Angerman, N.S. and Jordan, R.B. (1969) Inorg.Chem. 8, 1824.

Angerman, N.S. and Jordan, R.B. (1970) J.Chem.Phys. 54, 837.

Angier, R.B., Boothe, J.H., Mowat, J.H., Waller, C.W. and Semb, J. (1952) J.Amer.Chem.Soc. 74, 408. Angier, R.B., Boothe, J.H., Hutchins, B.L., Mowat, J.H., Semb, J., Stokstad, E.L.R., Subbarow, Y., Waller, C.W., Cosulich, D.B., Fahrenbach, M.J., Hultquist, M.E., Kah, E., Northey, E.H., Seeger, D.R., Sickels, J.P. and Smith, J.M. Jr. (1946) Science 103, 667.

Arnold, J.T. and Packard, M.E. (1951) J.Chem.Phys. 19, 1608.

Atkins, P.W. and Kivelson, D. (1966) J.Chem.Phys. 44, 169.

Becker, J.W., Reeke, G.N., Wang, J.L., Cunningham, B.A. and Edelman, G.M. (1975) J.Biol.Chem. 250 , 1513.

Bernheim, R.A., Brown, T.H., Gutowsky, H.S. and Woessner, D.E. (1959) J.Chem.Phys. 30, 950.

Blackburn, B.J., Hruska, F.E. and Smith, I.C.P. (1969) Can.J.Chem. 47, 4491.

Blakley, R.L. (1954) Biochem.J. 58, 448.

Bloch, F. (1946) Phys.Rev. 70, 460.

Bloembergen, N. (1957) J.Chem.Phys. 27, 572.

Bloembergen, N. and Morgan, L.O. (1961) J.Chem.Phys. 34, 842.

Bock, R. M. (1960) "The Enzymes" (Boyer, P.D., Lardy, H. and Myrback, K. Editors) 2nd Ed., Vol. 2, Chapter 1, pp. 3, Acad.Press, New York.

Bond, T.J., Bardos, T.J., Sibley, M. and Shive, W. (1949) J.Amer.Chem.Soc. 71, 3825.

Bothner-By, A.A. and Glick, R.E. (1957) J.Chem.Phys. 26, 1651.

Bovey, F.A. (1972) "High Resolution NMR of Macromolecules", Acad.Press, New York.

Brent, T.P., Butler, J.A.V. and Crathorn, A.R. (1965) Nature 207, 176.

Bridger, W.A., Millen, W.A. and Boyer, P.D. (1968) Biochemistry 7, 3608.

Bridger, W.A. (1971) Biochem.Biophys.Res.Commun. 42, 948.

Bridger, W.A. (1974) "The Enzymes" (Boyer, P.D., Editor) 3rd ed., Vol.10, Chapter 18, pp. 581, Acad.Press, New York.

Broom, A.D., Schweizer, M.P. and Ts'O, P.O.P. (1967) J.Amer.Chem.Soc. 89, 3612.

Brown, F.F., Campbell, I.D., Henson, R., Hirst, C.W.J. and Richards, R.E. (1973) Eur.J.Biochem. 38, 54.

Brown, G.M. and Reynolds, J.J. (1963) Ann.Rev.Biochem. 32, 419.

Bugg, C.E., Thomas, J.M., Sundaralingam, M. and Rao, S.T. (1971) Biopolymers 10, 175.

Burlamacchi, L., Martini, G. and Tiezzi, E. (1970) J.Phys.Chem. 74, 3980.

Carr, H.Y. and Purcell, E.M. (1954) Phys.Rev. 94, 630.

Cleland, W. (1967) Ann.Rev.Biochem. 36, 77.

Codrington, R.S. and Bloembergen, N. (1958) J.Chem.Phys. 29, 600.

Cohn, M. (1951) Phosphorus Metab. Symp., 1st, Vol.1, 374.

Cohn, M. and Townsend, J. (1954) Nature 173, 1090.

Cohn, M. and Hughes, T.R. Jr. (1962) J.Biol.Chem. 237, 176.

Cohn, M. and Leigh, J.S. Jr. (1962) Nature 193, 1037.

Collingwood, J.C. and White, J.W. (1973) Mole.Phys. 25, 1241.

Consulich, D.B., Seeger, D.R., Fahrenbach, M.J., Roth, B., Mowat, J.H., Smith, J.M.Jr., and Hultquist, M.E. (1951) J.Amer.Chem.Soc. 73, 2554.

Danyluk, S.S. and Hruska, F.E. (1968) Biochemistry 7, 1938.

Daune, M. (1974) "Metal Ions in Biological Systems" (Sigel, H. Editor) Vol. 3, Chapter 1, pp. 1, Marcel Dekker, New York.

Diebler, H., Eigen, M. and Hammes, G. (1960) Z.Naturforsch. 15b, 554.

Dodgen, H.W., Jordan, A.D. and Jordan, R.B. (1973) J.Phys.Chem. 77, 2149.

Dorman, D.E. and Roberts, J.D. (1970) Proc.Nat.Acad.Sci. U.S.A. 65, 19.

Dwek, R.A. (1973) "Nuclear Magnetic Resonance (N.M.R.) In Biochemistry", Clarendon Press, Oxford.

Dwek, R.A., Williams, R.J.P. and Xavier, A.V. (1974) "Metal Ions in Biological Systems", (Sigel, H. Editor) Vol. 4, Chapter 3, pp. 61, Marcel Dekker, New York.

Eisinger, J., Shulman, R.G. and Szymanski, B.M. (1962) J.Chem.Phys 36, 1721.

Eyring, H. (1935) Chem.Rev. 17, 65.

Fiskin, A.M. and Beer, M. (1965) Biochemistry 4, 1289.

Freeman, R. and Hill, H.D.W. (1969) J.Chem.Phys. 51, 3140.

Freeman, R. and Hill, H.D.W. (1971) J.Chem.PHys. 54, 3367.

Frey, C.M. and Stuehr, J.E. (1972) J.Amer.Chem.Soc. 94, 8898.

Frey, C.M., Banyasz, J.L. and Stuehr, J.E. (1972) J.Amer.Chem.Soc. 94, 9198.

Frey, C.M. and Stuehr, J.E. (1973) "Metal Ions in Biological Systems" (Sigel, H. Editor) Vol.1, Chapter 2, pp. 51, Marcel Dekker, New York.

Frost, A.A. and Pearson, R.G. (1961) "Kinetics and Mechanism" (2nd ed) Chapter 3, pp.49, Wiley and Sons, New York.

Fuhr, B.J. and Rabenstein, D.L. (1973) Inorg.Chem. 12, 1868.

Fung, C.H., Mildvan, A.S., Allerhand, A., Komoroski, R. and Scrutton, M.C. (1973) Biochemistry 12, 620.

Glasoe, P.K. and Long, F.A. (1960) J.Phys.Chem. 64, 188.

Glassman, T.A., Cooper, C., Harrison, L.W. and Swift, T.J. (1971) Biochemistry 10, 843.

Glasstone, G., Laidler, K.J. and Eyring, H. (1941) "The Theory of Rate Processes", McGraw-Hill, New York.

Gotto, A.M., Neikle, A.W. and Touster, O. (1964) Biochem.Biophys.Acta 80, 552.

Greenberg, G.R. (1954) Fed.Proc. 13, 745.

Grinnell, F.L. and Nishimura, J.S. (1969) Biochemistry 8, 4126.

Guggenheim, E.A. (1926) Phi.Mag. 2, 538.

Gutowsky, H.S., McCall, D.W. and Slichter (1953) J.Chem.Phys. 21, 279.

Gutowsky, H.S. and Saika, A. (1953) J.Chem.Phys. 21, 1688.

Hager, L.P. (1962) "The Enzymes" (Boyer, P.D., Lardy, H. and Myrback, K. Editors) 2nd ed., Chapter 24, pp. 387, Acad.Press, New York.

Hall, C., Kydon, D.W., Richards, R.E. and Sharp, R.R. (1970) Proc.Roy.Soc., Series A, 318, 119.

Hammes, G.G. and Levison, S.A. (1964) Biochemistry 10, 1504.

Hammes, S., Maciel, G.E. and Waugh, J.S. (1961) J.Amer.Chem.Soc. 83, 2394.

Hammes, G.G. and Miller, D.L. (1967) J.Chem.Phys. 46, 1533.

Happe, J.A. and Morales, M. (1966) J.Amer.Chem.Soc. 88, 2077.

Heller, M.J., Jones, A.J. and Tu, A.T. (1970) Biochemistry 9, 4981.

Hift, H., Ouellet, L., Littlefield, J.W. and Sanadi, D.R. (1953) J.Biol.Chem. 204, 565.

Hiraga, S. and Sugino, Y. (1966) Biochem.Biophys.Acta 114, 416.

Hsieh, T. and Buchanan, J.M. (1967) Proc.Natl.Acad.Sci. 58, 2468.

Hughes, M.N. (1972) "The Inorganic Chemistry of Biological Processes", John Wiley and Sons, Toronto.

Hutchinson, D.W. (1964) "Nucleotides and Coenzymes", John Wiley and Sons, New York.

Inoue, H. and Nakagawa, T. (1966) J.Phys.Chem. 70, 1108.

Izatt, R.M., Christensen, J.J. and Rytting, J.H. (1971) Chem.Rev. 71, 439.

Jaenicke, L. (1964) Ann.Rev.Biochem. 33, 287.

Jardetzky, C.D. and Jardetzky, O. (1960) J.Amer.Chem.Soc. 82, 222.

Johnson, C.E.Jr. and Bovey, F.A. (1958) J.Chem.Phys. 29, 1012.

Jones, D.E. (1972) J.Mag.Res. 6, 191.

Jones, R., Dwek, R.A. and Walker, I.O.W. (1974a) Eur.J.Biochem. 47, 285.

Jones, R., Dwek, R.A. and Forsen, S. (1974b) Eur.J.Biochem. 47, 271.

Jones, A.J., Winkley, M.W., Grant, D.M. and Robins, R.K. (1970) Proc.Nat.Acad.Sci. U.S.A. 65, 27.

Kaufman, S. (1955) J.Biol.Chem. 216, 153.

Kennard, O., Isaacs, N.W., Motherwell, W.D.S., Coppola, J.C., Wampler, D.L., Larson, A.C. and Watson, D.G. (1971) Proc.R.Soc.Lond.A 325, 401.

King, J. and Davidson, N. (1958) J.Chem.Phys. 29, 787.

Kit, S. (1970) "Metabolic Pathways", (Greenberg, D.M. Editor) 3rd ed., Vol. 4, Chapter 20, pp. 69, Acad.Press, New York.

Koenig, S.H., Brown, R.D. and Studebaker, J. (1971) Cold Spring Harbor Symp.Quant.Biol. 36, 551.

Koenig, S.H. (1972) J.Chem.Phys. 56, 3188.

Koenig, S.H., Brown, R.D., and Brewer, C.F. (1973) Proc.Nat.Acad.Sci. U.S.A. 70, 475.

Kotowycz, G. and Hayamizu, K. (1973) Biochemistry 12, 517.

Kotowycz, G., Teng, N., Klein, M.P. and Calvin, M. (1969) J.Biol.Chem. 244, 5656.

Kraut, J. and Jensen, L.H. (1963) Acta Cryst, 16, 79.

Krebs, A. and Bridger, W.A. (1974) Can.J.Biochem. 52, 594.

Kuntz, G.P.P., Glassman, T.A., Cooper, C. and Swift, T.J. (1972) Biochemistry 11, 538.

Kuntz, G.P.P. and Kotowycz, G. (1975) Biochemistry, in press.

Kuntz, G.P.P. and Kotowycz, G. (1975) Biochemistry, in press.

Lam, Y.F. and Kotowycz, G. (1972) Can.J.Chem. 50, 2357.

Leitzmann, C., Wu, J.-Y. and Boyer, P.D. (1970) Biochemistry 9, 2338.

Luhby, A.L. and Cooperman, J.M. (1964) Adv.Metabolic Disorders 1, 264.

Luz, Z. and Meiboom, S. (1964) J.Chem.Phys. 40, 2686.

Martell, A.E. and Schwarzenbach, S. (1956) Helv.Chem.Acta 39, 653.

Martin, J.S. and Dailey, B.P. (1963) J.Chem.Phys. 38, 1722.

Mantsch, H.H. and Smith, I.C.P. (1972) Biochem.Biophys. Res.Commun. 46, 808.

McConnell, H.M. (1958) J.Chem.Phys. 28, 430.

McCormick, W.G. and Levedahl, B.H. (1959) Biochem.Biophys.Acta 34, 303.

McLachlan, A.D. (1964) Proc.Roy.Soc., Series A, 280, 271.

Mclaughlin, A.C. and Leigh, J.S. Jr. (1973) J.Magn.Res. 9, 296.

Mildvan, A.S. and Cohn, M. (1963) Biochemistry 2, 910.

Mildvan, A.S. and Cohn, M. (1965) J.Biol.Chem. 240, 238.

Mil van, A.S. and Engle, J.L. (1972) "Methods in Enzymology" (Hirs, C.H.W. and Timasheff, S.N. Editors) Vol.XXVI, Chapter 29, pp. 654, Acad.Press, New York.

Miles, D.W. and Urry, D.W. (1968) Biochemistry 7, 2791.

Mitchell, H.K., Snell, E.E. and Williams, R.J. (1941) J.Amer.Chem.Soc. 63, 2284.

Moffet, F.J. and Bridger, W.A. (1970) J.Biol.Chem. 245, 2758.

Moffet, F.J. and Bridger, W.A. (1972) Can.J.Biochem. 51, 44.

Mohan, M.S. and Rechnitz, G.A. (1974) Arch.Biochem.Biophys. 162, 194.

Montgomery, H., Chastain, R.V. and Lingafelter, E. (1966) Acta Cryst. 20, 731.

Morrison, J.F. and James, E. (1965) Biochem.J. 97, 37.

Muller, N. and Birkhahn, R.H. (1967) J.Phys.Chem. 71, 957.

Nakamura, H. and Sugino, Y. (1966) Cancer Res. 26, 1425.

Nishimura, J.S. (1972) Adv.Enzymol. 36, 183.

O'Reilly, D.E. and Poole, C.P. Jr. (1963) J.Phys.Chem. 67, 1762.

Pastore, E.J., Friedkin, M. (1962) J.Biol.Chem. 237, 3802.

Pastore, E.J., Friedkin, M. and Jardetzky, O. (1963) J.Amer.Chem.Soc. 85, 3058.

Pastore, E.J. (1971) Ann.N.Y.Acad.Sci. 186, 43.

Peacocke, A.R., Richards, R.E. and Sheard, B. (1969) Mol.Phys. 16, 177.

Pfeifer, M. (1962) Z.Nature A17, 279.

Pfeifer, H., Michel, D., Sames, D. and Sprihz, H. (1966) Mol.Phys. 11, 581.

Phillips, R.C. (1966) Chem.Rev. 66, 501.

Poe, M. (1973) J.Biol.Chem. 248, 7025.

Poole, C.P. Jr. and Farach, H.A. (1971) "Relaxation in Magnetic Resonance", Acad.Press, New York.

Poole, C.P. Jr. and Farach, H.A. (1972) "The Theory of Magnetic Resonance", Wiley-Interscience, New York.

Rabinowitz, J.C. (1960) "The Enzymes" (Boyer, P.D., Lardy, H. and Myrback, K., Editors) 2nd ed., Vol.2, Chapter 7, pp.185, Acad.Press, N.Y.

Ramaley, R.F., Bridger, W.A., Moyer, R.W. and Boyer, P.D. (1967) J.Biol.Chem. 242, 4287.

Randerath, K. and Randerath, E. (1964) J. Chromatogr. 16, 111.

Reed, G.H. and Cohn, M. (1970) J.Biol.Chem. 245, 662.

Reed, G.H. and Cohn, M. (1973) J.Biol.Chem. 248, 6436.

Reed, G.H., Leigh, J.S. Jr. and Pearson, J.E. (1971) J.Chem.Phys. 55, 3311.

Reuben, J. and Cohn, M. (1970) J.Biol.Chem. 245, 6539.

Reuben, J., Reed, G.H. and Cohn, M. (1970) J.Chem.Phys. 52, 1617.

Reuben, J. (1971) J.Chem.Phys. 75, 3164.

Reynard, A.M., Hass, L.F., Jacobsen, D.D. and Boyer, P.D. (1961) J.Biol.Chem. 236, 2277.

Robinson, J.L., Benson, R.W. and Boyer, P.D. (1969) Biochemistry 8, 2503.

Rubinstein, M., Baram, A. and Luz, Z. (1971) Mol.Phys. 20, 67.

Sarma, R.H., Dannies, P. and Kaplan, N.O. (1968) Biochemistry 7, 4359.

Sarma, R.H. and Kaplan, N.O. (1969) J.Biol.Chem. 244, 771.

Sarma, R.H. and Kaplan, N.O. (1970a) Biochemistry 9, 539.

Sarma, R.H. and Kaplan, N.O. (1970b) Biochemistry 9, 557.

Sauberlich, H.E. and Baumann, C.A. (1948) J.Biol.Chem. 176, 165.

Scatchard, G. (1949) Ann.N.Y.Acad.Sci. 51, 660.

Schneider, W.G., Bernstein, H.J. and Pople, J.A. (1958) J.Amer.Chem.Soc. 80, 3497.

Schneider, P.W., Brintzinger, H. and Erlenmeyer, H. (1964) Hel.Chem.Acta 47, 992.

Schweizer, M.P., Broom, A.D., Ts'O, P.O.P. and Hollis, D.P. (1968) J.Amer.Chem.Soc. 90, 1042.

Shive, W., Ackermann, W.W., Gorden, M., Getzendaner, M.E. and Eakin, R.E. (1947) J.Amer.Chem.Soc. 69, 725.

Slichter, P. (1963) "Principles of Magnetic Resonance", Harper and Row, New York.

Smith, G.W. (1964) J.Mol.Spectrosc. 12, 146.

Smith, R.M. and Alberty, R.A. (1956a) J.Phys.Chem. 60, 180.

Smith, R.M. and Alberty, R.A. (1956b) J.Amer.Chem.Soc. 8, 2376.

Solomon, I. (1955) Phys.Rev. 99, 559.

Solomon, I. and Bloembergen, N. (1956) J.Chem.Phys. 25, 261.

Stadtman, E.R. (1957) "Methods in Enzymology" (Colowick, S.P. and Kaplan, N.O., Editors) Vol.3, pp. 931, Acad. Press, New York.

Sternlicht, H., Shulman, R.G. and Anderson, E.W. (1965a) J.Chem.Phys. 43 3123.

Sternlicht, H., Shulman, R.G. and Anderson, E.W. (1965b) J.Chem.Phys. 43, 3133.

Sternlicht, H., Jones, D.E. and Kustin, K. (1968) J.Amer.Chem.Soc. 90, 7110.

Sundaralingam, M. (1969) Biopolymers 7, 821.

Swift, T.J. and Connick, R.E. (1962) J.Chem.Phys. 37, 307.

Szent-Gyorgyi, A.G. (1957) "Bioenergetics", pp. 64, Acad.Press, New York.

Taqui Khan, M.M. and Martell, A.E. (1962) J.Phys.Chem. 66, 10.

Taqui Khan, M.M. and Martell, A.E. (1966) J.Amer.Chem.Soc. 88, 668.

Thakkar, A.L. and Wilham, W.L. (1971) Chem.Commun. 320.

Todd, A. (1958) Science 127, 787.

Ts'O, P.O.P. and Chan, S.I. (1964) J.Amer.Chem.Soc. 86, 4176.

Ts'O, P.O.P., Kondo, N.S., Schweizer, M.P. and Hollis, D.P. (1969) Biochemistry 8, 997.

Ts'O, P.O.P., Melvin, I.S. and Olson, A.C. (1963) J.Amer.Chem.Soc. 85, 1289.

Ts'O, P.O.P., Schweizer, M.P. and Hollis, D.P. (1969) Ann.N.Y.Acad.Sci. 158, 256.

Uhr, M.L., Marcus, F. and Morrison, J.F. (1966) J.Biol.Chem. 241, 5428.

Vallee, B.L. (1960) "The Enzymes" (Boyer, P.D., Lardy, H. and Myrback, K. Editors) 2nd ed., Chapter 15, pp. 225, Acad. Press, New York.

Villafranca, J.J. and Wedler, F.C. (1974) Biochemistry 13, 3286.

Vold, R.L., Waugh, J.S., Klein, M.P. and Phelps, D.E. (1968) J.Chem.Phys. 48, 3831.

Wahba, A.J. and Friedkin, M. (1962) J.Biol.Chem. 237, 3794.

Walsh, C.T. Jr., Hildebrand, J.G. and Spector, J.B. (1970) J.Biol.Chem. 245, 5699.

Waugh, J.S. and Fessenden, R.W. (1957) J.Amer.Chem.Soc. 79, 846.

Wee, V., Feldman, I., Rose, P. and Gross, S. (1974) J.Amer.Chem.Soc. 96, 103.

Whiteley, J.M. and Huennekens, F.M. (1967) Biochemistry 6, 2620.

Whiteley, J.M. (1971) Ann.N.Y.Acad.Sci. 186, 29.

Wiberg, J.S. (1958) Arch.Biochem.Biophys. 73, 337.

Williams, D.R. (1970) "The Metals of Life" Van Nostrand Reinhold Company, London.

Wilson, R. and Kivelson, D. (1966) J.Chem.Phys. 44, 154.

Yamamoto, O. and Yanagisawa, M. (1970) Anal.Chem. 42, 1463.

Zalkin, A., Forrester, J.D. and Templeton, D.H. (1964) Inorg.Chem. 3, 529.

Zetter, M.S., Grant, M.W., Wood, E.J., Dodgen, H.W. and Hunt, J.P. (1972) Inorg.Chem. 11, 2701.

Zetter, M.S., Dodgen, H.W. and Hunt, J.P. (1973) Biochemistry 12, 778.

Zimmerman, J.R. and Foster, M.R. (1957) J.Phys.Chem. 61, 282.

APPENDIX A

COMPUTER PROGRAM FOR THE CALCULATION OF THE SPIN-LATTICE RELAXATION TIME T_1

The values of T_1 are calculated by means of a linear-least-squares analysis of the data obtained from ($180^\circ - \tau - 90^\circ$) pulse sequence. When the thermal equilibrium magnetization, M_∞, is known, the standard equation described in Chapter II[Eq. (II-29)] is used. This equation is rewritten here as follows:

$$\ln (M_\infty - M_{\tau_i}) = \ln (2M_\infty) - \frac{\tau_i}{T_1} \qquad \text{(A-1)}$$

Therefore, a plot of $\ln(M_\infty - M_\tau)$ vs the time interval gives a line with slope $-1/T_1$.

In addition to the above procedure, another method, which does not require the knowledge of M_∞, can also be used. The principle (Guggenheim, 1926) and the applications of this method are well known from kinetic studies (Frost and Pearson, 1961). The procedure is now described in terms of the NMR parameters.

First of all, the M_{τ_i} data are sorted into

pairs in which the time difference between the two values of the magnetization is an appropriately chosen constant Δt . A schematic diagram is included to illustrate the pairing:

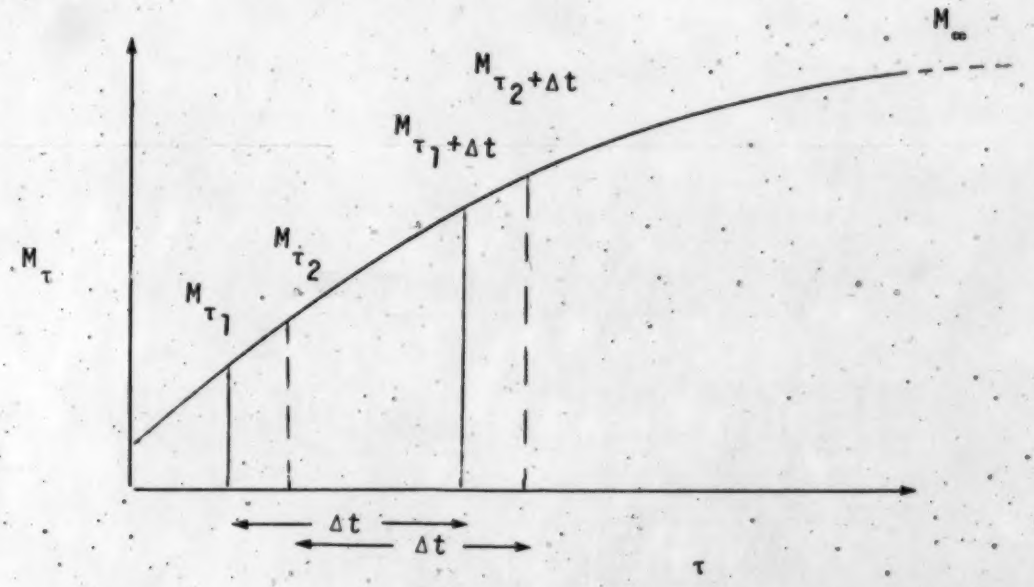

(A-2)

At time τ_i , the corresponding magnetization is given by Eq. (A-1) which may be rewritten in the following form:

$$M_{\tau_i} = M_\infty \left\{ 1 - 2 \exp\left(\frac{-\tau_i}{T_1}\right) \right\} \qquad \text{(A-3)}$$

Similarly, for time $\tau_i+\Delta t$,

$$M_{\tau_i+\Delta t} = M_\infty \left\{ 1 - 2 \exp\left[\frac{-(\tau_i + \Delta t)}{T_1} \right] \right\} \qquad \text{(A-4)}$$

Taking the difference between these two equations, one obtains

$$\ln \left(M_{\tau_i+\Delta t} - M_{\tau_i} \right) = \ln \left(2M_\infty \left[1 - \exp\left(\frac{-\Delta t}{T_1} \right) \right] \right) - \frac{\tau_i}{T_1}$$

$$= \ln K - \frac{\tau_i}{T_1} \qquad \text{(A-5)}$$

For all pairs of data points with the same value of Δt , K is a constant. Therefore, Eq. (A-5) indicates that the natural logarithm of the difference between the two data points also varies linearly with the time τ_i . Hence the slope of the plot of $\ln(M_{\tau_i+\Delta t} - M_{\tau_i})$ vs τ_i also gives a value for $-1/T_1$.

Both of the above techniques are included in the computer program for data treatment. The program is written in the FORTRAN IV language. The listing of the program and the documentation describing the input and output formats and various options are given as follows.

```
C
C      T1  LINEAR FITTING.
C     ============================
C     SUBROUTINES USED IN THIS PROGRAM:
C        LSQSM,TRS,IWT,GUGGEN,NULL
C
C     CARD INPUT:
C
C     CARD(0)  MAIN CONTROL CARD
C              ISXP,NULO,IG,IDEL,IH,TABLE,WT,INTR,FR
C              (8(I1,1X),F10.0)
C
C        ISXP: SET TO 1 IF DATA IS FROM BRUKER SXP .
C              SPECTROMETER.
C        NULO: SET TO 1 IF ONLY REQUIRED TO ESTIMATE T1
C              VALUE (SEE SUBROUTINE NULL)
C          IG: SET TO 1 IF GUGGENHEIM TREATMENT IS USED
C              (SEE SUBROUTINE GUGGEN)
C        IDEL: NUMBER OF HT BETWEEN THE CONJUGATE PAIR USED
C              IN THE GUGGENHEIM TREATMENT.
C          IH: THE INDEX OF THE INITIAL DATA POINT (THE HEAD)
C              TO BE USED IN THE CALCULATION OF T1.
C       TABLE: SET TO 1 IF DETAILED OUTPUT  IS
C              REQUIRED(SEE SAMPLE OUTPUT)
C          WT: SET TO 1 IF WEIGHTING IS APPLIED TO THE INPUT
C              DATA.
C        INTR: MAXIMUM NUMBER OF ITERATIONS TO ESTIMATE
C              HT(0).
C          FR: FREQUENCY OF THE EXPERIMENT(MHZ).
C
C
C     CARD  (1)
C           TITLE
C           (20A4)
C
C     CARD (2)
C           NPT,WT,TABLE,TAU(1),DEL,HTO
C           (3I3,3F6.3)
C           NPT = NUMBER OF DATA PTS.
C           WT = WEIGHTING OPTION.
C           TABLE= PRINT TABLE OPTION.
C           TAU(1)= THE FIRST TAU INPUT.
C           DEL= INCREMENT IN TAU. (OPTION INPUT FOR TAU.S
C                IF DEL=0.0)
C           HTO= MZ (0).
C
C     CARDS(2-A) IFF DEL=0.0.
C           TAU(I)
C           (10(F5.3,5X))
C           INCREASING ORDER AS THE HT.
C
```

```
C      THE CARDS (3).....
C            HT(I)   OR HT(I) AND WTH(I) IF IH=0
C            WHERE HT(I) IS THE HEIGHT OF THE SIGNAL
C            AT TAU(I), AND WHT(I) IS THE WEIGHT
C            APPLIED TO THE HT(I).
C           FORMATS:

C           10(F6.3,1X)      OR  7(F6.3,1X,I1,2X)
C
C       MAIN  PROGRAM
C       =============
C
      REAL*8 D(5),STD(5)
      DIMENSION TAU(50),HT(50)
      INTEGER*4 TIT(20),TABLE,WTH(50),WT
      NC=5
      ICARD=1
       READ(5,112)ISXP,NULO,IG,IDEL,IH,TABLE,WT,INTR,FR
112   FORMAT(8(I1,1X),F10.0)
1     IF(ISXP.EQ.0)GOTO  120
C      ITER : ITERATION COUNTER
      ITER=0
      CALL TRS(ICARD,TIT,NPT,NC,TAU(1),DEL,HTO,HT,NTR)
      IF(ICARD.EQ.0) GOTO 99
      GOTO 3
120     READ(5,100,END=99) (TIT(I),I=1,20)
100   FORMAT(20A4)
      READ(5,101)NPT,WT,TABLE,TAU(1),DEL,HTO ,NTR
101   FORMAT(3I3,3F6.3,1X,I1)
      IF(DEL.GT.0.0) GOTO 11
       READ(5,104) (TAU(I),I=1,NPT)
 104   FORMAT(10(F5.3,5X))
11    IF((WT.EQ.0).OR.(IH.EQ.0)) GOTO 2
      READ(5,102) (HT(J),WTH(J),J=1,NPT)
102   FORMAT(7(F6.3,1X,I2,2X))
      GOTO3
2     READ(5,103)  (HT(J),J=1,NPT)
103   FORMAT(10(F6.3,1X))
      IF(DEL.LE.0.0) GOTO 41
3      DO 4 J=2,NPT
4     TAU(J)=TAU(J-1)+DEL
41    IF(ISXP.EQ.0)GOTO 42
      WRITE(6,111)FR,(TIT(I),I=1,20)
111   FORMAT('0',///'TITLE :',F8.4,2X,'MHZ',2X,2A4,
     &I1,3X,17A4)
      GOTO 43
42    WRITE(6,115)FR,(TIT(I),I=1,20)
115   FORMAT('0',///'TITLE :',F8.4,2X,'MHZ',2X,20A4)
 43   IF(NTR.GT.0) GOTO  44
      NTR=INTR
```

```
44     DIF=FLOAT(IDEL)*DEL
       WRITE(6,113)ISXP,IG,IH,IDEL,DIF,
      &TABLE,WT,NTR,NPT,TAU(1),DEL,HTO
       IF(TABLE.EQ.1) GOTO 51
       WRITE(6,116)(HT(J),J=1,NPT)
116    FORMAT(/,T5,'INPUT HT :',/(4X,10(F6.3,2X)))
113    FORMAT(//,4X,'CONTROLS :',T30,'ISXP =',I2,/T5,
      &'GUGGEN. =',I2,T30,'INIT.EFF.PT.=',I2,T60,
      &'INIT.CON.PAIR =+',I2,T90,'DELTA =',F7.3,/T5,
      &'PRINT TABLE =',I2,T30,'WT APPLIED =',I2,T60,
      &'REPEAT # =',I2,T90,'NPT =',I2/,T5,'INIT. TAU =',F7.3,
      &T30,'INCREMENT =',F7.3,T60,'MZ (0) =',F7.3)
       CALL NULL(NPT,NC,WT,WTH,IH,DEL,HT,TAU,SLR,HTINF)
       WRITE(6,105)SLR,HTINF
105    FORMAT(//,6X,'NULL-PT. ESTIMATION :',T50,
      &'1./ T1 =',E10.4,T80,'HTO (WT.AVE.=',F7.3)
       IF(NULO.NE.1) GOTO 50
       WRITE(6,109)
       GOTO 1
50      IF(DEL.GT.0.0) GOTO   51
       WRITE(6,114)(TAU(I),I=1,NPT)
114    FORMAT(T5,'INPUT TAU :',/,(4X,10(F6.3,2X)))
51     IF(WT.EQ.0) GOTO 52
       IF((WT.EQ.1).AND.(ISXP.EQ.0)) GOTO 6
       CALL IWT(NPT,NC,WTH,IH)
       GOTO 6
52     DO 5 I=1,NPT
5      WTH(I)=1
6      IDD=IDEL
60      ITER=ITER+1
       IF((HTO.GT.0.0).AND.(IG.NE.1)) GOTO 61
       IDD=IDD+ITER-1
       CALL GUGGEN(ICARD,IDD,DEL,NC,NPT,HTO,HT,WTH,IH,TAU,
      &T1,T1R,T1ST,HTCAL)
       GOTO 71
61     DO 7 I=1,NPT
       D(1)=TAU(I)
       D(2)=1.0D00
C...A SAFETY CHECK HERE
       DELTA=HTO-HT(I)
       IF(DELTA.LE.0.0) GOTO 98
       D(3)=ALOG(DELTA)
       MW=WTH(I)
       CALL LSQSM(0,2,D,MW,IFN,STD)
7      CONTINUE
       CALL LSQSM(1,2,D,MW,IFN,STD)
       IF( D(1).EQ.0.0) GOTO 98
       T1= -1./SNGL(D(1))
       T1R=1./T1
       T1ST=T1*T1*SNGL(STD(1))
```

```
      HTCAL=EXP(SNGL(D(2)))/2.
71    IF(ICARD.EQ.-9) GOTO 98
      WRITE(6,106)T1R,T1,T1ST,HTCAL,  HTO
106   FORMAT(T5,'1./T1 =',E10.4,T35,'T1 (SEC) =',F8.4,
     1T60,'STD.DEV =',F10.6,//T5,'MZ(0) CAL. =',F8.4,
     2T35,'MZ(0) OBS. =',F8.4,//)
      IF((TABLE.EQ.0).AND.(ITER.GE.NTR)) GOTO 1
      WRITE(6,107)
107   FORMAT(5X,' ====    TABLE    =====    '//,4X,
     1'TAU(SEC)',4X,'MZ(OBS)',3X,'MZO-MZ(I)',4X,
     2'WEIGHT',4X,'MZ(CAL)',6X,'DIFF')
      DO 8 I=1,NPT
      CAL=HTCAL*(1.-2.*EXP(-TAU(I)/T1))
      DD=HTO-HT(I)
      DIF=HT(I)-CAL
8     WRITE(6,108)TAU(I),HT(I),DD,WTH(I),CAL,DIF
108   FORMAT(5X,F6.3,5X,F7.4,5X,F7.4,5X,I2,7X,F7.4,5X,F6.3)
      WRITE(6,109)
109   FORMAT(//,'  =======          ==========       ',
     2'=======  ')
      IF(ITER.GE.NTR) GOTO 1
      IF(IG.EQ.1) GOTO 60
      HTO=HTINP
      GOTO 60
98    WRITE(6,117)HTO,(HT(J),J=1,NPT)
117   FORMAT('-','ERROR IN INPUT DATA ********** HT/-HT(',
     1'I).LE.0.0 *****',/T5,'INPUT CHECK :  HTO=',
     2E10.4,//T5,'HT :',/,(10(E10.4,2X)))
     &(10(E10.4,2X)))
      ICARD=-9
      GOTO 1
99     WRITE(6,110)
110   FORMAT(//,5X,'=== DATA EXHAUSTED. === ')
      STOP
      END
```

```
      SUBROUTINE LSQSM( ILQ,NM,U,MWT,IFN,STD)
    C
    C  PROGRAMED BY DR.MCCLUNG AND DR.BIRSS,CHEM.DEPT.
    C DOCUMENTATIONS SEE CHEM 570 PHYSICAL CHEM MANUAL.
      IMPLICIT REAL*8(A-H,O-Z)
      REAL*8 DABS,DSQRT,FLEV/0.00D0/,R(5,5),U(5),X(5),SEY,STD(5)
      INTEGER*4 IND/0/
      IF( ILQ.NE.0) GO TO 102
      IF ( IND.EQ.0) GO TO 19
    1 N=NM+1
      M=M+MWT
      DO 2 I=1,N
      DO 2 J=I,N
    2 R(I,J)=R(I,J)+MWT*U(I)*U(J)
      RETURN
  102 WT=M
      NM1=N-1
      PRINT 901, M,NM1
      DO 6 I=1,N
      M=I-1
      X(I)=DSQRT(R(I,I))
      IF (X(I).LT.1.D-8) GO TO 6
      DO 5 J=1,I
      IF (X(J).GE.1.D-8) GO TO 3
      Z=0.0D0
      GO TO 4
    3 Z=R(J,I)/(X(I)*X(J))
    4 R(I,J)=Z
      R(J,I)=Z
    5 CONTINUE
    6 CONTINUE
    7 VMIN=1.D+70
      VMAX=0.0D0
      DO 9 I=1,NM1
      IF (R(I,I).LE.1.D-4) GO TO 9
      V=DABS(R(I,N)*R(N,I)/R(I,I))
      IF (X(I).LT.0.0D0) GO TO 8
      IF (V.LE.VMAX) GO TO 9
      VMAX=V
      IMAX=I
      GO TO 9
    8 IF (V.GE.VMIN) GO TO 9
      VMIN=V
      IMIN=I
    9 CONTINUE
```

```
      IF (R(N,N).LT.1.D-10) GO TO 16
      IF (VMIN*WT/R(N,N).LT.FLEV) GO TO 10
      IF (VMAX*WT/(R(N,N)-VMAX).GT.FLEV) GO TO 11
      GO TO 16
   10 K=IMIN
      WT=WT+1.D0
      GO TO 12
   11 K=IMAX
      WT=WT-1.D0
   12 X(K)=-X(K)
      Z=1.D0/R(K,K)
      DO 13 J=1,N
   13 R(K,J)=Z*R(K,J)
      R(K,K)=Z
      DO 15 I=1,N
      IF (I.EQ.K) GO TO 15
      Z=-R(I,K)
      R(I,K)=0.0D0
      DO 14 J=1,N
   14 R(I,J)=R(I,J)+Z*R(K,J)
   15 CONTINUE
      GO TO 7
   16 SEY=X(N)*DSQRT(R(N,N)/WT)
      IFN=0
      PRINT 902, SEY
      DO 18 I=1,NM1
      IF (X(I).LT.0.0D0) GO TO 17
      U(I)=0.0D0
      PRINT 903, I,U(I)
      GO TO 18
   17 U(I)=-R(I,N)*X(N)/X(I)
      VMIN=-SEY*DSQRT(R(I,I))/X(I)
      STD(I)=VMIN
      IF (VMIN.LT.DABS(U(I))) IFN=1
   18 CONTINUE
      PRINT 905
   19 M=0
      DO 20 I=1,5
      DO 20 J=1,5
   20 R(I,J)=0.0D0
      IF (IND.NE.0) RETURN
      IND=1
      GO TO 1
    1 FORMAT('1',5X,'LINEAR LEAST SQUARES FIT FOR ',I4,'
     1I4,'  PARAMETERS IN THE MODLE. '//)
    2 FORMAT(//,6X,'OBSERVED-CALCULATED STANDARD DEVIATION ='
  903 FORMAT (I4,E18.8,20X,'INDETERMINABLE BY SUBMITTED DATA'
  905 FORMAT ('0')
      END
```

```
      SUBROUTINE TRS(ICARD,TIT,NPT,NC,TAU1,DEL,BHT,RHT,NTR)
C     ================
C
C
C     THE SUBROUTINE CONVERTS THE DIGITAL OUTPUTS
C     THE BRUKER SXP T1 EXPERIMENTS, WHEN THE DIODE
C     DETECTION MODE IS USED, INTO THE USUAL INPUT
C     FORMATS OF THE MAIN PROGRAM.
C
C     THE NEW INPUT CARDS ARE :
C
C     CARD (0)  CONTROL CARD
C               AS DEFINED IN THE MAIN PROGRAM.
C
C     CARD (1)  TRAIL INDEX,  TITLE
C               (6X,I1,18A4)
C
C     CARD (2)  ITAU(1), DEL, INTR
C               (I1,1X,F10.0,1X,I1)
C
C      ITAU(1) : INDEX OF THE INITIAL TAU.
C      DEL     : INCREMENT OF TAU.
C      INTR    : MAX. NUMBER OF ITERATIONS TO ESTIMATE
C                THE HT0.
C
C     CARD (3) NPH    (2I1)
C      NUMBER OF HT0 TO BE AVERAGED.
C
C     CARD (4) HT0 VALUES.  (10(I6,1X))
C
C     CARD (5) NPT (I2) : NUMBER OF DATA POINTS.
C
C     CARD (6) HT VALUES.   (10(I6,1X))
C
C
C....
      INTEGER*4 TIT(17),NTIT(17),WT,TABLE,HT(50),HTO(15),
     1AVH,TLE(17)
      REAL*4 RHT(50)
      INTEGER*4 TR(2)/'TRIA','L = '/ ,HEAD(2)/'TRIA','L 1 '/
C... HERE ARE SOME DEFINE OPTIONS AND SCALINF FACTOR
C...FOR THE MAGNITUDE OF HT.
      FACT=10000.
C...  END OF DEFINED.
       IF(ICARD.EQ.-9) GOTO 17
      READ(5,100,END=16)IN,(NTIT(I),I=1,17)
100   FORMAT(6X,I1,18A4)
20    TIT(1)=TR(1)
      TIT(2)=TR(2)
      TIT(3)=IN
```

```
      IF(IN.GT.1) GOTO 2
      DO 1 J=1,17
1      TIT(J+3)=NTIT(J)
2      READ(5,103) ITAU,DEL ,NTR
103   FORMAT(I1,1X,F10.0,1X,I1)
      IF(ITAU.GT.0) GOTO 21
      NTR=NTRO
      ITAU=ITAUO
      DEL=DELO
      TAU1=DEL*ITAU
      IF(TAU1.LE.0.0) GOTO 17
       GOTO 6
21    TAU1=DEL*ITAU
C...CHECK
       IF(TAU1.LE.0.0) GOTO 17
      READ(5,104)K1,K2
104   FORMAT(2I1)
      IF((K1.EQ.1).AND.(K2.EQ.0)) GOTO 3
      K=K1
      IF(K.EQ.0) GOTO 6
      GOTO 4
3      K=10
4     READ(5,105) (HTO(I),I=1,K)
105   FORMAT(10(I6,1X))
      AVH=0
      DO 7 I=1,K
7      AVH=HTO(I)+AVH
      AVH=AVH/K
6     READ(5,106)NPT
106   FORMAT(I2)
      IF(NPT.LE.0) GOTO 17
      READ(5,107) (HT(I),I=1,NPT)
107   FORMAT(10(I6,1X),10X)
      NH=HT(1)
      NC=0
       NPT1=NPT-1
      DO 8 J=1,NPT1
      IF(NH.LE.HT(J+1)) GOTO 8
      NH=HT(J+1)
      NC=J+1
8     CONTINUE
       NC1=NC+1
      IF(NH.GE.0) GOTO 12
      DO 10 I=1,NC
10    RHT(I)=FLOAT(NH-HT(I))/FACT
      DO 11 J=NC1,NPT
11    RHT(J)=FLOAT(HT(J)-NH)/FACT
      BHT=FLOAT(AVH-NH)/FACT
       GOTO 15
12    DO 13 J=1,NC
13    RHT(J)=-FLOAT(HT(J))/FACT
```

```
      DO 14 J=NC1,NPT
14    RHT(J)=FLOAT(HT(J))/FACT
      BHT=FLOAT(AVH)/FACT
15    ITAUO=ITAU
      NTRO=NTR
      DELO=DEL



       RETURN
C...SEARCH FOR NEW SET OF DATA
17    WRITE(6,108)TAU1,K,NPT
108   FORMAT('-','ERROR INPUT ****',/'0','TAU1',E10.4,5X,
     1' K ',I2,5X,'NPT =',I3,//'-','** SEARCH FOR    ',
     3'  ANOTHER SET OF DATA BEGINS :***** ',///)
18    READ(5,109) (TLE(J),J=1,17)
109   FORMAT(18A4)
      IF(TLE(1).NE.HEAD(1)) GOTO 18
      IF(TLE(2).NE.HEAD(2)) GOTO 18
      IN=1
      DO 19 J=3,17
19    NTIT(J-2)=TLE(J)
       ICARD=1
      GOTO 20
16    ICARD=0
      RETURN
      END
C
C
```

```
C
      SUBROUTINE IWT(NPT,NC,WTH,IH)
      INTEGER*4 WTH(50)
C
C
C     THE SUBROUTINE IS ACTIVATED BY SETTING
C     WT = 1 IN THE CARD (0).
C
C     THIS IS A USER SUPPLIED SUBROUTINE,
C     WHEN SPECIAL WEIGHTING AND TRUNCATION OF THE
C     INPUT DATA ARE DESIRED.
C
C
      RETURN
      END
C
      SUBROUTINE NULL(NPT,NC,WT,WTH,IH,DEL,HT,TAU,SLR,HTINF)
C
C
C     THE SUBROUTINE USES NULL-POINT METHOD TO ESTIMATE
C     THE T1 AND THE AVERAGE HT(0) VALUES.
C
C      NULL-POINT, NC, IS THE INFLECTION POINT (THE TAU
C      VALUE) AT WHICH THE MAGNETIZATION VECTOR IN THE
C      T1 EXPERIMENT CHANGES ITS SIGN.
C
      REAL HT(50),TAU(50)
      INTEGER WT,WTH(50)
      DIF1=ABS(HT(NC)-HT(NC-1))
      DIF2=ABS(HT(NC)-HT(NC+1))
      TNUL=TAU(NC-1)+(2.-DIF2/DIF1)*DEL
      SLR=ALOG(2.)/TNUL
      SUM=0.0
      WM=0.0
      NCN=NC-2
      NCP=NC+2
      IF(IH.EQ.0) IH=1
      DO 3 J=IH,NCN
      WM=WM+WTH(J)*HT(J)/(1.-2.*EXP(-TAU(J)*SLR))
      SUM=SUM+FLOAT(WTH(J))
3     CONTINUE
      DO 4 J=NCP,NPT
      WM=WM+WTH(J)*HT(J)/(1.-2.*EXP(-TAU(J)*SLR))
      SUM=SUM+FLOAT(WTH(J))
4     CONTINUE
      HTINF=WM/SUM
      RETURN
      END
```

```
      SUBROUTINE GUGGEN(ICARD,IDEL,DEL,NC,NPT,HTO,HT,WTH,IH,
     &T1,T1R,T1ST,HTCAL)
C     GUGGENHEIM TREATMENT (E.A. GUGGENHEIM. PHI.,MAG.,
C     2,538,1926) EQUATION:
C          LN(HT(J+DELT)-HT(J))   =  B - TAU(J) / T1
C
C          J = IH,  NPT-IDEL
C
C          B  = LN(  2 *  HTO *( 1 - EXP(-IDEL*DEL/T1)  )  )
C
C      SUBROUTINE USED : LSQSM
C
      REAL HT(50),TAU(50)
      INTEGER*4 WTH(50)
      REAL*8 D(5),STD(5)
C   CHOOSE THE DELTA
      IF(IDEL.LE.0)IDEL=NC
      IEND=NPT-IDEL
      IF(IH.EQ.0) IH=1
      IF(IH.GE.IEND) RETURN
      WRITE(6,100)IH,IEND
      IS=IH

100   FORMAT(//,6X,'GUGGENHEIM TREATMENT :',T60,'INIT.PT.='
     1,I2,T90,'FINAL PT.=',I2)
      DO 2 J=IS,IEND
      D(1)=TAU(J)
      D(2)=1.0D0
      DELTA=HT(J+IDEL)-HT(J)
      IF(DELTA.GT.0.0)GO TO 1
      ICARD=-9
      RETURN
1     D(3)=ALOG(DELTA)
      MW=WTH(J)
2     CALL LSQSM(0,2,D,MW,IFN,STD)
      CALL LSQSM(1,2,D,MW,IFN,STD)
      IF(D(1).NE.0.0) GOTO 3
      ICARD=-9
      RETURN
3     T1=-1./SNGL(D(1))
      T1R=1./T1
      T1ST=T1*T1*SNGL(STD(1))
      HTCAL=EXP(SNGL(D(2)))/(2*(1.-EXP(-T1R*FLOAT(IDEL)
     1*DEL)))
      RETURN
      END
```

APPENDIX B

SPIN-LATTICE RELAXATION RATES FOR THE THREE-SITE-SYSTEM

For a nucleus involved in the three-site exchange system given in Chapter III Eq. (III-9), the spin-lattice relaxation rate due to the metal ion complexes is described in this section. The relevant equations for the fast exchange limit are derived in terms of the equations for a two-site exchange system. [same notation defined in Chapter III are used here].

In the fast exchange region (high temperatures), where $k_{32} >> T_{2,3}^{-1}$ [Chapter II, Section B-2A(ii)], the same condition is also valid for the spin-lattice relaxation:

$$k_{32} >> T_{1,3}^{-1} \qquad \text{(B-1)}$$

Hence, a rapid exchange between species 2 and species 3 ($2 \rightleftharpoons 3$) exists. The individual spin-lattice relaxation times, $T_{1,2}$ and $T_{1,3}$, will then be averaged out and only a single effective relaxation time, denoted by $T_{1,5}$ is observed (McLaughlin and Leigh, 1973):

$$T_{1,5}^{-1} = f_2 T_{1,2}^{-1} + f_3 T_{1,3}^{-1} \qquad \text{(B-2)}$$

where f_2 and f_3 are, respectively, the mole fraction of the two species:

$$f_2 = \frac{[\underline{2}]}{[\underline{2}] + [\underline{3}]} \qquad f_3 = \frac{[\underline{3}]}{[\underline{2}] + [\underline{3}]}$$

The total concentration is then $[\underline{5}]$, where

$$[\underline{5}] = [\underline{2}] + [\underline{3}].$$

Therefore, in the fast exchange region, the three-site system resembles a "pseudo-" two-site exchange system and may be represented in the following notation:

$$\underline{1} \rightleftharpoons \underline{5}$$

where $$\underline{5} = \left[\underline{2} \rightleftharpoons \underline{3}\right]$$

The system now consists of a major diamagnetic species $\underline{1}$ and a minor paramagnetic species $\underline{5}$. Since the nucleus exchanges between species $\underline{1}$ and $\underline{5}$, the observed relaxation rate is (O'Reilley and Poole, 1963; Luz and Meiboom, 1964):

$$T_{1p}^{-1} = \frac{P_5}{k_{51}^{-1} + T_{1,5}} \qquad \text{(B-3)}$$

where $$P_5 = \frac{[\underline{2}] + [\underline{3}]}{[\underline{1}]}$$

Furthermore, the NMR exchange rates are related to the equilibrium concentrations of the corresponding species (Gutowsky *et al*, 1953; Gutowsky and Saika, 1953) in the following manner:

$$\frac{k_{ij}}{k_{ji}} = \frac{[j]}{[i]} \qquad \text{(B-4)}$$

The exchange between 5 and 1 can now be expressed in terms of the original process:

$$k_{s1} = \frac{[1]}{[2]+[3]} k_{15} = \frac{[1]}{[2]+[3]} (k_{12}+k_{13})$$

Since $k_{12} >> k_{13}$ [Eq. (III-10)], therefore,

$$k_{s1} = \frac{[1]}{[2]+[3]} k_{12} = \frac{[2]}{[2]+[3]} k_{21} = f_2 k_{21}. \qquad \text{(B-5)}$$

When Eqs. (B-2) and (B-5) are substituted into Eq. (B-3), one obtains

$$T_1 p^{-1} = \frac{P_s}{(f_2 k_{21})^{-1} + (f_2 T_{1,2}^{-1} + f_3 T_{1,3}^{-1})^{-1}} \qquad \text{(B-6)}$$

In the high temperature region, where

$$f_2 k_{21} \gg (f_2 T_{1,2}^{-1} + f_3 T_{1,3}^{-1}) ,$$

i.e. $$k_{51} \gg T_{1,5}^{-1}$$

the expression (B-6) further simplified to

$$T_1 p^{-1} = \frac{[2]}{[1]} T_{1,2}^{-1} + \frac{[3]}{[1]} T_{1,3}^{-1} \qquad \text{(B-7)}.$$

This is the desired equation in Chapter III (Eq. III-17).